Sphalerons and the Vacuum Structure of Gauge Theories

Giovanni G. van Marion

July 13, 2020

Abstract

Semi-classical techniques exist that study quantum field theories by looking at their special classical field configurations. Examples include solitons, instantons and sphalerons. For each of these we will discuss to different degrees what defines them, how to find them, why they exist, what they say about the classical and quantum theoretic vacuum structures of their associated theories and what phenomena they help us probe. In these discussions, topological considerations turn out to be crucial. Our focus will be on the sphaleron, a potential energy saddle point, in the electroweak sector of the standard model. It might make baryon and lepton number violating processes possible in collider experiments and its thermal cousin might be an ingredient in explaining the origin of the matter-antimatter asymmetry of the observable universe. We examine this process and explore a recent proposal that claims it could be resonant.

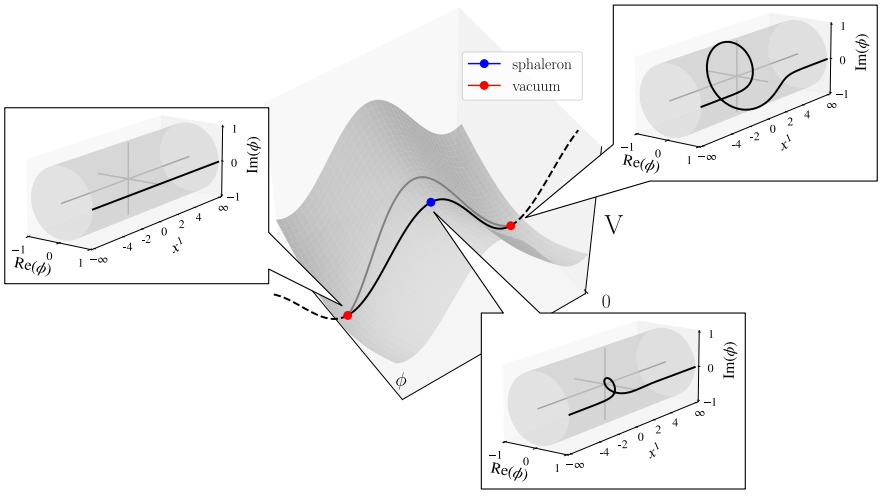

Master Thesis - Physics

Institute: Van Swinderen Institute
Supervisor / First Examiner: prof. dr. Daniël Boer
Secondary Examiner: prof. dr. Rob G.E. Timmermans

university of groningen / faculty of science and engineering

Contents

Chapter 1

Introduction

The standard model (SM) has been a phenomenally successful theory of particle physics. Its backbone, which is also the foundation of many models in solid state physics, is quantum field theory (QFT), the most successful theoretical framework that can combine the principles of classical mechanics, special relativity and quantum mechanics (QM). In particle physics, QFT is used to compute cross sections of reactions and decay rates of particles. In addition to the usual pertubative contribution to these quantities probed using, for instance, Feynman diagrams, semiclassical methods exist to examine a the non-perturbative features.

"Semiclassical" is a broad term, it refers to any model which is part quantum and part classical. Lots of these techniques analyze field theories by considering their special classical field configurations. An example is the instanton, they are event configurations of minimal Euclidean action, which help us compute tunneling amplitudes and which tells us about the gauge field vacuum. Other examples of special field configurations include solitons (such as monopoles and vortices) or sphalerons. Bringing together the literature on these special field configurations and the techniques and contexts in which they appear will be the subject of this thesis: For each these three we discuss to different extend what defines them, how to find them, when they exist and what predictions can be made with them. Our primary focus will be understanding the sphaleron. As we will get to see, a thorough understanding of the relation between the space of classical field configurations (and how it appears it different gauges) and the quantum states of the actual QFT is paramount. As it turns out, the appearance of such configurations can have a gauge-dependent character. Especially the relation between the classical and quantum theoretic vacuum structure of the models is important, which both instantons and sphalerons help us probe.

The most well known application of a sphaleron is seen in the SM. The bosonic component of electroweak (EW) sector is known to have one[14][28][23] as well as a thermal variant. In theory, it plays a crucial role in making baryon and lepton number violating reactions possible. These could occur in collider experiments using the regular EW sphaleron or they might have occurred in the early universe using the thermal EW sphaleron. If those reactions are found to exist, then they might ultimately help explain the origin of the matter-antimatter asymmetry of the observable universe[26][32]. During our discussions, we keep coming back to this EW sphaleron and its applications.

Outline

In chapter 2 we discuss solitons, which are the most straightforward kind of special configuration to introduce. They are the non-trivial minima of the potential energy functional of a theory. In the chapter, we introduce further concepts, such as field configuration spaces, homotopy groups and the relevance of scaling arguments such as those used in proving Derrick's theorem. While these topics are discussed in regards to solitons, they are crucial ingredients to assess the existence of the other special classical field configurations that occur within this thesis.

In chapter 3 we discuss the aforementioned instantons, which are solutions of so-called Euclidean equations of motion of a theory. They help us compute tunneling amplitudes in both QM and QFT. We derive the famous BPST-instanton[5] in pure Yang-Mills theory, which is a component of the EW and quantum chromodynamics (QCD) sector of the SM. We discuss the gauge-dependent character of the classical vacuum structure. They give rise to two physically equivalent, but conceptually different quantum pictures of the gauge field vacuum.

In chapter 4 we discuss sphalerons: saddle points of the potential energy functional. They exist on the smallest possible barriers between vacua, which makes them the most energetically favorable channels for vacuum-to-vacuum transitions. Before deriving the EW sphaleron itself, we derive the sphaleron (and instanton) in the $(1+1)$-dimensional Abelian Higgs model, which is a toy model for the full EW theory.

In chapter 5 we introduce fermions into our theories and discuss their consequences. We will see how they effect the vacuum structure of the gauge sectors of the SM. We will see why sphalerons (and instantons) are related with the violations of fermionic quantum numbers, such as the possible SM baryon and lepton number violating reactions. We do so by studying the effect of bosonic fields on fermions semiclassically. Then we'll discuss the possibility that these reaction in the SM might be resonant.

In chapter 6 we summarize, discuss and conclude out findings.

Chapter 2

Solitons and the Topology of Field Configuration Space

In this chapter we discuss the most straightforward class of special classical field configuration relevant to QFT: solitons[12, ch.6][11, ch.15]. Solitons are essentially *non-dissipative* wave-packets. By definition, they are *static*, *stable*, and have *finite potential energy*. They are *static* in the sense that their profile does not change when they move and they are *stable* in the sense that at least under a small perturbation the soliton will not fall apart / decay towards a vacuum configuration.

Objects like this can appear in theories with certain non-linear wave equations. This non-linearity gives rise to self-reinforcement of waves that can balance out against natural dispersion. Light traveling through glass can exhibit such a soliton, where dispersion, characterized by the glass's refractive index, balances out against the amplifying Kerr effect. Note that these solitons exist in some sense accidentally: the balance of forces can still be tipped, perturbing the wave hard enough will break the stability. In particular, these regular solitons have no conservation law that keeps them around. On the other hand, the solitons that we are interested in are called *topological solitons*. They are stable under a variation of any size, the reason being the existence of *topological conservation laws*: We will see that there is no way for the soliton to reach the vacuum by decay, because these configurations are not continuously connected. Instead, they are separated by an infinitely large potential energy barrier.

The goal of this chapter will be to introduce solitons while also serving as a foundation for the rest of this thesis, introducing the mathematics that will keep coming back. The chapter's outline is as follows: We begin this chapter in section 2.1 by familiarizing ourselves the most forthright example of a topological soliton: the (anti-) kink configuration in a relativistic $(1 + 1)$-dimensional real scalar field theory (a ϕ^4-theory). This soliton can simply be computed as we go along. In section 2.2, we subsequently present the general argument of why topological solitons exist and why they are stable, which also applies to field theories with continuous symmetries like gauge theories and those of which that undergo spontaneous symmetry breaking (SSB). We also discuss the concept of field configuration space, which provides a topological picture of this argument. We apply the general argument to theories with continuous symmetries in section 2.3. We also learn to characterize solitons

by introducing winding numbers and homotopy groups. We close the section by giving the example of the solitons called monopoles in the SSB $SO(3)$ $(3+1)$-dimensional Georgi-Glashow model. In section 2.4, we discuss Derrick's theorem, which demonstrates how topological arguments are ultimately insufficient to guarantee the existence of solitons. One must check, in addition, that solitons cannot disappear by rescaling of the fields. The theorem has a much wider application, similar scaling arguments can also preclude the existence of the instantons and sphalerons mentioned in chapter 1. We will henceforth refer to topological solitons simply as solitons for the rest of this thesis, except when the distinction is important.

2.1 The (Anti-) Kink Soliton in Scalar Field Theory

We begin our discussion of solitons in field theories by studying the so-called kink and anti-kink soliton. This is the traditional approach employed in many sources[11, ch.15 §2][12, ch.6 §2][21]. The model is a simple relativistic $(1+1)$-dimensional real scalar field theory[1]. Let us begin by reviewing this model while deriving the solitons themselves. After this section we generalize our results for solitons in general.

The dynamics of the field ϕ is given by the following Lagrangian:

$$\mathcal{L} = \frac{1}{2}\,\partial_\mu\phi\partial^\mu\phi - \mathcal{V}(\phi), \quad \text{where} \quad \mathcal{V}(\phi) = \frac{1}{2}(\phi^2-1)^2. \quad (2.1)$$

The potential $\mathcal{V}$ used is that of a double well potential, making this a ϕ^4-theory, see figure 2.1. Given the action $S = \int d^2x\,\mathcal{L}$, the equation of motion (e.o.m.) can be found using the stationary action principle. The result is

$$\partial_\mu\partial^\mu\phi = -\frac{\partial\mathcal{V}}{\partial\phi}. \quad (2.2)$$

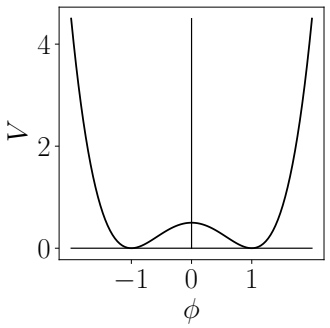

Figure 2.1: A generic double well potential.

Even though we work in a relativistic setting, in any particular reference frame we can break the energy E of the configuration into a kinetic T and potential V component at each moment in time: $E[\phi] = T[\phi] + V[\phi]$. In this specific case,

$$T[\phi] = \int dx\,\frac{1}{2}(\partial_0\phi)^2 \quad \text{and} \quad V[\phi] = \int dx\,\left[\frac{1}{2}(\partial_1\phi)^2 + \mathcal{V}(\phi)\right]. \quad (2.3)$$

Both are functionals of the particular configuration. As expected, E is conserved within such a frame, but it is not Lorentz invariant.

Actually solving for solitons in this particular theory is straightforward, one simply minimizes V by variation. The e.o.m. tells us that any extremum of V, which includes our minima, produces a static configuration: $\partial_\mu\partial^\mu\phi = 0$ (extreme satisfy $\delta V = 0$, hence $\frac{\partial\mathcal{V}}{\partial\phi} = 0$). In general, static configurations are not necessarily stable, but minima are. The argument why this is true parallels the equivalent argument in classical (particle) mechanics

[1] Let us stick, like we do in the entirety of this thesis, to the $(+,-)$ metric convention.

(think of a particle rolling around in some potential, let loose near some minimum): If a configurations $\bar{\phi}$ is a minimum of V w.r.t. *all possible variations* $\delta\phi$, then one can always start the system close enough to $\bar{\phi}$ such that the configuration is stuck under time evolution in the neighborhood of $\bar{\phi}$, oscillating around this equilibrium. This is because the field energy is conversed (T is bounded) and only a limited region of fields configurations is accessible: Suppose we start the system, say at $t = T$, in the configuration $\phi = \phi_\mathrm{i}$ with $\dot{\phi} = \dot{\phi}_\mathrm{i}$ such that its energy $E = E_\mathrm{i}$. Then only ϕ_f obtained by continuously deforming ϕ_i such that $V[\phi_\mathrm{f}] < E_\mathrm{i}$ during the deformation, are accessible configurations. Otherwise a potential energy barrier prevents the field from reaching ϕ_f.

Before we continue, let us be clear about the precise meaning of deformation, the concept returns quite often: We mean that one constructs a family of field configurations $\phi(x;\mu)$, continuous for all values of the parameter $\mu \in [0,1]$ everywhere in space, which begins and ends at the required fields. In the aforementioned example, $\phi(x,\mu=0) = \phi_\mathrm{i}$ and $\phi(x;\mu=1) = \phi_\mathrm{f}$. In mathematics, such a family of functions is called a *homotopy*. Two functions that can be continuously connected are said to be homotopic.

The extremization that will lead us to the solitons is

$$\delta V = \delta\left(\int dx\,\left[\frac{1}{2}(\partial_1\phi(x))^2 + \mathcal{V}(\phi(x))\right]\right) = 0. \tag{2.4}$$

Notice the form of this variational problem, it is functionally identical to the minimization of the "action" V of a particle of unit mass at "position" ϕ as a function of "time" x rolling in the flipped potential $-\mathcal{V}(\phi)$. We can therefore solve this problem as we would solve any other classical mechanics problem. There is just one boundary condition that we need not forget that carries over the original classical field theory problem: We would like to find finite V solutions only. If we look at the potential energy functional, equation 2.3, then we must conclude that $\phi(x)$ must approach a zero of the potential $\mathcal{V}(\phi)$ as $x \to \pm\infty$. Otherwise the potential energy $V[\phi]$ of the soliton will blow up. We discard the possibility that $\bar{\phi}(\infty) = \bar{\phi}(-\infty) = \pm 1$. Solving the problem with these boundary conditions gives us the vacuum configurations $\bar{\phi}(x) \equiv \phi_0^\pm(x) = \pm 1$ for which $V[\phi_0^\pm] = 0$. They *are* the static and stable global minima of V (the functional is positive definite), but not the non-trivial soliton solutions we are looking for.

In case the $\bar{\phi}(\infty) = -\bar{\phi}(-\infty) = \pm 1$, we could write down the corresponding Euler-Lagrange equations for $\delta V = 0$ and solve the system from there. Let us instead solve our trajectory starting from "energy" conservation of the "particle" system of "action" V. Since the particle tends asymptotically to a zero of $\mathcal{V}$, the solution has zero "energy":

$$\frac{1}{2}\left(\frac{d\phi}{dx}\right)^2 + (-\mathcal{V}(\phi)) = 0, \quad \text{hence} \quad x = \pm\int_{\phi(x_0)}^{\phi(x)} d\phi' \frac{1}{\sqrt{2\mathcal{V}(\phi')}}. \tag{2.5}$$

The solution can simply be integrated to give

$$\bar{\phi}(x) \equiv \phi_\pm(x) = \pm\tanh(x - x_0), \tag{2.6}$$

for which $V[\phi_\pm] = \frac{4}{3} > 0$.

The stability of these configurations is discussed in lots of sources[12, ch.6 §2.2][21]. One writes out all small perturbations $\delta\phi(x)$, which vanish as $x \to \pm\infty$ to satisfy the finite

V condition, in terms of some basis. One then shows that there are no negative modes (variations that lower the V), by showing that all eigenvalues of the linearized problem are greater than zero. This turns out to be true, except for the existence of a zero mode (a variation that keeps V constant), which corresponds to shifting the solution $\phi_\pm$ left to right: $\delta\phi(x) = \pm\frac{\partial\phi}{\partial x}(x)$. This is not surprising, the solution we obtained has translation invariance, just as any solution of a Lagrangian with translation invariance should have. The solution is still considered a soliton as the profile of the wave does not change when it moves.

2.2 Topological Solitons and Field Configurations Space

We have solved the (anti-) kink solitons by stationarizing V, which were stable under all (small) perturbations. This means they are, at least, regular solitons. We have not shown, however, whether they are topological solitons. We will now argue why they are. Recall from this chapter's introduction that a configurations being a topological solitons means that its decay is prevented by it and the vacua not being continuously connected. They must therefore be (topologically) stable under arbitrary large variations: They can be seen to carry a topological charge, conserved by a topological conservation law.

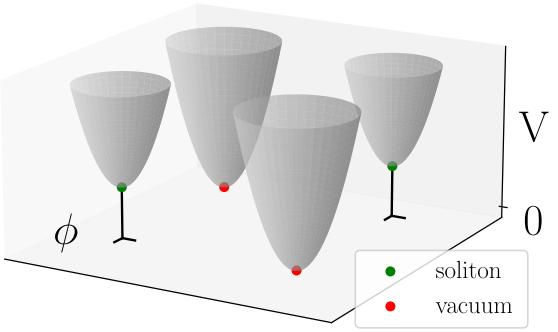

Figure 2.2: Schematic figure that graphs V above a two dimensional cross section of C_V for the theory containing the (anti-) kink solitons.

Actually, we have already mentioned the reason why the (anti-) kink is a topological soliton indirectly: *Any* finite V configuration, such as the (anti-) kinks $\phi_\pm$ or vacua $\phi^0_\pm$, have constrained asymptotic field values (asymptotics) to keep their V finite: They must always approach a zero of $\mathcal{V}$ (which are ± 1) as $x \to \pm\infty$. If we try and deform any finite V configuration into another with at least one different asymptotic, then for some intermittent value(s) of the deformation parameter μ one (or both) of the asymptotics must go from $+1$ to -1 (or vice versa). For those intermediate values of the parameter, V blows up. This happens, in particular, when deforming any of the vacua or solitons into another: One needs to cross an infinitely high potential energy barrier. Since time evolution is also a continuous deformation, there is no way the (anti-) kink soliton can decay into a vacuum, even if the configuration is hit by an arbitrary large variation $\Delta\phi$. Those change the configurations potential energy by a large, but finite amount. We would need an infinite (kinetic) energy to change the asymptotics.

Each of these four configurations are still part of the domain of V, which is *the space of finite V field configurations* C_V. The fact that they cannot be continuously deformed into each other means that this space C_V must consist of disconnected components. Figure 2.2 illustrates this point, we have graphed V above a two-dimensional cross section[2] of C_V. The

[2]We can only show a cross section in three dimensions. C_V is, in general, infinite dimensional.

plot captures the idea of the sectors, each containing a vacuum or (anti-) kink soliton, with an infinitely large potential energy barriers between them. Note how each configuration is the global minimum[3] of its own component, this is why solving $\delta V = 0$ produced them. The true global minima of the V on the whole space are, of course, the vacua themselves (the solitons have a positive non-zero V, they hover above the plane).

Since the asymptotics of the fields cannot change, the difference between the corresponding field values is a conserved quantity, a topological charge q. For the model that we are considering,

$$q[\phi] = \frac{1}{2}\int d\phi = \frac{1}{2}\int_{-\infty}^{+\infty} dx\, \partial_1\phi = \phi(+\infty) - \phi(-\infty), \tag{2.7}$$

where $q[\phi_\pm] = \pm 1$. The fact that requiring finiteness of V leads to q being conserved is known as a topological conservation law. They have a completely different origin as the usual Noether charges and currents, as they are not a consequence of the symmetries of the Lagrangian. Each of the configurations inside a component of C_V share the same q. We can thus characterize each sector (and configuration) using the label q.

2.2.1 The Existence of Solitons and the Topology of C_V

C_V having disconnected components is a necessary requirement for the existence of solitons. It occurs quite generally as C_V inherits its topology from the space of field asymptotics: As in the scalar field theory, deforming the asymptotics is enough to know V blows up. In particular, it is independent of how the fields are deformed anywhere else on the line.

In a theory with d spatial dimensions, these asymptotics are simply mappings from the boundary of space $\partial\mathbb{R}^d$ (which was the set $x \in \mathbb{R} = \{-\infty, +\infty\}$ for the previous scalar field theory) to the zero's of the potential term appearing within V, $\ker \mathcal{V}$ (which was the set $\phi \in \ker \mathcal{V} = \{-1, +1\}$). In other words,

$$C_V \cong \mathrm{Maps}(\partial\mathbb{R}^d \to \ker \mathcal{V}). \tag{2.8}$$

Thus, when there are multiple such maps that cannot be continuously deformed into each other (or when the set of much mappings it self discrete, which happend in the scalar field theory), then that disconnectedness carrier over into C_V, such as in figure 2.2.

We note, however, that the condition is not sufficient to prove the existence of solitons. In section 2.4 we consider Derrick's theorem, which shows how a scaling argument can preclude their appearance, even though C_V has disjoint sectors.

Before we end this section, let us be clear about the meaning of $\partial\mathbb{R}^d$: In general when $d > 1$, we mean the space of coordinates the fields still depend on if the limit $|\vec{x}| \to \infty$ of the fields is taken ($\vec{x} \in \mathbb{R}^d$). For instance, in a two dimensional space, when we can write our fields using the polar coordinates r and θ, a field $\phi(r, \theta)$ only depends on θ when $r \to \infty$. Therefore $\partial\mathbb{R}^2 \cong S^1$.

[3] Is such a figure, regular (non-topological) solitons would appear as local minima in each sector. This reflects their ability to decay if perturbed hard enough, there is no topological conservation law keeping them away from the vacua. They are instead separated by a finite height barrier.

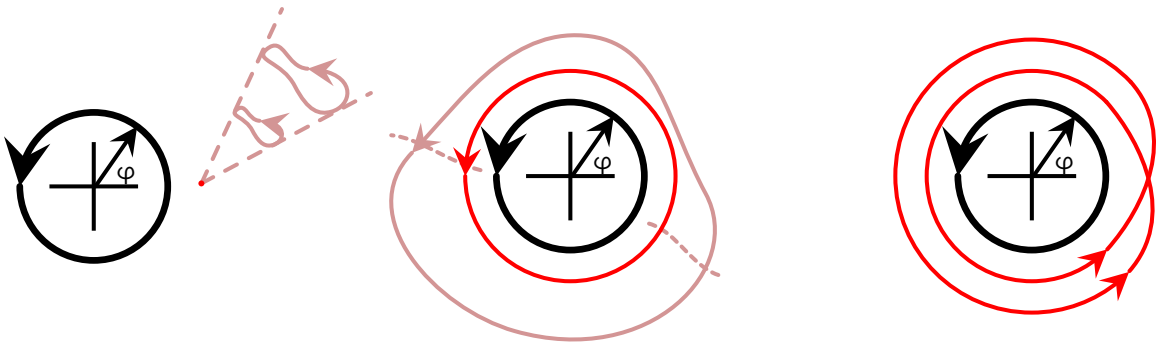

Figure 2.3: A visualization of a mapping of $S^1 \to S^1$, showing mappings with winding numbers 0, 1 and 2 in order. For each point on the red outer ring (the domain) one projects down radially onto the black inner ring (the codomain). From left to right we see the trivial mapping (winding number 0; the whole domain is mapped onto a single point), the identity mapping (winding number 1; each point is mapped onto itself) and a mapping of winding number 2. Homotopies (deformations) of the first two mappings are also drawn in beige, by definition they belong in the same homotopy class as the winding number cannot change disjointly under smooth deformations.

2.3 Continuous Symmetries and Homotopy Classes

In the previous example, we saw how C_V separated in four components because there were four discrete ways to map $\partial\mathbb{R} = \{\pm\infty\}$ into $\ker \mathcal{V} = \{\pm 1\}$. In this section, we discuss the same problem, but for theories where both $\partial\mathbb{R}^d$ and $\ker \mathcal{V}$ are continuous spaces instead. The resulting sector structure of C_V, one again, hints at the possibility of solitons.

Let us explain what changes by considering a theory with a complex scalar field $\phi(x^\mu)$ in $(2+1)$-dimensions, where the potential term

$$\mathcal{V}(\phi) = \frac{1}{2}\left(|\phi|^2 - 1\right) \tag{2.9}$$

with $U(1)$ symmetry appears in the potential energy functional V. Furthermore, let us write our fields in polar coordinates, $\phi = \phi(r, \theta)$. Further details of the model are not relevant, we only assume that ϕ is required to approach a zero of $\mathcal{V}$ for V to converge.

In this model, this potential has degenerate zero's: $\ker \mathcal{V} = \{e^{i\theta} \,|\, \theta \in [0, 2\pi]\} \cong S^1$. Moreover, if we let $r \to \infty$, then ϕ becomes a function of θ alone, as we discussed above: $\partial R^2 \cong S^1$. The asymptotics of ϕ, let us explicitly name these $\phi^\infty(\theta)$ ($\phi^\infty(\theta) = \lim_{r\to\infty} \phi(r, \theta)$), are therefore elements of the set $\mathrm{Maps}(\partial\mathbb{R}^2 \to \ker \mathcal{V}) = \mathrm{Maps}(S^1 \to S^1)$.

Mappings from $S^1 \to S^1$ have a *winding number* or *index* q, corresponding to the number of times the codomain is covered by the domain. Figure 2.3 illustrates a few of such mappings (in red) with winding number 0, 1 and 2, as well as other mappings (in a less saturated beige) to which these red mappings are homotopic (i.e. continuously deformable). To find out what any particular mapping does, project a point along the red loop (the domain) radially down onto the black circle (the codomain). The picture demon-

strates visually that two mappings with different winding numbers cannot be continuously connected, while mappings with the same winding number can, they are are said to belong to the same *homotopy class* (an equivalence class under winding numbers). Note that there are also mapping with the opposite orientation (obtained by reversing the red arrow), we label these mapping with a negative winding number.

Since C_V inherits the structure of $\mathrm{Maps}(S^1 \to S^1)$, there are a countably infinite number of sectors: one for each homotopy class of labeled by winding number q. In each we expect a soliton. Configurations whose asymptotics have different winding numbers are not continuously connected and must be separated by infinitely high potential energy barriers. Suppose $\phi^\infty(\theta) \equiv 1 \cdot u(\theta) = e^{if(\theta)}$, then q in terms of u is given by

$$q[u] = \frac{-i}{2\pi}\int_0^{2\pi} u^{-1}(\theta)\frac{du(\theta)}{d\theta}d\theta \quad \text{and} \quad q[f] = \int df = \frac{1}{2\pi}\left(f(2\pi) - f(0)\right). \tag{2.10}$$

2.3.1 Homotopy Groups and Notation

For our example it is easy to construct a single element from each homotopy class $f(\theta) = f_n(\theta) = n\theta$ with winding number n. It is possible to endow the set of homotopy classes with a group multiplication property $\times$, which is nothing more than connecting a representative element of each class back to back. For example,

$$g(\theta) = (f_n \times f_m)(\theta) = \begin{cases} f_n(2\theta) & \text{if} \quad 0 \le \theta \le \pi, \\ f_m(2\theta - 2\pi) & \text{if} \quad \pi \le \theta \le 2\pi \end{cases} = f_{n+m}(\theta). \tag{2.11}$$

This group is written as $\Pi_1(S^1)$ which is called the 1st *homotopy group* of S_1, where the subscript 1 tells us that we consider the group structure of mapping S^1 onto the argument (also S^1). We see immediately that the group structure is the same as that of the integers under addition $(\mathbb{Z}, +)$ (generally shortened to just $\mathbb{Z}$), i.e. that

$$\Pi_1(S^1) \cong (\mathbb{Z}, +). \tag{2.12}$$

There also exists homotopy groups of higher order denoted by $\Pi_n(X)$, where we consider the group structure of mapping S^n onto X. An example is $\Pi_n(S^n) \cong \mathbb{Z}$ in analogy with the example above. Note that homotopy groups satisfy the composition law

$$\Pi_n(\mathrm{Maps}(S^m \to X)) = \Pi_{n+m}(X). \tag{2.13}$$

Most importantly, one can also extend the concept of homotopy groups to include a $\Pi_0(X)$, the *first* or *fundamental homotopy group*, with which the group structure of the connected components of X are meant. In terms of homotopy groups, solitons might exist if C_V's fundamental homotopy group is non-trivial, i.e. $\Pi_0(C_V) \neq \mathbb{1}$. In the (2+1)-dimensional model, for instance,

$$\Pi_0(C_V) = \Pi_0(\mathrm{Maps}(\partial\mathbb{R}^2 \to \ker \mathcal{V})) = \Pi_0(\mathrm{Maps}(S^1 \to S^1)) = \Pi_1(S^1) = \mathbb{Z}. \tag{2.14}$$

For more information on homotopy groups and classes, see [11, ch.16 §1][12, ch.7 §3.2].

2.3.2 SSB and Homotopy Classes

In some gauge theories with gauge group G, the zeros of the potential are only invariant under some proper subgroup H of G. The theory's fields have different symmetries when expended around this vacuum then the original fields had. Theories like this are said to have SSB. For these theories[12, p.217]

$$\ker \mathcal{V} \cong G/H, \tag{2.15}$$

where G/H is the coset space. It is important to realize that H need not be an invariant subgroup. In that case the result is not a group either, but it might very well be some manifold. It is therefore possible to look for mappings from the boundaries of space into G/H, rather than solving $\ker \mathcal{V}(\phi)$, when deciphering the field configuration space.

In our previous example $H = \mathbb{1}$, since each $z \in \ker \mathcal{V}(\phi)$ gets rotated away under all $u(\theta) = e^{i\theta} \in U(1)$, except for the trivial $u(0) = 1$ element. This is knows as complete symmetry breaking. In this case, $G/H = U(1)/\mathbb{1} = U(1) \cong S^1$ (an example of complete symmetry breaking). This agrees with our earlier discussion $\ker \mathcal{V} \cong S^1$.

2.3.3 The $SO(3)$ Georgi-Glashow Model

Let us finish our discussion on solitons in theories with continuous symmetries with a well known model in which we can verify the validity of equation 2.15 visually. This is the so-called Georgi-Glashow model[11, p.466][12, p.197, p.207]. It is a $SO(3)$ (non-Abelian) gauge theory in (3+1) dimensions containing a single triplet of Higgs scalars $\boldsymbol{\phi} = (\phi_1, \phi_2, \phi_2)$ as well as three gauge field A^a_μ (one for each generator τ^a of $SO(3)$). This model is not to be confused with the the $SU(5)$ GUT theory also know by that name. Let us employ vector notation, $\boldsymbol{A}_\mu = \frac{i}{g} A^a_\mu \frac{\tau^a}{2}$, $\boldsymbol{F}_{\mu\nu} = \frac{i}{g} F^a_{\mu\nu} \frac{\tau^a}{2}$. The details of the theory are given by:

$$\mathcal{L} = -\frac{1}{2} \operatorname{Tr}(\boldsymbol{F}_{\mu\nu} \boldsymbol{F}^{\mu\nu}) + \frac{1}{2} (\boldsymbol{D}_\mu \boldsymbol{\phi})^* (\boldsymbol{D}^\mu \boldsymbol{\phi}) + \mathcal{V}(\boldsymbol{\phi}). \tag{2.16}$$

$$\boldsymbol{D}_\mu = \partial_\mu \phi + \boldsymbol{A}_\mu \boldsymbol{\phi}. \tag{2.17}$$

$$\mathcal{V}(\boldsymbol{\phi}) = \frac{\lambda}{2} (\boldsymbol{\phi} \cdot \boldsymbol{\phi} - 1)^2. \tag{2.18}$$

As we can see the $\ker \mathcal{V}$ is given by the field values for which $|\boldsymbol{\phi}| = 1$, which is nothing else than a 2-sphere. In other words $\ker \mathcal{V} \cong S^2$. The boundary of space $\partial \mathbb{R}^3 \cong S^2$ as well. The field configuration space is therefore divided into disconnected components given by maps from $S^2 \to S^2$, i.e. by $\Pi_0(C_V) \cong \Pi_2(S^2) = \mathbb{Z}$. So this theory has a countably infinity number of sectors too. The model contains all of these solitons, they are referred to as monopoles.

Let us see if we can obtain the same conclusion based on the principle expressed by equation 2.15. For this model the symmetry remaining after SSB is the stabilizing subgroup $H = SO(2)$ rotations of $G = SO(3)$ around a particular $|\boldsymbol{\phi} = 1|$ vector. Our task will be to find the manifold to which the set of (left) cosets $G/H = SO(3)/SO(2)$ is isomorphic, which ought to be S^2. Note that it will not be another Lie subgroup, since the $SO(2)$ subgroup is not invariant.

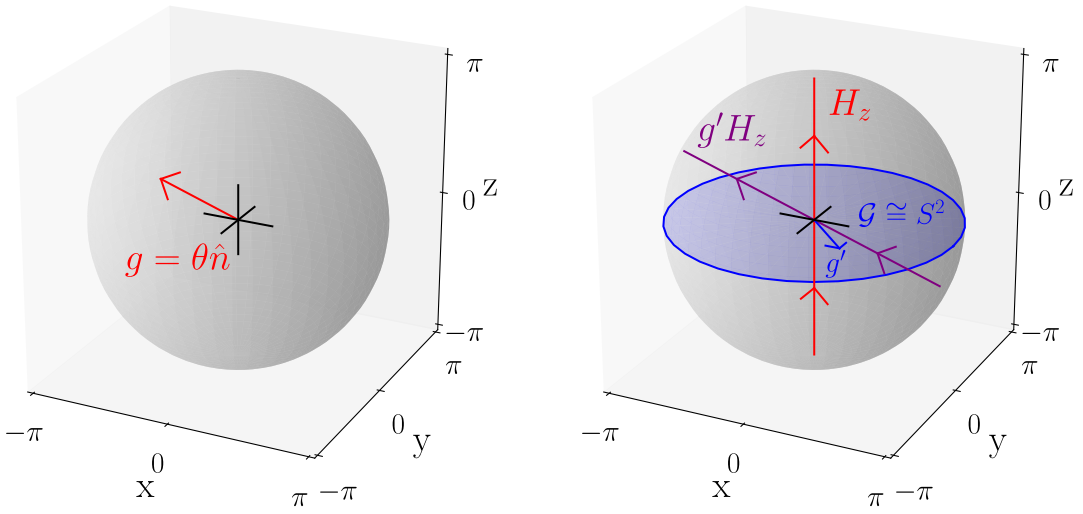

Figure 2.4: Demonstration that $SO(3)/SO(2) \cong S^2$. All points of $g \in SO(3)$ are displayed as points in and on a sphere of radius π: $g = \theta\hat{n}$, where θ is the (right handedly oriented) rotation angle around the axis specified by $\hat{n}$.

We choose to take a geometrical approach to tackle this problem. Let us therefore begin by visually representing all the elements of $SO(3)$. We do this in the conventional way: Draw each element g of $SO(3)$ as a point inside and on a sphere of radius π in $\mathbb{R}^3$. The distance θ to the origin of any given point g will be the rotation angle and the direction $\hat{n}$ will be the axis of rotation (using the right hand rule to orient the rotation direction). The left side of figure 2.4 shows this construction. It is important to realize that antipodal points on the sphere's surface are identified, they correspond to equivalent $\pm\pi$ rotations around the given axis. For instance, $H_{\hat{z}}$, the rotations around the $\boldsymbol{\phi} = (0, 0, 1)$, is the oriented line running through the center of the ball between the poles, see the right side of figure 2.4. Note that, because of the identification, such a line is actually a closed non-contractible loop (NCL) in $SO(3)$. This is how it should be, the parameter space of $SO(2)$ is S^1.

The right side of figure 2.4 shows us why $G/H \cong S^2$: w.r.t. the reference subgroup $H_{\hat{z}}$, each other $SO(2)$ subgroup H can be reached by a unique element $g' = \theta'\hat{n}' \in \mathcal{G} \subset G$, which are the points in the xy-plane (Note that geometrically, $g'H_{\hat{z}} = H_{\hat{z}\times\theta'\hat{n}'}$). It appears that $\mathcal{G}$ is not an S^2, since it is a disk. This is not exactly true: Not just the antipodal points, but the entire rim of the disk map $H_{\hat{z}} \to H_{-\hat{z}}$, which shows that, as far as the cosets are concerned, we need to treat the elements on the edge as one. The disk gets compactified to a sphere: $G/H \cong \mathcal{G} \cong S^2$.

2.4 Derrick's Theorem

Sometimes a theory has a soliton in isolation, but when we try to add other fields the solitons suddenly ceases to exist. One way that this can happen is through one of several "scaling

arguments"[27]. Qualitatively, a sector of field configurations space loses its minimum, even though C_V still has disconnected components. Hence, there is no longer any configuration that can resemble a soliton. Similar scaling arguments can also be used to rule out the instantons and sphalerons that are the topic of the upcoming chapters.

For the case of solitons there is a no-go theorem called Derrick's theorem[12, p.194] that exploits such an argument to preclude their existence. It applies in the case of (D+1) dimensional gauge theories with scalar fields only.

Let the theory's scalar fields be assembled into some big vector $\boldsymbol{\phi}$ with Lagrangian

$$\mathcal{L} = \frac{1}{2}(\partial_\mu \boldsymbol{\phi})(\partial^\mu \boldsymbol{\phi}) - \mathcal{V}(\boldsymbol{\phi}) \tag{2.19}$$

and where the potential $\mathcal{V}(\boldsymbol{\phi})$ is positive-definite with zeros at $\boldsymbol{\phi}_0$: $\mathcal{V}(\boldsymbol{\phi}_0) = 0$. Then the only static solutions of finite energy (to which solitons belong) for $D \geq 2$ are the vacua, i.e. $\boldsymbol{\phi}(x^\mu) = \boldsymbol{\phi}_0$.

To see why this is the case, consider the following argument. Recall that finite energy solutions minimize the potential energy functional:

$$V[\boldsymbol{\phi}] = V_1[\boldsymbol{\phi}] + V_2[\boldsymbol{\phi}] \quad \text{where,} \quad V_1[\boldsymbol{\phi}] = \frac{1}{2}\int d^D x (\nabla \boldsymbol{\phi})^2 \quad \text{and} \quad V_2[\boldsymbol{\phi}] = \int d^D x \mathcal{V}(\boldsymbol{\phi}) \tag{2.20}$$

The argument is based on the way different terms in the Lagrangian scale when scaling the solution $\boldsymbol{\phi}_\lambda(\vec{x}) \to \boldsymbol{\phi}(\lambda \vec{x})$. Under this transformation $\nabla\boldsymbol{\phi}(\vec{x}) \to \lambda^2 \nabla\boldsymbol{\phi}(\lambda\vec{x})$, therefore (after a change of variables), $V[\boldsymbol{\phi}]$ scales as

$$V[\boldsymbol{\phi}_\lambda] = \lambda^{2-D} V_1[\boldsymbol{\phi}] + \lambda^{-D} V_2[\boldsymbol{\phi}]. \tag{2.21}$$

If the solution is really stationary it must be at a minimum of the potential, so $\frac{d}{d\lambda} V[\boldsymbol{\phi}_\lambda] = 0$ at $\lambda = 1$, in other words

$$(D-2)V_1[\boldsymbol{\phi}] + DV_2[\boldsymbol{\phi}] = 0 \tag{2.22}$$

However, since $V_1[\boldsymbol{\phi}]$ and $V_2[\boldsymbol{\phi}]$ are positive-definite, when $D > 2$, $V_1[\boldsymbol{\phi}]$ and $V_2[\boldsymbol{\phi}]$ must vanish. In other words the solutions must be the vacua $\boldsymbol{\phi}(x^\mu) = \boldsymbol{\phi}_0$, since their energy vanishes. Even in the case $D = 2$, it can be shown that this cannot be satisfied by non-trivial solutions.

The same principle can be applied to the EW theory in the search for instantons. Here we apply a scaling argument to the Euclidean action $S_E[\boldsymbol{\phi}, \boldsymbol{A}_\mu]$ in $\mathbb{R}^4$ rather then the potential energy functional $V[\boldsymbol{\phi}, \boldsymbol{A}_\mu]$. This rules out the pure Yang-Mills instantons in that theory[30, p.459]. However, the same argument cannot be used to rule out sphalerons in that particular theory[28][27, §4].

Chapter 3

Instantons and the Gauge Theory Vacuum

In this chapter we will meet *instantons*, which, like solitons, are another example of a special classical field configuration with importance to physics. As we will get to see, they are solutions of the *Euclidean equations of motion* found by minimizing the *Euclidean action* S_E of various field theories.

Mathematically, instantons and solitons are more than superficially similar: They live in C_{S_E}, the space of finite S_E field configurations, a space analogous to C_V. Minimizing S_E over C_{S_E} to find instantons is similar to minimizing V over C_V to find solitons. The instanton's existence is therefore similarly related to the non-trivial topology of C_{S_E}, this space can consist of disconnected components ($\Pi_0(C_{S_E}) \neq \mathbb{1}$) just as C_V does. They can thus be classified using the elements of $\Pi_0(C_{S_E})$, hence labeled by topological charges (i.e. winding numbers). Despite this similarity, their physical applications are quite different. Solitons reveal static objects, like monopoles and vortices, that appear in certain theories. Instantons, on the other hand, are relevant when discussing quantum tunneling. As a classical solution they connect a theory's classical vacua together over the so-called *Euclidean time* (or Imaginary time). They therefore appear as an "event" taking place over Euclidean time, transforming one vacuum into another. These are the same vacua as those appearing in C_V, they are generally isolated and separated by potential energy barriers through which the instantons are said to tunnel.

To be precise, instantons are used to compute *transition amplitudes* (or tunneling amplitudes) in the path integral between classical vacuum configurations in both quantum mechanics (QM) and quantum field theory (QFT). With classical vacuum configurations, we mean the same as in the last chapter: the minima x_0 of the potential $V(x)$ in QM and the minima $\mathbf{\Phi}_0$ of $V[\mathbf{\Phi}]$ in QFT. When there is an instanton connecting two such vacua, then, in terms of wave functions[1], there is a non-zero probability amplitudes for a state that is approximately localized at one of these classical vacua (close to a delta spike) to be found at the other an arbitrarily long time later. It is the instanton's Euclidean action

[1] Wave functions are generally used in quantum mechanics, but have their use in field theory too. The wave function picture in field theory is called the *Schrödinger functional formalism.*

that ultimately determines these amplitudes. The higher the barrier between the vacua, the longer such approximately localized state will last. Essentially they are the approximate ground (or vacuum) states of the theory. In terms of wave functions, the true stationary (hence tunneling invariant) ground state must be localized (in superposition) near all the classical vacua; the existence of the instanton (and its resulted tunneling) have clued us in to this fact.

Consider, for instance, the particle in the double well potential. It is one of the simplest examples of a quantum mechanical system with tunneling. The potential is,

$$V(x) = \frac{1}{2}(x^2 - a^2)^2, \tag{3.1}$$

see figure 3.1. In this problem, the classical vacua are $x_0 = \pm a$ and there are two instantons: one connecting $x_0 = a$ to $x_0 = -a$ and vice versa. Both approximate ground states $|\pm a\rangle$ are required to build a true stationary ground state $|\Omega\rangle \sim \frac{1}{\sqrt{2}}(|a\rangle + |-a\rangle)$ of the system.

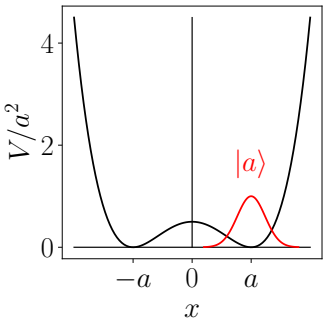

Figure 3.1: Double well potential, with approximate ground state $|a\rangle$.

In gauge theory we run into additional complications: The classical vacuum structure depends on which gauge fixing one chooses. Since instantons interpolate between classical vacua, the instantons change their appearance when changing gauge. Upon quantization, there are some subtleties associated with discerning which approximate vacuum states exist and between which of those instantons determine the transition amplitudes. In other words, there is some subtly involved in *relating the classical vacuum structure* (like the zero's $\pm a$) *with the quantum theoretic vacuum structure* (like the states $|\pm a\rangle$) in gauge theories. As we will get to see, the issue comes down to the physicality of large gauge transformations. An example of such a theory is the *pure* $SU(2)$ *Yang-Mills* theory in (3+1)-dimensions.

In the *pure* $SU(2)$ *Yang-Mills* theory, Belavin, Polyakov, Schwarz and Tyupkin, discovered a countably infinite number of instantons classified by topological charges[5] ($\Pi_0(C_{S_E} = \mathbb{Z})$). The unit winding number instanton is now known as the *BPST-instanton*, named after its discoverers. At the time, the theory was expected to have only a single classical vacuum, while it *appears* as if these instantons contradict that fact. Jackiw and Rebbi were the first to make sense of these instantons by interpreting the theory's vacuum structure[22] and they were later followed by Callan, Dashen and Gross[9] who came to the same conclusion. As it turns out, the true vacuum state $|\Omega\rangle$ is characterized by a so-called vacuum angle θ.

For this thesis, investigating how the classical vacuum structure (and hence an instanton) changes when changing gauge is important. For instance, the $SU(2)$ sphaleron has a similar gauge fixing-dependent appearance as the BPST-instanton. Moreover, understanding the difference between the quantum theoretic vacuum structures of quantum chromodynamics (QCD) (which is similar to pure Yang-Mills) and the electroweak (EW) theory (which as the $SU(2)$ sphaleron) is important to understand the work by Tye and Wong on resonant tunneling in the EW theory[37].

In this chapter, we discuss the aforementioned topics as follows: In section 3.1, we begin this chapter with a brief overview of tunneling in quantum mechanics. First, we discuss

the *transmission amplitude* computed in the WKB approximation, which is also been put to use in field theory (in the Schrödinger functional formalism). Afterwards we compute using instantons the transition amplitude of tunneling between the approximate ground states $|\pm a\rangle$ in the double well problem. This section is meant as an introduction to working with instantons. In section 3.2 we derive the BPST-instanton itself. In section 3.3, we show how the instanton changes between different gauges and we present one possible way of thinking about the quantum theoretic vacuum structure of the pure $SU(2)$ Yang-Mills theory. We draw upon an analogy between it and the *quantum mechanical pendulum*. We use the comparison to interpret the vacuum angle θ that characterizes the ground state.

3.1 An Overview of Quantum Tunneling

In this section we discuss two techniques that are used to make quantitative predictions about quantum tunneling in both quantum mechanical and quantum field theory. Firstly, we briefly discuss the computation of transmission amplitudes using WKB approximation. Secondly, we discuss tunneling using instantons. This section is meant as a rudimentary introduction to quantum tunneling (especially using instantons), for that reason we present a quantum mechanical example for either technique.

3.1.1 The WKB Approximation

In short, the WKB approximation is all about computing approximate wave functions $\psi(x)$ that solve the time-independent Schrödinger equation, given what their energy E should be. The primary application of the technique is to approximate the spectrum of bound states of some system. Central to the procedure is the patching together of wave functions in classically allowed regions ($E > V(x)$) with classical forbidden regions ($E < V(x)$).

By analyzing the time-independent Schrödinger equation, one can show that in regions where $E \gg V(x)$ and $E \ll V(x)$ the wave function is given by

$$\psi(x) \approx Ae^{\pm\frac{i}{\hbar}\sqrt{2m(E-V(x)}\,x} \quad \text{and} \quad \psi(x) \approx Ae^{-\frac{1}{\hbar}\sqrt{2m(V(x)-E)}\,x} \quad \text{respectively.} \tag{3.2}$$

These approximations are then assumed to hold all the way up to the classical turning points where $E = V(x)$. The patching is done in such away that $\psi(x)$ is differentiable at these points.

The patching together of wave functions makes the technique ideal for scattering calculations where some particle impinges on some barrier. The incoming plane wave solutions can be joined up with an outgoing transmitted wave on the other side of the barrier (which is partially a forbidden region). The ratio (or relative magnitude) of the amplitudes of wave functions on either side of the barrier $T(E)$ helps us compute the transmission amplitude (the probability for the particle to tunnel through), which is simply $|T(E)|^2$. The magnitude of $T(E)$ is given by

$$|T(E)| = \exp\left(-\frac{1}{\hbar}\int_{x_1}^{x_2} dx\sqrt{2m(V(x)-E)}\right), \tag{3.3}$$

where x_1 and x_2 are the turning points at either side of the barrier. This straightforward form is a consequence of the assumption that the amplitude simply decays exponentially throughout the forbidden part of the barrier, see equation 3.2.

The WKB approach has also been applied to field theory. The technique is used to compute the so-called most probable escape paths (MPEPs) along which fields will most likely tunnel between them[8]. This domain of techniques is closely related to the work by Tye and Wong[37] we discuss in chapter 5. For further details on the WKB procedure see, for example, Griffiths[19].

3.1.2 Tunneling Using Instantons

We will now discuss another technique that can be used to make quantitative predictions about tunneling in QM and QFT. In certain scenarios, the technique reproduces the WKB procedure's results[8][38]. The technique uses instantons, which we will apply to the problem from the introduction: the double well potential. This is *the* conventional pedagogical examples used to explain instantons. For instance, it is used in the famous paper "The Uses of Instantons" by Coleman[12, ch.7 §1]. To be precise, we will go ahead and compute the probability amplitude $\langle -a| \exp\left(-\frac{i}{\hbar}HT\right)|a\rangle$. This is the transition amplitude for a particle initially in the approximate ground state $|-a\rangle$ to transition to $|a\rangle$, given a specified transition time T (that we will have to make arbitrarily large later, see below). The dominant contribution to this quantity is calculated using the instanton. Even though we discuss instantons in the context of quantum mechanics, the idea can be extended straightforwardly to field theory. This section will act as an introduction to the concept of the instanton and we will connect it to the previous chapter by comparing it to the soliton.

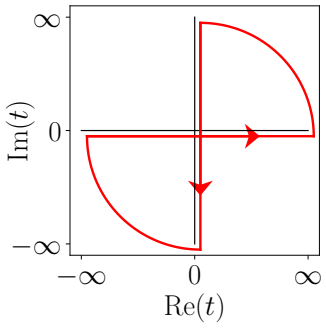

Figure 3.2: Equivalent integrating over the real and imaginary axis.

The transition amplitude can be written down in term of the path integral

$$\langle -a| e^{-\frac{i}{\hbar}HT}|a\rangle = \int \mathcal{D}q\, e^{\frac{i}{\hbar}S[q]}, \tag{3.4}$$

where

$$S[q] = \int_{-\frac{T}{2}}^{\frac{T}{2}} dt\, \mathcal{L}(q,\dot{q}) = \int_{-\frac{T}{2}}^{\frac{T}{2}} dt\, \left[\frac{1}{2}\left(\frac{dq}{dt}\right)^2 - V(q)\right] \tag{3.5}$$

is the action for a classical particle trajectory used in quantum mechanics.

To find the dominant contribution to the amplitude 3.4, one would like to apply some sort of steepest descent method (the stationary phase approximation) to the path integral expression. However, it is tricky to apply such an approximation to the amplitude as is. This is because a sum of rotating phases $e^{\frac{i}{\hbar}S}$ does not have the same nice converge properties a regular exponent $e^{-\frac{1}{\hbar}S}$ would. We therefore start by manipulating this amplitude's exponent such that it becomes of this regular $e^{-\frac{1}{\hbar}S}$ form. It is then argued that in the vicinity of the classical trajectory $q_{cls.}(t)$ neighboring paths interfere constructively within this amplitude

in what is known as the semiclassical limit: $\hbar \to 0$. Instantons enter the picture when we apply a, more or less, regular steepest descent method to this newly obtained amplitude.

To turn the complex exponent into a reguler one we start with a so-called *Wick rotation*. One analytically continues the action integral, equation 3.5, such that we can equivalently integrate over the imaginary axis instead, see figure 3.2. The new coordinate along which we integrate is known as the imaginary time τ. Even though both integrals are only equal in the limit $T \to \infty$ (since then the contributions along the arcs vanish), the equivalence of the integrals is generally assumed. This is because proving that the analytical continuation exists and is well defined is definitely not straightforward. Nonetheless, the procedure works for the applications in physics. The result of the continuation is usually summarized as the following *active* transformation

$$t \to -i\tau. \tag{3.6}$$

One can choose to give the Wick-rotated time a new index, $x_0 \to -ix_4$, we choose to keep the index the same: $x_0 \to -ix_0$. The transformed time coordinate is also known as the Euclidean time, since for these field theories the Wick rotation turns the regular spacetime interval into[2]:

$$dx_\mu dx^\mu = dx_0^2 - dx_i^2 \to (-idx_0)^2 - dx_i^2 = -(dx_0^2 + dx_i^2) \equiv -dx_\mu^2, \tag{3.7}$$

which is the negative of the now Euclidean distance dx_μ^2.

The Wick rotation turns the action into the so-called *Euclidean action* S_E:

$$iS[q] \to -S_E[q] = \int_{-\frac{T}{2}}^{\frac{T}{2}} d\tau \left[\frac{1}{2}\left(\frac{dq}{dt}\right)^2 + V(q)\right], \tag{3.8}$$

which can be seen as the negative of the action of a Newtonian particle rolling in a flipped potential $-V(x)$. The Wick rotation has done what we desired and has given us a simpler exponent in the path integral to work with:

$$\langle -a|\, e^{-\frac{i}{\hbar}HT}\, |a\rangle = \int \mathcal{D}q\, e^{-\frac{1}{\hbar}S_E[q]}. \tag{3.9}$$

Only the solutions that minimize the new $S_E[q]$ dominate this new path integral amplitude (a saddle point approximation essentially). These are the solutions of the *Euclidean equations of motion* generated by $\delta S_E = 0$:

$$\frac{d^2q}{d\tau^2} = \frac{dV}{dq} \tag{3.10}$$

In light of the double well potential, equation 3.1, this is similar to the last chapter's (anti-) kink soliton, see section 2.1. Since we are specifically looking to find the amplitude in going from the left to the right well, we need only to consider the *solutions* $q(\tau)$ that start and end at these vacua. This is the way in which the instanton interpolates between the two classical vacua $q_0 = \pm a$. Since we would like to work in the limit $T \to \infty$ (such

[2]Here we use the $(+,-,-,-)$ particle physics metric convention used throughout this thesis.

that the Wick rotation is exact) this must correspond to a particle motion that goes from hill to hill in this flipped potential $-V(x)$ in an arbitrary large amount of time. This can only be achieved by a zero "energy" motion $E(q_{\text{inst}}(\tau)) = 0$. Note that for this particular particle motion the energy is given by

$$E(q(\tau)) = \frac{1}{2}\left(\frac{dq}{d\tau}\right)^2 - V(q). \tag{3.11}$$

The instanton solution that takes us from $-a$ to a (between $\tau = \pm\infty$) is given by

$$q_{\text{inst.}}(t) = a \tanh\big(a(\tau - \tau_0)\big), \tag{3.12}$$

which we recall from equation 2.6 solves this e.o.m. This is the instanton event for the tunneling from $-a$ to a.

Given this instanton, the leading order contribution to the tunneling rate is

$$\langle -a|\, e^{-\frac{i}{\hbar}HT}\, |a\rangle \cong e^{-\frac{1}{\hbar}S_E[q_{inst}]}\big(1 + O(\hbar)\big). \tag{3.13}$$

Note the inverse power of $\hbar$ that remain inside the exponent, it makes the expression non-analytic. In other words, a perturbative expansion of the path integral in orders of $\hbar$ would not have picked up on the tunneling.

There is, unsurprisingly, also an instanton solution that takes us from a to $-a$ instead. This instanton is required to compute the reverse tunneling amplitude $\langle a|\exp\left(-\frac{i}{\hbar}HT\right)|-a\rangle$ (whose magnitude will by symmetry be equally large). That solution is simply $q'_{\text{inst.}} = -q_{\text{inst.}}$.

There was no way to deform the kink soliton into the antikink soliton without making V blow up intermittently. The same happens to S_E, of course, when one tries to deform $q_{\text{inst.}}$ into $q'_{\text{inst.}}$: Both C_V and C_{S_E} are made out of disconnected components ($\Pi_0(C_V)$ and $\Pi_0(C_{S_E})$ are non-trivial). Configurations in these spaces are characterized by their asymptotics (by which zero of the potential they approach as $\tau \to \pm\infty$) or equivalently by their topological charge (like equation 2.7). Each sector of C_{S_E} contains either a vacuum or instanton configuration.

This concludes the main goal that we set for ourselves in this section. See, for instance, Coleman[12, ch.7 §1] for further details of the procedure such as for dealing with the higher order corrections.

3.2 The BPST-Instanton in $SU(2)$ Yang-Mills

In this section we present the BPST-instanton in the pure (3+1)-dimensional $SU(2)$ Yang-Mills theory originally found by Belavin, Polyakov, Schwarz and Tyupkin[5]. We discuss the details of the theory, how to perform the wick rotation, the scale-invariance of the model, the topology of C_{S_E} and, ultimately, how to find the instanton solution. What is listed here is based on the advanced textbooks by Cheng and Li[11, ch.16], Coleman[12, ch.7 §3.5], and Rubakov[33, ch.13]. In the next section, we will discuss how the instanton appears in different gauges and what implications this has for its quantum theoretic interpretation.

3.2.1 The $SU(2)$ Pure Yang-Mills Theory

The pure $SU(2)$ Yang-Mills theory is a simple field theory consisting of nothing else than the three massless gauge fields A^a_μ corresponding to each of the three generator the $SU(2)$ gauge group.

The parameter space of $SU(2)$ is S^3, as each element of $U \in SU(2)$ can be labeled by two complex scalars α and β satisfying

$$U(\alpha,\beta) = \begin{pmatrix} \alpha & -\beta^* \\ \beta & \alpha \end{pmatrix}, \quad \text{such that} \quad |\alpha|^2 + |\beta|^2 = 1. \tag{3.14}$$

The hypersphere S^3 is defined implicitly by the constraint the real and imaginary components of α and β together satisfy. The group's generators are the three Pauli matrices τ^a. Their structure constant are $2\epsilon^{abc}$: $[\tau^a, \tau^b] = 2i\epsilon^{abc}\tau^c$ and their index is $\operatorname{Tr}\tau^a\tau^b = 2\delta^{ab}$.

The Lagrangian of the Yang-Mills theory is given by

$$\mathcal{L} = -\frac{1}{2}\operatorname{Tr}(\boldsymbol{F}_{\mu\nu}\boldsymbol{F}^{\mu\nu}), \tag{3.15}$$

which is the familiair Maxwellian term for non-Abelian gauge theories. It contains the field strength tensor $\boldsymbol{F}_{\mu\nu}$, which itself is given by

$$\boldsymbol{F}_{\mu\nu} = \frac{i}{g}[\boldsymbol{D}_\mu, \boldsymbol{D}_\nu] = \partial_\mu \boldsymbol{A}_\nu - \partial_\nu \boldsymbol{A}_\mu - ig[\boldsymbol{A}_\mu, \boldsymbol{A}_\nu]. \tag{3.16}$$

Here, the covariant derivative

$$\boldsymbol{D}_\mu = \partial_\mu - ig\boldsymbol{A}_\mu \tag{3.17}$$

does contain a coupling constant g, even though there are no other fields present to which the gauge fields couple. Here we have used the vector notation

$$\boldsymbol{A}_\mu = \frac{\tau^a}{2}A^a_\mu \quad \text{and} \quad \boldsymbol{F}_{\mu\nu} = \frac{\tau^a}{2}F^a_{\mu\nu}, \tag{3.18}$$

to simplify our notation. We can use the index relation of the Pauli matrices to get rid of the trace in the Lagrangian if necessary, the Lagrangian then becomes

$$\mathcal{L} = -\frac{1}{4}F^a_{\mu\nu}\,F^{\mu\nu\,a}. \tag{3.19}$$

Under a gauge transformation $U \in SU(2)$,

$$\boldsymbol{A}_\mu \to U^{-1}\boldsymbol{A}_\mu U + \frac{i}{g}U^{-1}\partial_\mu U \quad \text{and} \quad \boldsymbol{F}_{\mu\nu} \to U^{-1}\boldsymbol{F}_{\mu\nu}U. \tag{3.20}$$

These transformations will become important in a moment[3].

[3]Note that one regularly encounters different conventions, for instance, by puting the U on the left and $\partial_\mu U^{-1}$ on the right.

3.2.2 The Wick Rotation

Now that we have introduced the pure $SU(2)$ Yang-Mills theory we can begin the actual BPST-instanton derivation. As in section 3.1.2, this means beginning with a Wick rotation. For this particular problem we choose to transform $\boldsymbol{A}_0$ in addition to x_0. If we would simply let $x_0 \to -ix_0$, then the initially real F^a_{0i} (see equation 3.16) becomes

$$F^a_{0i} \to i\partial_0 A^a_i - \partial_i A_0 + g\epsilon^{abc} A^b_0 A^c_i, \tag{3.21}$$

which suddenly includes both imaginary and real contributions. This is not necessarily a problem, but we would rather like to keep the Euclidean action real if we can. By choosing to transform $\boldsymbol{A}_0$ in addition to x_0 we make F^a_{0i} completely imaginary. The covariant derivative then transforms covariantly under the Wick rotation itself.

$$x_0 \to -ix_0 \quad (\partial_0 \to i\partial_0) \quad \text{and} \quad \boldsymbol{A}_0 \to i\boldsymbol{A}_0 \tag{3.22}$$

imply $\boldsymbol{D}_0 \to i\boldsymbol{D}_0$ and hence

$$F^a_{0i} \to iF^a_{0i}. \tag{3.23}$$

We can use these transformations to figure out how the Lagrangian transforms starting from the action.

$$\begin{aligned} S[A] = \int d^4x\, \mathcal{L} &= \int d^4x\, - \left[\frac{1}{2} F^a_{0i}\, F^{0i\,a} + \frac{1}{4} F^a_{ij}\, F^{ij\,a}\right] \\ &= \int d^4x\, \left[\frac{1}{2}(F^a_{0i})^2 - \frac{1}{4}(F^a_{ij})^2\right], \end{aligned}$$

which Wick-rotates to

$$S_E[A] = \int d^4x\, \left[\frac{1}{2}(F^a_{0i})^2 + \frac{1}{4}(F^a_{ij})^2\right] = \int d^4x \frac{1}{4}(F^a_{\mu\nu})^2, \tag{3.24}$$

since $iS \to -S_E$ (recall equation 3.8). Hence, the Wick-rotated Lagrangian is given by

$$\mathcal{L} = \frac{1}{2}\,\mathrm{Tr}(\boldsymbol{F}_{\mu\nu}\boldsymbol{F}_{\mu\nu}), \tag{3.25}$$

which is similar to the original Lagrangian, equation 3.15, except for the Euclidean index contractions rather than Minkowski ones (recall that $dx^2_\mu = dx^2_0 + dx^2_i$).

With the Wick rotation completed, we have turned our (3+1) dimensional theory into a 4 dimensional one, i.e. with fields defined throughout $\mathbb{R}^4$.

3.2.3 Scale-Invariance of the Pure Yang-Mills Theories

A pure Yang-Mills theory's Lagrangian is entire scale-invariant. That is, it is left unchanged by a proper rescaling of the coordinates and fields:

$$x_\mu \to \lambda x_\mu \quad \text{and} \quad \boldsymbol{A}^{\text{inst}}_\mu(x) \to \lambda \boldsymbol{A}^{\text{inst}}_\mu(\lambda x). \tag{3.26}$$

This has two important consequences.

Firstly, any instanton solution $\boldsymbol{A}_\mu^{\text{inst}}(x)$ that we will find will have some free parameter that indicates its "size" (i.e. the spatial extend over which the fields are approximately non-trivial). This is because any rescaling of the solution will be a new instanton. Changing the free parameter will rescale the fields.

Secondly, it means that Derrick's theorem (see section 2.4) does not preclude the BPST-instanton's existence. In the theories where a soliton is prevented, the theorem works as proof by contradiction: There cannot be any solitons, since there always exists a scale transformation that lowers the potential energy of any suspected soliton (in pure Yang-Mills, the theorem refers to a trial instanton and its Euclidean action). Because Yang-Mills is scale invariant, S_E does not change under any rescaling.

The double well problem (section 3.1.2) demonstrated what is usually said about instantons: They tunnel through potential energy barriers between vacua. In pure Yang-Mills theories, this story is slightly different. Since pure Yang-Mills theories are length scale-invariant, they are also energy scale invariant. This means that there is no particular energy scale set by theory for process, including tunneling. In particular, there is no energy scale for the height of the barriers between the vacua. Any particular instanton does have a size (set by that free parameter we just mentioned) and does tunnel through a particular barrier (the height being its potential energy at its center in Euclidean time), but a rescaling will change both. A large instanton will traverse a small barrier and a small instanton a large one[30, p.460][33, p.281]. When the scale invariance is explicitly broken by, for instance, the inclusion of a new field, then this story stops being true. The instanton action might become scale dependent. Therefore, one needs to consider whether scaling arguments, like Derrick's theorem, do not start to rule out their existence.

3.2.4 The Topology of C_{S_E}

In this section we will demonstrate that $\Pi_0(C_{S_E}) = \mathbb{Z}$, hence that C_{S_E} is made out of a countably infinite number disconnected components. We will find an expression for the topological charge (i.e. winding number) that can be used to determine to which sector any particular finite S_E configuration belongs. This charge is determined, once again, by the asymptotics of the fields. In the next section, we will show that each of these disconnected component has an instanton. This topological charge can be used to characterize each them.

Let the distance to the origin of $\mathbb{R}^4$ be ρ, that is $\rho^2 = x_0^2 + x_i^2$. Then, for any field configuration to have finite S_E, it needs to approach asymptotically, that is as $\rho \to \infty$, a configuration such that $\boldsymbol{F}_{\mu\nu} \to 0$, see equation 3.24. In other words, $\boldsymbol{F}_{\mu\nu}$ must vanish at each point Ω of the "boundary" of Euclidean spacetime $\partial\mathbb{R}^4$. With this boundary we mean that $\boldsymbol{A}_\mu$ is only a function of the angular variables Ω describing the direction towards which the point $\rho = \infty$ was approached, recall the discussion in section 2.3 . Since we consider $\mathbb{R}^4$, the points on this boundary Ω make up the continuous space $\partial\mathbb{R}^4 \cong S^3$. Not just $\boldsymbol{A}_\mu = 0$, but any *pure gauge* configuration

$$\boldsymbol{A}_\mu(x) \xrightarrow{\rho\to\infty} \frac{i}{g} U^{-1}(\Omega)\partial_\mu U(\Omega), \tag{3.27}$$

makes $\boldsymbol{F}_{\mu\nu}$ vanish asymptotically. As was true for solitons, C_{S_E} inherits its topology from

the space of these mappings U:

$$C_{S_E} \cong \text{Maps}(\partial\mathbb{R}^4 \to SU(2)) \tag{3.28}$$

Since the parameter space of $SU(2)$ is also an S^3, $U(\Omega)$ is a mapping from $S^3 \to S^3$. These cannot all be continuously connected to each other: $\Pi_0(C_{S_E}) \cong \Pi_3(S^3) \cong \mathbb{Z}$. C_{S_E} is made out of a countably infinite number of disconnected components, like C_V was for the Georgi-Glashow model, recall section 2.3.3.

An expression for the topological charge in terms of the mapping U is given by

$$Q[U] = \frac{1}{24\pi^2} \int d\sigma_\mu \epsilon_{\mu\nu\rho\sigma} \,\text{Tr}\left(U^{-1}(\partial_\nu U)U^{-1}(\partial_\rho U)U^{-1}(\partial_\sigma U)\right), \tag{3.29}$$

where $d\sigma_\mu$ is the (outward pointing) oriented surface integral over this boundary. Alternatively, it is also possible to calculate the winding number of the solution from $\boldsymbol{F}_{\mu\nu}$ throughout $\mathbb{R}^4$:

$$Q[F] = -\frac{g^2}{16\pi^2} \int d^4x \,\text{Tr}(\boldsymbol{F}_{\mu\nu}\tilde{\boldsymbol{F}}_{\mu\nu}), \tag{3.30}$$

where $\tilde{\boldsymbol{F}}_{\mu\nu} = \frac{1}{2}\epsilon_{\mu\nu\rho\sigma}\boldsymbol{F}_{\rho\sigma}$ is the so-called dual of $\boldsymbol{F}_{\mu\nu}$.

To see why these two expressions agree, construct the following *gauge dependent* current:

$$K_\mu = 4\epsilon_{\mu\nu\rho\sigma} \,\text{Tr}\left(\boldsymbol{A}_\nu \partial_\rho \boldsymbol{A}_\sigma - \frac{2}{3} ig \boldsymbol{A}_\nu \boldsymbol{A}_\rho \boldsymbol{A}_\sigma\right), \tag{3.31}$$

whose divergence is related to the field strength tensor $\partial_\mu K_\mu = 2\,\text{Tr}(\boldsymbol{F}_{\mu\nu}\tilde{\boldsymbol{F}}_{\mu\nu})$. Using this property we deduce that

$$\int d^4x \,\text{Tr}(\boldsymbol{F}_{\mu\nu}\tilde{\boldsymbol{F}}_{\mu\nu}) = \frac{1}{2}\int d^4x \,\partial_\mu K_\mu = \frac{1}{2}\int d\sigma_\mu \lim_{\rho\to\infty} K_\mu, \tag{3.32}$$

where the last equality follows from Stokes's theorem. What remains to be shown is whether $\lim_{\rho\to\infty} K_\mu$ is indeed the integrand of equation equation 3.29. To see that it is indeed the same, realize that the first term in the definition of K_μ does not contribute to the surface integral: Since the action must be finite, see equation 3.24, $\boldsymbol{F}_{\mu\nu}$ must vanish *faster* than ρ^{-2}. Since $\partial_\rho \boldsymbol{A}_\sigma$ is a term inside $\boldsymbol{F}_{\mu\nu}$, it must do the same. Furthermore, since $\boldsymbol{F}_{\mu\nu}$ contains a term that is a product of two $\boldsymbol{A}_\mu$, $\boldsymbol{A}_\mu$ must vanishes faster than ρ^{-1}. We know that $d\sigma_\mu \cong \rho^3 d\Omega$. Therefore, the first term in the integrand vanishes fast enough not to contribute to the surface integral. Since only the second term survives and since the gauge fields at infinity are given by equation 3.27, we deduce that $\lim_{\rho\to\infty} K_\mu$ is given by

$$\lim_{\rho\to\infty} K_\mu = -\frac{4}{3g^2}\epsilon_{\mu\nu\rho\sigma} \,\text{Tr}\left(U^{-1}(\partial_\nu U)U^{-1}(\partial_\rho U)U^{-1}(\partial_\sigma U)\right), \tag{3.33}$$

which is what we still needed to show that equation 3.30 is indeed correct.

3.2.5 Constructing the BPST-Instanton

Now that we have shown that C_{S_E} consists of countably infinite number of disjoint components and that within each sector instantons are not prevented by Derrick's theorem, we can go ahead and look for the instantons themselves. We will not be required to solve the Euclidean equations of motion directly. Instead, these instantons can be found to satisfy the simple relation

$$\boldsymbol{F}_{\mu\nu} = \pm\tilde{\boldsymbol{F}}_{\mu\nu}. \tag{3.34}$$

To see why, we begin with the seemingly trivial identity:

$$\int d^4x \,\mathrm{Tr}\left((\boldsymbol{F}_{\mu\nu} \pm \tilde{\boldsymbol{F}}_{\mu\nu})^2\right) \geq 0. \tag{3.35}$$

Since $(\boldsymbol{F}_{\mu\nu} \pm \tilde{\boldsymbol{F}}_{\mu\nu})^2 = 2(\boldsymbol{F}_{\mu\nu}\boldsymbol{F}_{\mu\nu} \pm \boldsymbol{F}_{\mu\nu}\tilde{\boldsymbol{F}}_{\mu\nu})$, we can conclude that

$$S_E = \frac{1}{2}\int d^4x \,\mathrm{Tr}(\boldsymbol{F}_{\mu\nu}\boldsymbol{F}_{\mu\nu}) \geq \frac{1}{2}\left|\int d^4x \,\mathrm{Tr}(\boldsymbol{F}_{\mu\nu}\tilde{\boldsymbol{F}}_{\mu\nu})\right| = \frac{8\pi^2|Q|}{g^2}, \tag{3.36}$$

which is known as the Bogomol'nyi bound. It is an inequality for S_E which holds within each individual disconnected component of C_{S_E} (the inequality depends on that sector's particular Q). Suppose that we move around within that sector (assuming $Q \neq 0$), then if the action is ever to attain its minimum value $S_E = \frac{8\pi^2|Q|}{g^2}$, we must have found that sector's configuration of minimal S_E, i.e. its instanton with topological charge Q. Since this inequality followed from equation 3.35, this equality is saturated when $\boldsymbol{F}_{\mu\nu} = \pm\tilde{\boldsymbol{F}}_{\mu\nu}$.

Based on an ansatz[33, ch.13 §2] one can find the aforementioned BPST-instanton ($Q = 1$). Its configuration is given by

$$\boldsymbol{A}_\mu^{\mathrm{BPST}}(x) = \frac{i}{g}\left(\frac{\rho^2}{\rho^2+\lambda^2}\right)U^{-1}(x)\partial_\mu U(x) \quad \text{where} \quad U(x) = \frac{x_0 + i\vec{\tau}\cdot\vec{x}}{\rho}. \tag{3.37}$$

Alternatively, its time and space components are separately given by

$$\boldsymbol{A}_0^{\mathrm{BPST}}(x) = \frac{1}{g}\frac{\vec{\tau}\cdot\vec{x}}{\rho^2+\lambda^2}, \quad \boldsymbol{A}_i^{\mathrm{BPST}}(x) = \frac{1}{g}\frac{-\tau_i x_0 + (\vec{\tau}\times\vec{x})_i}{\rho^2+\lambda^2}. \tag{3.38}$$

On the boundary $\boldsymbol{A}_\mu(x)$ tends to $U^{-1}(x)\partial_\mu U(x)$ which in the limit only depends on $\frac{x_\mu}{\rho}$. In other words $U(x)$ becomes a mapping depending only on the direction towards which we approach the boundary $\partial\mathbb{R}^4$. One can check using equation 3.29 that $Q[U] = 1$ as we desired. The free parameter λ is the scale paramater we discussed in section 3.2.3, which determines the spatial extend of the instanton.

3.3 Instantons and the Vacuum Structure of Yang-Mills

In the previous section we have presented the BPST-instanton in the pure $SU(2)$ Yang-Mills theory, but the configuration does not look like what we expect. As we have claimed in the introduction and then demonstrated when discussing the double well problem: An

instanton is supposed to look like an event in imaginary time, it has to be a configuration that connects classical vacua between $x_0 = \tau = \pm\infty$. However, because we have not fixed the gauge and determined the classical vacuum structure of the theory, this is currently not possible.

Moreover, we have not spoken about the resulting quantum picture (the quantum theoretic vacuum structure) that this classical picture (the classical vacuum structure) implies (upon quantization). In the double well problem, this was straightforward: there were two classical vacua $\pm a$ and two approximate ground states $|\pm a\rangle$ from which the true vacuum $|\Omega\rangle$ was built. As it turns out, because Yang-Mills is a gauge theory, there is some subtlety involved with the resulting quantum picture. In general, configurations related by gauge transformations, that is gauge equivalent configurations, are considered physically the same: they should be identified. However, some care needs to be taken when applying this idea to large gauge transformations (we will explain these in a moment) that appear when fixing the gauge in specific ways.

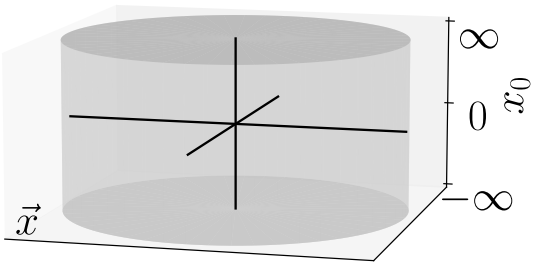

Figure 3.3: Schematic depiction of $\mathbb{R}^4$ (and its boundary $\partial\mathbb{R}^4$) as a cylinder. It is used to picture the Yang-Mills instantons as tunneling events: As configurations connecting the initial pure gauge vacuum on the cylinder's bottom lid to another on the top. Circular horizontal slices are all points of space $\mathbb{R}^3$ at individual moments of imaginary time x_0.

3.3.1 The Supplemented Temporal Gauge: Instantons and Classical Vacuum Structure

In this section we determine the classical vacuum structure of the theory by working in the temporal gauge $\boldsymbol{A}_0 = 0$. We will also impose a subsidiary gauge fixing condition motivated by Hamiltonian quantization, this is what the "supplemented" refers too. This gauge gives the BPST-instanton the desired event structure. Our choice of gauge is not arbitrary, the temporal gauge is the *traditional gauge* used to study this instanton. The procedure can be found in a variety of sources[11, ch.16 §2][33, ch.13], which have been used for this section. In the next section, we give this classical picture its quantum mechanical interpretation.

Working in the temporal gauge requires us to impose $\boldsymbol{A}_0 = 0$ everywhere on $\mathbb{R}^4$. The remaining gauge transformations must then be time-independent $U(\vec{x})$. A classical vacuum is a configuration for which $\boldsymbol{F}_{\mu\nu} = 0$, they are *pure gauges*. Since only time-independent gauge transformations remain, any vacuum configuration will, at the very least, be a pure

gauge of the form

$$\boldsymbol{A}_i^{\text{vac.}}(\vec{x}) = \frac{i}{g} U^{-1}(\vec{x}) \partial_\mu U(\vec{x}). \tag{3.39}$$

This is not yet the whole story of the classical vacuum structure. At this point, all vacua can still be continuously connected by gauge transformations and should therefore be identified.

To deduce the classical vacuum structure of the theory and to turn the BPST-instanton into an event, we picture $\mathbb{R}^4$ as well as its boundary $\partial\mathbb{R}^4$ as the inside and surface of a "cylinder" respectively, see figure 3.3. Taking imaginary time slices through the cylinder gives us all of space $\mathbb{R}^3$ at different moments x_0. The instanton will live on the inside, taking us from one initial vacuum on the bottom lid to another final vacuum on the top lid, both of the form of equation 3.39. We already know from section 3.2.4 that the fields on the bottom and top lid, as well as the sides, must be pure gauges $U(\Omega)$, which has been required for S_E to converge.

To determine the classical vacuum structure we need to characterize which classical vacua on the top and bottom lids can be connected by an instanton in between. Let us, for convenience, choose the vacuum on the bottom to be $\boldsymbol{A}_\mu = 0$. We can do so by exploiting the remaining gauge freedom to fix $\boldsymbol{A}_i = 0$ at $x_0 = -\infty$. The question then becomes which classes of vacua can be tunneled into on the top. Note that $\boldsymbol{A}_\mu = 0$ is the vacuum corresponding to $U(\vec{x}) = \mathbb{1}$, which is the required pure gauge configuration on the bottom lid.

In determining the classical vacuum structure, we need to be more precise about the pure gauge configuration occurring on the sides of the cylinder (that is, the boundaries of space $\partial\mathbb{R}^3$ at all x_0). Because the barrier through which the instanton tunnels is finite in height for any particular instanton, the field configuration at any imaginary time slice x_0 is some configuration of finite potential energy

$$V[\boldsymbol{A}] = \frac{1}{2} \operatorname{Tr}[\boldsymbol{F}_{ij} \boldsymbol{F}_{ij}]. \tag{3.40}$$

This means, in particular, that the fields on the sides of the cylinder are required to have $\boldsymbol{F}_{\mu\nu} = 0$ for $V[\boldsymbol{A}]$ converge. Therefore $\boldsymbol{F}_{0i} = \partial_0 \boldsymbol{A}_i = 0$ on the sides: The asymptotics of the fields cannot evolve over x_0.

For now, we need to make sure U approaches a constant value on the boundary. We choose to set

$$\lim_{|\vec{x}| \to \infty} U(\vec{x}) \to \mathbb{1} \quad \text{for all } x_0 \tag{3.41}$$

as an additional gauge condition. This condition is motivated by the Hamiltonian formulation of the theory, which we will get to discuss. Equation 3.41 has effectively compactified all of space $\mathbb{R}^3$ at each slice into an S^3. In particular, this equation holds for the vacuum on the top lid. Let us refer to the temporal gauge with this additional constrained the *supplemented temporal gauge*.

Now we know precisely which vacua can be accessed by an instanton and how to characterize them: The gauge function $U(\vec{x})$ that specifies a vacuum on the top of the cylinder is therefore actually a map from $S^3 \to SU(2) \cong S^3$, those can not all be continuously connected: $\Pi_3(S^3) = \mathbb{Z}$. *The classical vacuum structure is therefore periodic: it consists of a*

countably infinite number of homotopy classes of vacua characterized by a winding number depending on $U(\vec{x})$, i.e. they are vacua that are topologically distinct. Vacua within a class are gauge equivalent and therefore identified.

These classes of vacua are referred to as *Chern-Simons vacua*, since the winding number of the map is the so-called *Chern-Simons number* N_{CS}: a property of the gauge fields in the supplemented temporal gauge. When $\boldsymbol{A}_\mu$ described a vacuum, then N_{CS} can be computed in terms of $U(\vec{x})$,

$$N_{\mathrm{CS}}[\boldsymbol{A}] = -\frac{1}{24\pi^2}\int d^3x \epsilon_{ijk}\,\mathrm{Tr}(U^{-1}(\partial_i U)U^{-1}(\partial_j U)U^{-1}(\partial_k U)). \tag{3.42}$$

A example of a vacuum with $N_{\mathrm{CS}} = 1$ is given by the gauge function

$$U(\vec{x}) = \exp\left[\frac{i\pi\vec{\tau}\cdot\vec{x}}{\sqrt{r^2+\lambda^2}}\right] \tag{3.43}$$

through equation 3.39. The vacuum on the bottom of the cylinder, $\boldsymbol{A}_\mu = 0$ has $N_{\mathrm{CS}} = 0$.

Now that we know the vacuum structure, we can stop keeping $\boldsymbol{A}_i = 0$ on the bottom of the cylinder. As it turns out, the instanton in each sector of C_{S_E} can connect multiple CS-vacua together, not just $\boldsymbol{A}_\mu = 0$ to another. As an example, consider the BPST-instanton itself, which we still wanted to turn into an event. It still has to be put in the supplemented temporal gauge, which is achieved by applying the gauge transformation

$$U'(x) = \exp\left[\frac{i\vec{\tau}\cdot\vec{x}}{\sqrt{r^2+\lambda^2}}\left(\tan^{-1}\left(\frac{x_0}{\sqrt{r^2+\lambda^2}}\right)+\left(n+\frac{1}{2}\right)\pi\right)\right] \tag{3.44}$$

to the components of $\boldsymbol{A}_\mu^{\mathrm{BPST}}$ from equation 3.38, according to equation 3.20. The final and initial vacua between which the BPST-instanton tunnels $\boldsymbol{A}_\pm^{\mathrm{vac.}}$ become

$$\begin{aligned}\boldsymbol{A}_\pm^{\mathrm{vac.}}(x) &= \lim_{x_0=\tau\to\pm\infty} U'^{-1}(x)\boldsymbol{A}_i^{\mathrm{BPST}}(x)U'(x) + \frac{i}{g}U'^{-1}(x)\partial_i V(x)\\ &= \lim_{x_0=\tau\to\pm\infty}\frac{i}{g}U'^{-1}(x)\partial_i U'(x)\end{aligned} \tag{3.45}$$

respectively, where only the pure gauge part due to U' remains.

$$\lim_{x_0=\tau\to+\infty} U'(x) = \exp\left[i\pi\frac{\vec{\tau}\cdot\vec{x}}{\sqrt{r^2+\lambda^2}}(n+1)\right] \quad \text{and} \tag{3.46}$$

$$\lim_{x_0=\tau\to-\infty} U'(x) = \exp\left[i\pi\frac{\vec{\tau}\cdot\vec{x}}{\sqrt{r^2+\lambda^2}}n\right], \tag{3.47}$$

which, according to equation 3.42, define vacua with $N_{\mathrm{CS}} = n+1$ and $N_{\mathrm{CS}} = n$ respectively.

That $\Delta N_{\mathrm{CS}} = (n+1) - n = 1$, given that $Q[\boldsymbol{A}_\mu^{\mathrm{BPST}}] = 1$, is no coincidence: As it turns out $Q = \Delta N_{\mathrm{CS}}$ for all instantons in the pure Yang-Mills theory. To see why, let us compute Q from equation 3.29 for an instanton in the supplemented temporal gauge. For that, we must perform an integral over $\partial\mathbb{R}^4$, that is, the outside of the cylinder C. Since the $U = \mathbb{1}$ on the sides, only the top T and bottom B contribute. On the bottom $d\sigma_\mu\,\epsilon_{\mu\nu\rho\sigma} =$

$d^3x\ -n_\mu\epsilon_{\mu\nu\rho\sigma} = -d^3x\,\epsilon_{0ijk}$, given the "upwards" pointing normal vector $n_\mu = (1,0,0,0)$, while on the top $d\sigma_\mu\,\epsilon_{\mu\nu\rho\sigma} = d^3x\,\epsilon_{0ijk}$.

$$\begin{aligned} Q[\boldsymbol{A}^{inst}] &= \frac{1}{24\pi^2}\int_C d\sigma_\mu\epsilon_{\mu\nu\rho\sigma}\,\mathrm{Tr}\left(U^{-1}(\partial_\nu U)U^{-1}(\partial_\rho U)U^{-1}(\partial_\sigma U)\right) \\ &= \frac{1}{24\pi^2}\left(\int_T d^3x\,\epsilon_{0ijk} - \int_B d^3x\,\epsilon_{0ijk}\right)d\sigma_\mu\,\mathrm{Tr}\left(U^{-1}(\partial_i U)U^{-1}(\partial_j U)U^{-1}(\partial_k U)\right) \\ &= N_{\mathrm{CS}}[A_+^{\mathrm{vac.}}] - N_{\mathrm{CS}}[A_-^{\mathrm{vac.}}] = \Delta N_{\mathrm{CS}}, \end{aligned} \tag{3.48}$$

where we used the fact that $\epsilon_{0ijk} = \epsilon_{ijk}$. Hence, $Q = \Delta N_{\mathrm{CS}}$.

Before discussing the quantum picture of these vacua, let us emphasize the following: Consider two CS-vacua, say defined by $U_1(\vec{x})$ and $U_2(\vec{x})$ through equation 3.39. Vacua with different N_{CS} cannot be continuously deformed into each other because of equation 3.41, that is, as long as the fields are tied up as $|\vec{x}| \to \infty$. If, on the other hand, they have the same arbitrary N_{CS}, then there exists a *small time-independent gauge transformation* $\tilde{U}(\vec{x})$ that connects them. $\tilde{U}$ being small means that it is continuously connected to $U = \mathbb{1}$, the trivial gauge transformation. By construction, small time-independent gauge transformations always satisfy equation 3.41. Because $\tilde{U}$ is connected to $U = \mathbb{1}$, if $\tilde{U}$ would itself be used to define a vacuum, then it would have $N_{\mathrm{CS}} = 0$. Note however that vacua with different N_{CS} *are connected* by gauge transformations: They are instead *large time-independent gauge transformations*, like the one which defined the vacuum with $N_{\mathrm{CS}} = 1$ (equation 3.43). In other words, the expression for N_{CS} can be used to label vacua themselves, but also to count the windings of the large gauge transformations that map between them.

3.3.2 The Quantum Theoretic Vacuum Structure of Yang-Mills

We will now present two quantum pictures of the vacuum of the $SU(2)$ Yang-Mills theory. As we will see, these two views ultimately agree on the physics: For any pure Yang-Mills theory, the true physics is determined by so-called vacuum angle θ, which shows up in instanton corrections to various quantities, including Green's functions and the vacuum energy[33, App.2].

We begin with the conventional textbook view[11, ch.16 §2][33, ch.13 §2][20][34], which agrees with the original interpretation found in the paper by Jackiw and Rebbi[22] and in the paper by Callen, Dashen and Gross[9]. It consists of analyzing the theory's quantum theoretic vacuum structure using (canonical) Hamiltonian quantization in the temporal gauge $\boldsymbol{A}_0 = 0$. To summarize, this is an incomplete gauge fixing where *small time-independent gauge transformations* remain. Classically, systems which have gauge freedom (remaining) are *constrained Hamiltonian systems*. This remaining gauge freedom is generated, after quantization, by the Noether charge of these small tine-independent gauge transformations: This charge turns out to be Gauss's law. States related by gauge transformations must be identified, this makes the preceding discussion of the classical vacuum structure in the supplemented temporal gauge relevant: Each homotopy class of CS-vacua given by $N_{\mathrm{CS}} = n$ (whose elements are related by the remaining small tine-independent gauge transformations) must obtain its own approximate vacuum state $|n\rangle$ (called an n-vacuum). According to this view, the resulting quantum theoretic vacuum structure is analogous to that of the

"quantum mechanical particle in a periodic potential": The true vacuum state $|\theta\rangle$ (called the θ-vacuum) will be a superposition of all these n-vacua.

Afterwards, we will present an alternative view on the quantum theoretic vacuum structure which, according to Rubakov[33, p.277], originated from Manton's original paper on the EW sphaleron[28]. In that paper, the sphaleron was derived in a physical gauge. This means that the gauge fields $\boldsymbol{A}_\mu$ are uniquely determined by $\boldsymbol{F}_{\mu\nu}$[7]. This does not mean that $\boldsymbol{A}_0 = 0$ cannot be part of such a gauge. In the EW sphaleron derivation Manton uses the the radial gauge $n^i \boldsymbol{A}_i = 0$ (an example of an axial gauge) together with $\boldsymbol{A}_0 = 0$ *without* imposing the supplementary condition of equation 3.41. This appears to be over-fixing the gauge, but since the sphaleron is a static configuration traversed at some moment in time we can always make sure that $\boldsymbol{A}_0 = 0$ is satisfied at the sphaleron point in addition to imposing the radial gauge condition globally or vice versa. As Manton points out in that paper, a switch between the views can be realized by letting go of $\boldsymbol{A}_r = 0$ while imposing the aforementioned subsidiary boundary condition. In these gauges, there is a *single unique classical vacuum*[33, p.277]. Hence, upon quantization there is only a single vacuum state $|\Omega\rangle$. To cast the traditional view in terms of the new one, the classical CS-vacua and their states $|n\rangle$ must henceforth be identified. This means identifying states related by large gauge transformations, ones that, according to Hamiltonian quantization are not supposed to be identified: This is, ultimately, the central disagreement between the views[20]. Upon identification, the quantum theoretic vacuum structure appears analogous to the so-called "quantum mechanical pendulum"[33, p.278][28][20][3][7][34]. By inclusion of a new θ-dependent term in the original Lagrangian, the equivalence of the views can be established: $|\Omega\rangle$ obtains the same θ-dependent instanton corrections as $|\theta\rangle$ had.

Because the classical vacuum structure differs between the supplemented temporal and physical gauges, instantons appear different as well. In the prior gauge, instantons tunnel between n-vacua, while in physical gauges, they tunnel between $|\Omega\rangle$ and itself along an NCL in C_{S_E}. Let us now discuss these two views in more detail.

3.3.3 Gauss's Law, Gauge Fixing and Hamiltonian Quantization

Consider the theory of free electromagnetism, for which $\mathcal{L}(A, \partial A) = -\frac{1}{4}\int d^3x\, F_{\mu\nu}F^{\mu\nu}$. The Euler-Lagrange equations $\partial_\mu F^{\mu\nu} = 0$, in addition to equations of motion, contain a famous constraint equation called Gauss's law[4]:

$$G = -\partial_i F^{i0} = -\partial_i(\partial^i A^0 - \partial^0 A^i) = -\partial_i E^i = 0. \tag{3.49}$$

Free electromagnetism is a gauge theory, so as long an any gauge freedom remains, there is no unique way of time evolving any particular set of initial conditions forward: For any solution of the equations of motion there is another a gauge transformation away. Gauge fixing is thus required. One way, for instance, to classically deal with Gauss's law is to choose to work in the temporal gauge $A_0 = 0$. Gauss's law is then no longer needed dynamically: Once the initial conditions satisfy Gauss's law, it is automatically satisfied for all time [33, ch.4 §2].

[4]This is a constraint equation because it relates single time derivatives of the fields (except for A_0, whose time derivative do not appear at all).

As it turns out, there is an important relation between Gauss's law and gauge freedom that becomes evident in the Hamiltonian formulation of the above Lagrangian system[34][7].

Gauss's Law in the Hamiltonian Formalism

A Hamiltonian supposedly generates some unique time evolution. Therefore, as long as there is some gauge freedom remaining (and hence the aforementioned ambiguity in time evolution is present), there is no unique Hamiltonian. In particular, the canonical momenta are not independent[34]. This makes a gauge field theory a *constraint Hamiltonian system*. This shows up in the Legendre transform required to produce the Hamiltonian: The transform between the positions / velocities and the canonical positions / momenta is not invertible[34]. Instead, additional Lagrange multiplier terms involving the dependent canonical momenta must be added to the Hamiltonian to pick out a unique dynamics (i.e. to fix the gauge freedom). The canonical momenta π^μ are found by taking a functional derivative w.r.t. to the canonical positions A_μ,

$$\pi^\mu = \frac{\partial \mathcal{L}}{\partial_0 A_\mu} = F^{\mu 0}, \tag{3.50}$$

which tells us that $\pi^i = E^i$ and $\pi^0 = 0$. This is one of these constraints, telling us that A_0 is not really a dynamical variable (there was no velocity $\partial_0 A_0$ anywhere in $\mathcal{L}$). The Hamiltonian

$$\begin{aligned} H &= \int d^3x \, [\pi^\mu \partial_0 A_\mu - \mathcal{L}] + \int d^3x \lambda \pi^0 \\ &= \int d^3x \, \left[E^i (E^i - \partial_i A_0) + \frac{1}{2}(E^i E^i - B^i B^i) \right] + \int d^3x \lambda \pi^0 \\ &= \int d^3x \, \left[\frac{1}{2}(E^i E^i + B^i B^i) + A_0 (\partial_i E^i) \right] + \int d^3x \lambda \pi^0, \end{aligned} \tag{3.51}$$

where $B_i = -\frac{1}{2}\epsilon_{ijk} F^{ij}$. Therefore, in additional to the previous constraint, free electromagnetism contains an additional constraint containing Gauss's law, $\int d^3x \, A_0 (\partial_i E^i)$, for which A_0 is the Lagrange multiplier field.

Working in the temporal gauge $A_0 = 0$ (where A_i and E_i are the canonical variables) uses up the gauge freedom allowed by the momentum constraint[34]. Gauss's law also seems to disappear (its term in the Hamiltonian vanishes), but the freedom generated by the constraint is retained, which are small time-independent gauge transformations. Working in the temporal gauge means working in the supplemented temporal gauge when considering this Hamiltonian system. Gauss's law is the charge associated with this symmetry: Given a gauge function $U = e^{i\alpha}$ that generates such a gauge transformation ($\lim_{|\vec{x}|\to\infty} \alpha(\vec{x}) = \text{const.}$), $A_i \to A_i - \frac{1}{g}\partial_i \alpha$. Therefore its charge

$$\begin{aligned} Q &= \int d^3x \, j^0 = \int d^3x \, \pi^i \delta A_i \\ &= -\frac{1}{g} \int d^3x \, E^i \partial_i \alpha = -\frac{1}{g} \int d^3x \, (\partial_i E^i) \alpha, \end{aligned} \tag{3.52}$$

where the last step's integration by parts was made possible by α's gauge transformation being small. In analogy with free electromagnetism, this is why we imposed the condition equation 3.41 in the pure Yang-Mills theory, it was in anticipation of using Hamiltonian mechanics to analyze the theory. In particular, this constant that α approaches as $|\vec{x}| \to \pm\infty$ can be chosen[34] to be $U = \mathbb{1}$.

Gauss's law in Quantum Field Theory

These observations are important when canonically quantizing this system in the (thus supplemented) temporal gauge. It is this Hamiltonian when quantized that has its remaining small time-independent gauge freedom generated by exponentiating the Gauss's law charge in operator form. In field theory, we use Gauss's law in this form to directly define which states are physical[33, p.265][34][12, p.291], rather than using it to constrain initial conditions as opposed to the classical field theory:

$$G\,|\Psi\rangle_{\text{phys.}} = 0. \tag{3.53}$$

This is the same idea as in the Gupta-Bleuler quantization of free electromagnetism: First constructing a Hilbert space that is too large (because $A_0 = 0$ is an incomplete gauge fixing) and then subsequently reducing it by picking out physical states. Non-physical states, on the other hand, can evolve however they want[34]. Since Gauss's law generates small time-independent *gauge* transformations, *states* that can be connected by exponentiating G are considered physically equivalent, hence identified.

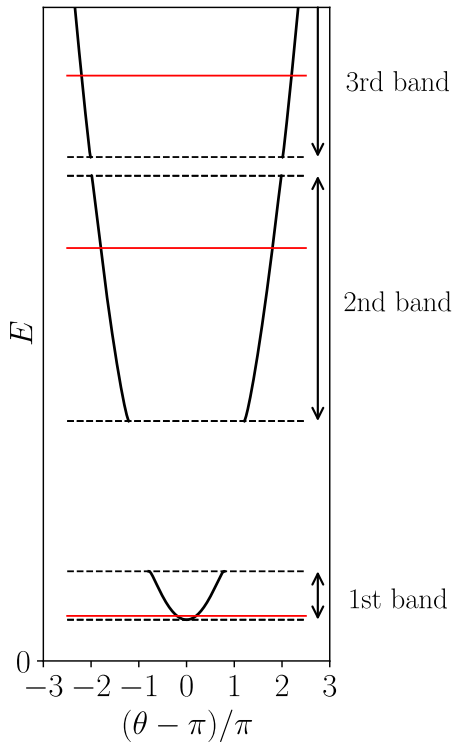

Figure 3.4: Band structure of the periodic potential, θ is extended beyond its first Brillouin zone. The red levels are a θ-sector. (E expansion taken from NIST Digital Library of Mathematical Functions §28)

A similar story goes on with electromagnetism's non-Abelian sister, the pure Yang-Mills theory. From this point of view large gauge transformations are not taken to connect physically equivalent states: Only the homotopy class of CS-vacua with the same N_{CS} should be identified. The theory must thus have a countably infinite number of approximate vacuum states $|n\rangle$ with tunneling between them. Out of these we will need to build the true vacuum state, which turns out to be $|\theta\rangle$. The model's quantum theoretic vacuum structure is analogous to the quantum mechanical system of the "particle in the periodic potential", which we will discuss in the next section.

3.3.4 The Traditional Picture: The Particle in the Periodic Potential

Consider the problem of a quantum mechanical particle in a sinusoidal periodic potential with physically distinct minima. For instance, think of a single electron placed in some

infinitely large crystal where the nuclei are spaced some fixed distance apart. The minima are unique lattice sites, there is no need for (periodic) boundary conditions to be imposed on the electron's wave function. Let us, for convenience, space them a distance 2π apart and let us choose the barriers to have height q. The time-independent Schrödinger equation for this particular system, including its Hamiltonian H, is

$$i\hbar\frac{d}{dt}\psi = H\psi = \left(-\frac{d^2}{dx^2} + q(1-\cos(x))\right)\psi(x), \tag{3.54}$$

which goes by the name of the Mathieu equation ($\hbar$ and m have been set to 1). The classical vacuum structure of the problem are simply the set of minima $x_0 = 2\pi n$.

The spectrum of this theory is given in figure 3.4, it is made out of bands. In terms of wave functions, any state of such a system is the product of a plane wave term given by a pseudo-momentum $\theta \in [0, 2\pi]$ and a truly periodic wave function ϕ:

$$\psi_\theta(x) = e^{-i\theta\frac{x}{2\pi}}\,\phi(x), \quad \text{where} \quad \phi(x \pm 2\pi) = \phi(x), \tag{3.55}$$

they are referred to as *Bloch waves*. States within any particular band share the same ϕ, but have different θ. The structure is consequence of the commutation of the H and the translation operator T, $T\psi(x) = \psi(x - 2\pi)$, that moves the entire wave function 2π to the right. The states are simultaneous eigenstates of both operators, $e^{i\theta}$ being the eigenvalue of T for any particular state. Because T translates wave functions, θ measures the (negative of) the phase shift which the wave function picks up between neighboring wells: $\psi_\theta(x - 2\pi) = e^{i\theta}\psi_\theta(x)$.

To discuss the quantum mechanical vacuum structure, consider an approximate ground state wave function localized near the n-th well. Like the double well potential, there will be tunneling (hence instantons) between states like these. The true ground state will be a superposition of all them. Let us drop the wave function notation in favor of brakets and call these n-vacua $|n\rangle$. States $|\theta\rangle$ in the lowest band are of the form

$$|\theta\rangle = \sum_n e^{-in\theta}\,|n\rangle\,, \tag{3.56}$$

which a have pseudo-momentum θ: $T\,|\theta\rangle = e^{i\theta}\,|\theta\rangle$ since $T\,|n\rangle = |n+1\rangle$.

The Analogy for Pure Yang-Mills

It is this system to which the pure Yang-Mills theory is analogous in the traditional view[11, ch.16 §2][33, ch.13 §3][20][3][34]. The translation operator T is replaced by a large gauge transformation with $N_{\mathrm{CS}} = 1$, mapping the class of Chern-Simons vacua with $N_{\mathrm{CS}} = n$ into the class with $N_{\mathrm{CS}} = n + 1$. Each class has a single state $|n\rangle$, since the configurations amongst a class are identified. Moreover, each field state[5] has its own pseudo-momentum θ. The instantons tunnel between these $|n\rangle$ vacua, i.e. they help us compute transition

[5] Jackiw and Rebbi write down their states using Wave functionals $\Psi_\theta[\boldsymbol{A}]$, we instead continue using braket notation as employed in the book by Cheng and Li[11, p.486].

amplitudes of the form $\langle n| \exp(-iHt) |m\rangle$. The potential energy barriers through which they tunnel are given by the specific size of the instantons chosen.

Not just the bottom rung of the lowest band $|\theta = 0\rangle$, but the entire lowest band itself $|\theta\rangle$ can be considered to be made out of vacuum states in Yang-Mills. Such a claim is not made about an electron in a crystal: θ is indeed a conserved quantity, however, in quantum mechanics, that is simply an idealization. Not only is a real crystal not infinitely large, we could also, in theory, perform a position measurement x to change θ ($[T, x] \neq 0$). Such operation do not exist in Yang-Mills: All gauge-invariant operators O leave θ intact[33, p.277]. In other words, N_{CS} (to which x is the analogue) is not measurable[6]. Only ΔN_{CS} can be observed. The system is essentially a continuum of mutually non-interacting ladders specified by θ: $\langle\theta'| \exp(-iHt) |\theta\rangle \sim \delta(\theta - \theta')$. These ladders are referred to as *superselections sectors*. The lowest energy state in each of these ladders is the state $|\theta\rangle$, the lowest energy state amongst them all is $|\theta = 0\rangle$. If we would live in a pure Yang-Mills world, the question would be in which sector: θ is a true universal constant of the theory and most importantly a true physical quantity: matrix elements of operators such as O on $|\theta\rangle$ have θ-dependent instanton corrections / contributions of the form[33, p.277] $e^{i\theta} \langle n + 1| O |n\rangle \sim e^{-S_E[\boldsymbol{A}^{\text{BPST}}]}$.

The Consequences for the Path Integral

In this section we will compute the effect of sitting in a particular θ-sector for the path integral in the way it is presented in the Book by Cheng and Li[11, p.487]. It turns out that having $|\theta\rangle$ be the ground state changes the theory's Lagrangian.

As we have seen, the Yang-Mills theory can have any of many θ-vacua. Different $|\theta\rangle$ belong in different non-interacting sectors of the theory,

$$\langle\theta'| e^{-iHt} |\theta\rangle = \delta(\theta - \theta')I(\theta). \tag{3.57}$$

In terms of the n-vacua this means that

$$\langle\theta'| e^{-iHt} |\theta\rangle = \sum_{m,n} e^{im\theta'} e^{-in\theta} \langle m| e^{-iHt} |n\rangle \tag{3.58}$$

$$= \sum_{m,n} e^{-i(n-m)\theta} e^{im(\theta'-\theta)} \int [\mathcal{D}A]_{n-m} \, e^{-\frac{i}{\hbar}\int dx_0 \, d^3x \, \mathcal{L}}, \tag{3.59}$$

where we inserted the $|\theta\rangle$'s in terms of the n-vacua according to equation 3.56. $\int [\mathcal{D}A]_{n-m}$ denotes a path integral over only those configurations for which $N_{\text{CS}}[\boldsymbol{A}] = n - m$, as those are the only configurations able to connect these $|n\rangle$ and $|m\rangle$. Since, $\sum_m e^{im(\theta'-\theta)} = \delta(\theta - \theta')$ we conclude that

$$I(\theta) = \sum_{\nu} e^{-iQ\theta} \int [\mathcal{D}A]_{\nu} \, e^{-\frac{i}{\hbar}\int dx_0 \, d^3x \, \mathcal{L}}, \tag{3.60}$$

[6] For related reasons, the states $|n\rangle$ cannot be proper states for the gauge fields. They do not satisfy the so-called *cluster decomposition principle*[11, p.491]. That means that the expectation value of a product of widely separated operators does not vanish as their separation is increased: $\lim_{|x-y|\to\infty} \langle n| O^\dagger(x) O(y) |n\rangle \neq 0$.

where $Q = n - m$. We can absorb this winding number into the path integral by using equation 3.30 (in Minkowski space). We then get to see that

$$I(\theta) = \sum_{\nu} \int [\mathcal{D}A]_{\nu} \, e^{-\frac{i}{\hbar} \int dx_0 \, d^3x \, \mathcal{L}_{\text{eff}}}, \tag{3.61}$$

where the effective Lagrangian $\mathcal{L}_{\text{eff}}$ is given by

$$\mathcal{L}_{\text{eff}} = \mathcal{L} - \frac{\theta g^2}{16\pi^2} \operatorname{Tr}(\boldsymbol{F}_{\mu\nu} \tilde{\boldsymbol{F}}^{\mu\nu}). \tag{3.62}$$

This is the result of having a θ-vacuum: In the pure Yang-Mills theory the Lagrangian obtains a P and CP odd θ-term. In this model (or one with additional scalar fields) θ show up in various physical quantities because that term gets to violate the same symmetries.

With additional fermions the story gets more complicated, both the Lagrangian of QCD and EW sector of the SM contain a Yang-Mills component ($SU(3)$ and $SU(2)$ resectively). QCD inherits its quantum theoretic vacuum structure, including the vacuum angle θ, from the pure Yang-Mills theory wholesale. On the other hand, in the EW sector θ becomes unphysical. The fermions are responsible for this effect. The difference has to do with the anomalous global symmetries such a model obtains. We will discuss this topic in the next chapter, see section 5.1. Generally, the existence of mass or Yukawa terms is crucial in deducing the physicality of θ.

3.3.5 The Alternative Picture: The Quantum Mechanical Pendulum

In this section we discuss the aforementioned alternative view of the quantum theoretic vacuum structure of the pure Yang-Mills theory[33, p.277][28][20][3][7][34]. It is the view that turns the "particle in the periodic potential" picture into the one of the "quantum mechanical pendulum". The view has been motivated by working in physical gauges. In those gauges, the classical vacuum structure consists of only a single vacuum, for Yang-Mills theory this is $\boldsymbol{A}_{\mu} = 0$. Hence, there is also only a single vacuum state $|\Omega\rangle$.

Turning the Crystal into a Pendulum

Since we have already discussed "the particle in the periodic potential" point of view at length, there is no need for us to requantize the theory in a physical gauge. In physical gauges, there is only a singe classical vacuum. Hence, there is only a single vacuum state $|\Omega\rangle$. To compare the two views, we can simply identify the classical Chern-Simons vacua connected by large gauge transformations. Consequently, the corresponding states $|n\rangle$ will also be identified. The path between them becomes an NCL in C_{S_E}. In doing this, the "quantum mechanical pendulum" point of view pops out immediately.

In terms of the "particle in the periodic potential", this means identifying the classical vacua $2\pi n$. This compactifies the potential's domain (an analogy for C_{S_E}) from $x \in \mathbb{R}$ into $x \in [0, 2\pi] = S^1$. This constraint carries over into the states $\psi(x)$ as a boundary condition: $\psi(x + 2\pi) = \psi(x)$. This boundary condition identifies all the states $|n\rangle$.

The system we have now obtained is precisely the "quantum mechanical pendulum": The Hamiltonian from equation 3.54 supplemented by this boundary condition is a Hamiltonian for a mass on a rod of length q, rotating around in a gravitational potential (stuck to some xy-plane with $\hbar = m = G = 1$), see figure 3.5. Because of the identification, x is now interpreted as measuring the angle of the pendulum from the vertical. The compactification makes sure that the pendulum having rotated around its suspension point returns to the same classical vacuum.

Manton discusses the perturbative features of this problem in his original paper[28], If the rod is really long ($q \gg 1$) and the excitations from the vertical really small, then the system is approximately an harmonic oscillator (the Gaussian ground state $|\Omega\rangle$ is depicted in figure 3.5). One can treat the anharmonicity perturbatively in $q^{-\frac{1}{2}}$, but such a procedure does not converge. This is loosely attributed to ignoring the tunneling present in this model[28]. The instantons that tunneled between the n-vacua in the tradition view have not disappeared. Instead, they become events that connect the vacuum to itself: they have tunneled the pendulum over its pivot point, which is, most importantly, along an NCL. There will always be some instanton corrections to the ground state $|\Omega\rangle$: it needs to be tunneling invariant. The instantons in the pure Yang-Mills theory change their appearance in precisely the same way: In these physical gauges, they help compute the amplitude $\langle\Omega| \exp(-iHt) |\Omega\rangle$.

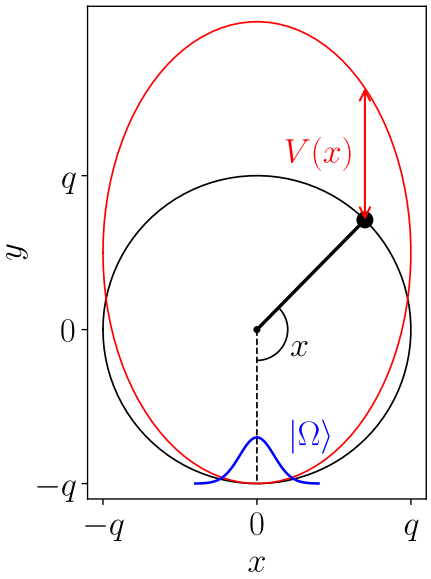

Figure 3.5: Pendulum and its potential including the ground state $|\Omega\rangle$ once quantized.

The original spectrum from figure 3.4 is no longer accurate. It would contain wave functions that are themselves not periodic in 2π: The boundary condition $\psi(x+2\pi) = \psi(x)$ holds for all states of the pendulum, not $\psi(x + 2\pi) = e^{i\theta}\psi(x)$. The superselection sector $\theta = 0$ is the Hilbert space of the pendulum, all the other states have become unphysical because we identified the minima. In particular, $|\Omega\rangle = |\theta = 0\rangle$.

The Vacuum Angle θ Survives

If only the $\theta = 0$ sector survives, one might rightfully wonder whether this means that the pure Yang-Mills theory cannot have a vacuum angle θ after all. As it turns out, it can. The two pictures must ultimately agree on the physics, because θ is physical / observable in the pure Yang-Mills theory.

Consider cloning the θ-term appearing the effective Lagrangian from equation 3.62 with a different angle, say θ', and adding it all the way back to our original Lagrangian[33, p.278][3][34] from equation 3.15. There is no problem in adding this new term, it does not modify the symmetries of the theory[7] or the equations of motion. It carries all the way

[7] At the very least, compared to the explicit C and CP odd term that exist when working in any non-zero

through back into the effective Lagrangian, changing $\theta \to \theta + \theta'$.

This term does something very special to the theory, it "mixes" the vacuum structure. *In the sector given by θ, instantons will now contribute a correction proportional to $e^{i(\theta+\theta')}$ rather then simply $e^{i\theta}$*. In other words, the instantons pick up an additional contribution θ' to the phase dynamically because of the new term. In particular, the state $|\theta = 0\rangle$, which is the vacuum state $|\Omega\rangle$ of the pendulum, now produces physics as if it has a vacuum angle θ', even though it satisfies the proper boundary condition. For instance, it now has the energy of the original state $|\theta'\rangle$ before adding the term, which is an energy larger than it used to have.

To conclude, manually adding an additional θ'-term rotates the physics of the states amongst themselves in each band. Most importantly, by setting $\theta' = \theta$ the pendulum mimics[8] the physics of the particular ladder / sector of the traditional crystal picture. The physics of either picture is therefore equivalent.

θ-sector.

[8]The new θ' term in the problem of the quantum mechanical pendulum resembles an Aharonov-Bohm term as if the pendulum was charged and swinging in a magnetic field perpendicular to the plane of rotation[34]. The instanton picks up a phase dynamically as it tunnels over and around the suspension point.

Chapter 4

Sphalerons: Saddle Point Configurations in Field Theory

In chapters 2 and 3 we concerned ourselves with solitons and instantons of various (Euclidean) field theories. In spite of their different physical contexts, both of them are critical point configurations that minimize their respective functionals V and S_E ($\delta V = 0$ or $\delta S_E = 0$). The origin of both configurations is topological: Keeping V or S_E finite breaks their configurations spaces C_V or C_{S_E} into disjoint components. Since both V and E are bounded from below (i.e. positive definite functionals), the existence of a minimum (i.e. solitons or instanton) in each sector disconnected from the vacuum is guaranteed as long as scaling argument do not preclude their existence.

In this chapter we concern ourselves with the so-called *sphalerons*[30, ch.11][33, ch.13 §4], another type of critical point of V: *saddle point configurations*. They were originally studied by Taubes[35] and also have a topological origin rooted, in this case, in Morse theory[27]. What intuitively distinguishes a saddle point from a minimum is clear: Solitons, as minima, are stable under all variations[1], while sphalerons have one or more specific variations, known as *negative modes*, that lower their energy; making them *unstable*. They are, however, still *static* if left unperturbed, since they are still critical point configurations[2]. Figure 4.1 shows a sketch of a cross section of configuration space on which V is graphed in a region with a typical saddle point. In the figure a single negative mode is visible. Such sphalerons reside on potential energy barriers between the classical vacua of a theory. In principle, sphalerons can have as many negative modes as we would like. The sphalerons we will study in this chapter will have just one.

The most famous example of a sphaleron can be found in the EW sector of the SM: an $SU(2)$ sphaleron rediscovered[14] by Manton and Klinkhamer[28][23]. It lives in the bosonic sector of the theory, it is a configuration in both the gauge fields and Higgs field. This sphaleron, as well as its thermal cousins (saddle points of the free energy functional F), are a key ingredient in predicted baryon and lepton number violating processes in the SM. Such processes might be observable in collider experiments (using the regular EW sphaleron)

[1] Except, possibly, the existence of zero modes. The (anti-) kink soliton we studied back in chapter 2 had such a mode that moved the lump back and forth.

[2] $\delta V = 0$, so they reside on a point without a potential gradient.

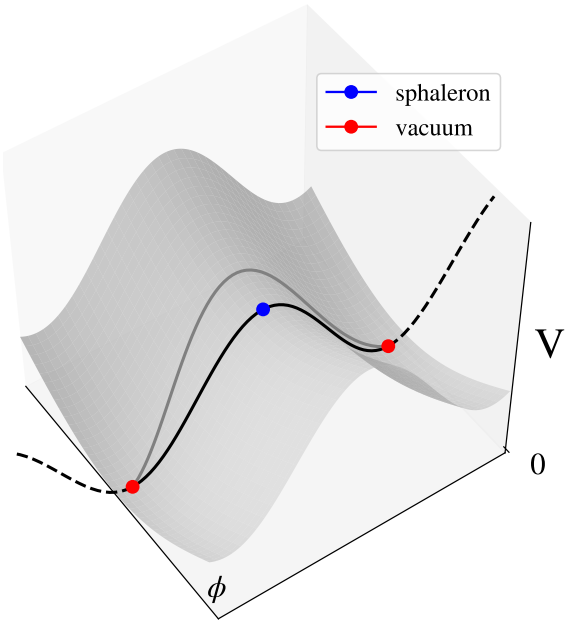

Figure 4.1: Qualitative figure showing the two dimensional cross section of C_V on which V is graphed in a region with a typical saddle point, i.e. sphaleron. At least one negative mode and one positive mode is visible. A path through C_V between CS-vacua is drawn that crosses the sphaleron at its apex. The grey line is an alternative path between these vacua that upon variation (minimizing the supremum of V along that line while keeping the ends fixed) will end up finding the sphaleron.

or they might have happened in the early universe (using the thermal EW sphaleron) and be (partially) responsible for the generation of the matter-antimatter asymmetry of the observable universe[33, ch.17 §4][26][32]. Understanding why such processes relate to sphalerons will be the discussed in the next chapter.

The main aim of this chapter is to discuss the sphaleron configurations themselves and to ultimately derive the EW sphaleron based on the literature. In section 4.1 we tie sphalerons to the content of the latter half of the previous chapter: The relation between sphalerons and the classical vacuum structure of gauge theories. We also discuss why they exist and what Manton refers to as the *minmax* procedure[27] by which we will find the EW sphaleron. Then we discuss the (1+1)-dimensional Abelian Higgs model and its sphaleron in section 4.2. This is in many ways a toy model of the full EW theory with a analytically solvable sphaleron. The topology of the configuration and its relation to the vacua is much more transparent than in the full EW sphaleron's case (which must, instead, be found numerically). Then we will discuss the EW sector of the SM and derive the EW sphaleron in section 4.3.

4.1 Sphalerons and Chern-Simons Vacua

In this section we discuss how the EW sphaleron relates to the classical vacuum structure of the EW sector, how the EW sphaleron has a gauge-dependent appearance, why sphalerons generally exist and how we will find them conceptually. The previous chapter's discussion of the pure Yang-Mills theory will be of help. The topics discussed in this section also apply to the (1+1)-dimensional Abelian Higgs model as well.

The EW theory's vacuum structure (in the absence of fermions) is analogous to the one of the pure Yang-Mills theory: In the temporal gauge $\boldsymbol{A}_0 = 0$ supplemented by the boundary condition 3.41 the vacuum structure is periodic, consisting of a countably infinite number of topologically distinct CS-vacua. While in a physical gauge, specifically combining the temporal $\boldsymbol{A}_0 = 0$ and radial $\boldsymbol{A}_r = 0$ gauge conditions (without a boundary constraint), there is only a single vacuum. We will use the latter gauge to derive the EW sphaleron, which might appear to be over-fixed. However, the sphaleron is simply a configuration at one moment in time, which is in general part of a larger path or trajectory. We can only impose one of the two conditions globally (at all times), but the other can be chosen to hold at sphaleron's time slice. Let us, for the moment, think about the sphaleron in the prior gauge with CS-vacua.

The EW sphaleron exists because the Higgs field introduces an explicit energy and length scale into the theory[27], as opposed to the pure Yang-Mills theory where the barriers between the CS-vacua were of arbitrary size (with large instantons tunneling through small barriers and vice versa, recall section 3.2.3). In the gauge with CS-vacua, the sphaleron therefore resides on some potential energy barrier of *finite physical height* between the CS-vacua. In other words, we cannot construct a path between the CS-vacua (that might or might not intersect the sphaleron) without $\mathrm{Tr}(\boldsymbol{F}_{\mu\nu}\boldsymbol{F}^{\mu\nu}) \neq 0$ somewhere along the path. On the other hand, the Euclidean EW sector has no true instanton anymore: Derrick's theorem rules out the existence of a stationary point of S_E[30, p.459]. Nonetheless, there exist instanton-like solutions that allow for tunneling in the EW theory[28].

How large the potential energy along a path must get depends on the path chosen and simply trying gives us only an upper bound on the smallest possible barrier. For reasons that will be made clear in the next chapter, it is the change of the CS-number of the gauge fields that is connected with the production of baryons and leptons. Therefore, the path that connects the vacua along the smallest possible barrier is the most physically interesting. It provides the most energetically favored "channel" along which baryon and lepton number violating processes are predicted to occur. This special path always traverses a saddle point, i.e. sphaleron, at its apex. The EW sphaleron energy therefore sets the energy scale at which baryon and lepton number violating processes are predicted to start occurring. For the regular EW sphaleron (relevant at zero temperature) this barrier has a height of ~ 9 TeV, a quantity calculated form the Higgs VEV and EW coupling constant. Since the sphaleron is situated half-way along a path between CS-vacua, it turns out that the CS-number of the sphaleron is half-integer. Figure 4.1 depicts a path that intersects the sphaleron on this smallest possible energy barrier.

Figure 4.1 also illustrates qualitatively how one attempts to find sphalerons in general: One varies a path with the ends fixed at the intended vacua, until the smallest barrier is

found. It is the point at which tangential variation of the path makes the energy go up. This is the *minmax* procedure Manton speaks about. We will essentially use this procedure to derive the sphalerons in this chapter. The parallel variation of the sphaleron in the direction along which V decreases most rapidly is what we call the sphaleron's negative mode. Note that the same tangential variation process cannot be used to look for sphalerons with more than a single negative mode: Graphs like figure 4.1 are simply sketches, they can only show two possible modes at once. Suppose, for instance, that a sphaleron has two negative modes. Then there exists a tangential variation of the path through the sphaleron that is able to lower the energy, the path "slides off". The graph looks like a local maximum restricted to those two modes. Of course V is still required to be positive definite for a sphaleron to exist and scaling arguments must still be considered.

In practice, we cannot be expected to vary over all possible paths between the CS-vacua, the d.o.f. would be too large. However, we can reduce this number by exploiting the so-called *principle of symmetric criticality*[30, ch.4 §3][33, ch.7 §3]. The principle claims that, at least in certain theories, we can expect critical point configurations like solitons and sphalerons to have additional symmetry. For instance, the BPST-instanton was rotationally symmetric, a symmetry of S_E. On the other hand, the instanton is not maximally symmetric. The instanton has a center, so it has no translation invariance. The vacua on the other hand do have maximal symmetry. If true, we can restrain our path to include only those configurations which are, for instance, spherically symmetric. One then substitutes the most general ansatz for a class of paths into V and solves the constrained minimization problem to find the sphaleron. Manton also emphasizes the importance of further proper gauge fixing when minmaxing[27]. Otherwise sphalerons can appear to have many zero modes, one associated to each infinitesimal gauge transformation (since V has gauge symmetry).

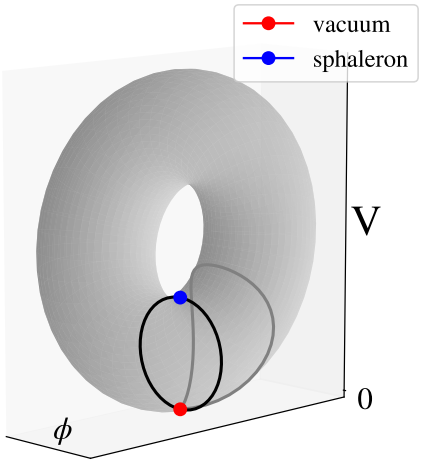

Figure 4.2: Qualitative figure showing a cross section of C_V on which V is graphed in a region where there is an NCL, $\Pi_1(C_V) = \mathbb{Z}$. The sphaleron resides on a barrier between the vacuum and itself.

We obtain a different picture of a sphaleron in a physical gauge with a single vacuum. The story is much the same as for the pure Yang-Mills instantons: sphaleron go from resting on a barrier between different CS-vacua, to a point on a barrier between the vacuum and itself, see figure 4.2. To find the EW sphaleron, we instead minmax the family of field configurations along this NCL. Therefore in gauges with a single vacuum, NCLs in C_V tend to have an associated sphaleron[27]. In other words, a non-trivial first homotopy group, such as $\Pi_1(C_V) = \mathbb{Z}$, can reveal the existence of sphalerons. The same is true for sphalerons with a larger number of negative modes. In that case one considers $\Pi_{\geq 2}(C_V)$. For instance, to find the $SU(3)$ sphaleron[24], which has two such modes, one considers the existence of non-contractible spheres in C_V, i.e. $\Pi_2(C_V)$.

4.2 The Abelian Higgs Model in (1+1) Dimensions

In this section we discuss one of the simplest theories that contains both an instanton and sphaleron, which is the Abelian Higgs model in (1+1) dimensions. The model is in many ways a simplified version of the EW theory's gauge and Higgs fields. For instance, the model has CS-vacua in the supplemented temporal gauge and its sphaleron has a single negative mode. This model makes it easier to demonstrate, for instance, how the sphaleron is situated on the barrier between these vacua.

The derivation of the instanton that follows is based on Rubakov's book[33, ch.13 §3] and Coleman's book[12, ch.7 §4]. The derivation of the sphaleron is based on the book by Manton and Sutcliffe[30, ch.11 §3]. These works discuss these solutions in different contexts and in different conventions, the aim here is in bringing them together in a consistent fashion.

The (1+1)-dimensional Abelian-Higgs model

The theory is a $U(1)$ gauge theory for which the Lagrangian is given by

$$\mathcal{L} = -\frac{1}{4} f_{\mu\nu} f^{\mu\nu} + |D_\mu \phi|^2 - \mathcal{V}(|\phi|^2), \quad \text{where} \quad \mathcal{V}(|\phi|^2) = \frac{1}{2}(|\phi|^2 - 1)^2. \tag{4.1}$$

Note the use of uncapitalized letters, they refer to Abelian quantities (or quantities that are a result of the $U(1)$ symmetry). The Lagrangian is similar to the one from scalar QED, with a Maxwell term and massive charged scalar. Here, the mass of the scalar (Higgs) is a consequence of the Abelian Higgs mechanism. This is due to the symmetry broken potential.

The field strength tensor and covariant derivative are

$$f_{\mu\nu} = \partial_\mu a_\nu - \partial_\nu a_\mu \quad \text{and} \quad D_\mu = \partial_\mu - i g a_\mu. \tag{4.2}$$

Under a local $U(1)$ gauge transformation $u(x) = e^{i\alpha(x)}$, the fields transform as

$$\phi \to u\phi = e^{i\alpha}\phi \quad \text{and} \quad a_\mu \to u^{-1} a_\mu u + \frac{i}{g} u^{-1} \partial_\mu u = a_\mu - \frac{1}{g}\partial_\mu \alpha. \tag{4.3}$$

The equations of motion for the theory are

$$D_\mu D^\mu \phi = -\frac{\partial \mathcal{V}}{\partial(|\phi|^2)}\phi \quad \text{and} \quad \partial_\mu f^{\mu\nu} = j^\mu. \tag{4.4}$$

Here, j^μ is the Noether current for the *global* $U(1)$ symmetry,

$$j^\mu = i g(\phi^* (D^\mu \phi) - \phi (D^\mu \phi)^*). \tag{4.5}$$

The Classical Vacuum Structure

The theory's potential energy functional is given by

$$V[\mathbf{\Phi}] = \int dx^1 \left[\frac{1}{2}(\partial_1 a_0)^2 + |D_1 \phi|^2 + \mathcal{V}(|\phi|^2)\right], \tag{4.6}$$

here $\mathbf{\Phi}$ is used to represent the joined collection of Higgs and gauge fields. Like the EW theory, whether this model has a periodic vacuum structure or not depends on the gauge chosen to minimize V. Let us consider the vacuum structure in the supplemented temporal gauge, $a_0 = 0$, first. The vacuum $\mathbf{\Phi}_{\text{vac.}}$ is then periodic.

Choosing to work in the temporal gauge leaves time-independent gauge transformations $u(x^1) = e^{i\alpha(x^1)}$ allowed. All terms in V must vanish simultaneously, therefore

$$\mathbf{\Phi}_{\text{vac.}}(x^1) = \left\{ \phi(x^1) = e^{i\varphi}\, u(x^1), \quad a_1(x^1) = \frac{i}{g} u(x^1)^{-1} \partial_\mu u(x^1) = -\frac{1}{g}\partial_1 \alpha(x^1) \right\}. \tag{4.7}$$

In other words, the remaining gauge d.o.f. a_1 is pure gauge. Note that both the ϕ and a_1 fields depend upon the same $u(x^1) = e^{i\alpha(x^1)}$, this is because the requirement that $D_1\phi = 0$ links the behavior of the Higgs field to the gauge field up to some arbitrary global phase $e^{i\varphi}$ (a phase since $|\phi| = 1$).

The vacua as given by equation 4.7 are not yet divided into homotopy classes: We need to compacitify space at each slice of time, such as we made happen for the pure Yang-Mills theory in section 3.3.1. We need to further impose an analogous supplementary gauge fixing condition such as equation 3.41. This divided the U's (hence the gauge fields A_i) into homotopy classes. The CS-number of the vacua could then be computed from A_i or U. Here, we need to impose a boundary condition on ϕ as well. We impose

$$\lim_{x^1 \to -\infty} \alpha(x^1) = 0, \qquad \lim_{x^1 \to +\infty} \alpha(x^1) = 2\pi n \quad \text{and} \quad \lim_{x^1 \to \pm\infty} \phi(x^1) = 1. \tag{4.8}$$

Note that the first two conditions make sure that $\lim_{x^1 \to \pm\infty} u(x^1) = 1$ and where we have eliminated the global phase freedom by setting[3] $e^{i\varphi} = 1$. The assumption compactifies space at each time slice into an S^1, the same as the gauge group manifold. The u's have therefore become mappings from $S^1 \to S^1$ which divide into homotopy classes ($\Pi_1(S^1) = \mathbb{1}$). Hence, the same is true for the vacua.

To figure out to which homotopy class a particular vacuum belongs one needs to know the right asymptotic of α, i.e. the integer n. Say, for instance, that for a given vacuum $\lim_{x^1 \to +\infty} \alpha(x^1) = 2\pi N$, then the CS-number of the vacuum is itself N:

$$\begin{aligned} N_{\text{CS}}[\mathbf{\Phi}_{\text{vac.}}] &= \frac{-g}{2\pi} \int dx^1\; a_1(x^1) = \frac{1}{2\pi i} \int dx^1\; u(x^1)^{-1} \frac{d}{dx^1} u(x^1) \\ &= \frac{1}{2\pi} \left(\lim_{x^1 \to \infty} \alpha(x^1) - \lim_{x^1 \to -\infty} \alpha(x^1) \right) \\ &= N. \end{aligned} \tag{4.9}$$

We can now convincingly call these CS-vacua. A possible choice for a CS-vacuum with $N_{\text{CS}} = n$ is given by the gauge mapping

$$u_n(x^1) \equiv e^{i\, n\pi(\tanh(x^1)+1)}. \tag{4.10}$$

[3] Simply requiring that $\lim_{x^1 \to \pm\infty} u(x^1) = 1$ (in addition to the condition on ϕ) is insufficient for this particular theory because $\partial\mathbb{R} = \{\pm\infty\}$ are two disconnected points. This would leave each vacuum specified by two integers instead of one that turns out to be CS-number. In Yang-Mills on the other hand, requiring that $U(\vec{x}) \to 1$ is enough because $\partial R^3 = S^2$ is connected.

The associated vacuum being

$$\mathbf{\Phi}_{\text{vac.}}(x^1) = \left\{ e^{i\,n\pi(\tanh(x^1)+1)}, \quad a_1(x^1) = -\frac{n\pi}{g}\text{sech}^2(x^1) \right\}, \tag{4.11}$$

as can be verified using equation 4.9

In the physical axial gauge $a_1 = 0$ there is only a single vacuum. This is because $a_0 = 0$ is required to make $V[\mathbf{\Phi}_{\text{vac.}}]$ vanish:

$$\mathbf{\Phi}_{\text{vac.}} = \left\{ \phi = e^{i\varphi}, \quad a_0 = 0 \right\}, \tag{4.12}$$

except for that same global phase freedom in ϕ (that we have chosen to be $e^{i\varphi} = 1$).

All in all we have the same periodic structure as the pure Yang-Mills theory did in the supplemented temporal gauge. Two vacua with CS-numbers 0 and 1 are plotted in figure 4.3. In section 4.2.3 we will derive the sphaleron that resides on the barrier between these two vacua.

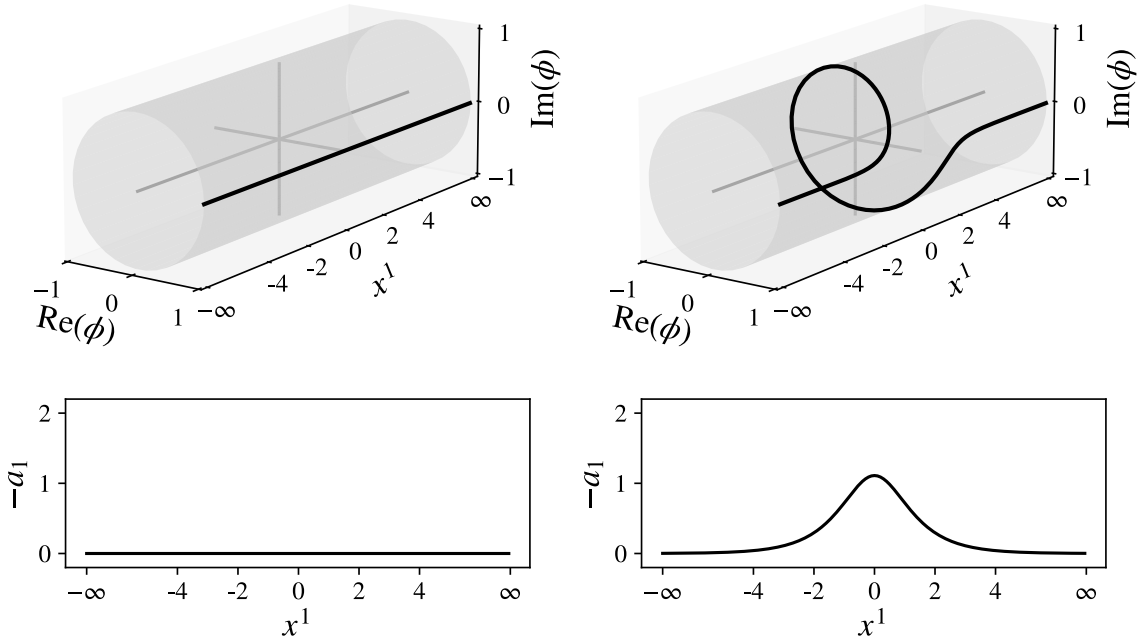

(a) Vacuum with $N_{\text{CS}} = 0$

(b) Vacuum with $N_{\text{CS}} = 1$

Figure 4.3: Two examples of CS-vacua in the Abelian Higgs model in the supplemented temporal gauge $a_0 = 0$. The top and bottom plot depict the Higgs field and gauge field respectively. The entire real axis (space) has been compressed asymptotically near the ends, but the relevant part around the origin is left undistorted.

4.2.1 The Landau-Ginzburg Theory

The Abelian Higgs Model model is more than a toy model of the EW theory. As it turns out, the instanton in this model is actually of physical relevance in an entirely different branch of physics[12, p.205]. To see why, consider the Euclidean action of this theory

$$S_E[\mathbf{\Phi}] = \int d^2x \left[\frac{1}{4}(f_{\mu\nu})^2 + (D_\mu\phi)^*(D_\mu\phi) + \mathcal{V}(|\phi|^2)\right]. \tag{4.13}$$

Its Lagrangian density is functionally identical to the static free energy density $\mathcal{F}$ of the Landau-Ginzburg theory of superconductors, here written down in vector notation.

$$\mathcal{F} = \frac{\hbar^2}{2m}\left|\left(\boldsymbol{\nabla} - \frac{iq}{\hbar c}\boldsymbol{A}\right)\psi\right|^2 - v|\psi|^2 + \frac{u}{2}|\psi|^4 + \frac{|\boldsymbol{\nabla}\times\boldsymbol{A}|^2}{8\pi}, \tag{4.14}$$

where ψ is the so-called *complex order parameter field*. The purpose of this theory is to describe the two-dimensional cross section of a superconductor (in the absence of time) near the superconducting transition in the presence of a protruding $\boldsymbol{B}$ field (caused by the $\boldsymbol{\nabla}\times\boldsymbol{A}$ term). ψ accounts for the behavior of the superconducting electrons and is proportional to their density. Due to the Euclidean nature of S_E, the x_0x_1-plane corresponds functionally to the xy-plane in this particular model.

In the Landau-Ginzburg model, minimizing the free energy produces a soliton called the Abrikosov-Nielsen-Olesen vortex[4], which is structurally the same as the instanton we are going to look for.

4.2.2 The Instanton in the Abelian Higgs model

In this section we derive an instanton that appears in the Abelian Higgs model and that corresponds with the vortex solitons discussed in the previous subsection. The derivation is based on those found in the books by Rubakov[33, ch.7 §3] and Coleman[12, ch.7 §4] and use vector notation borrowed from a paper discussing the Abrikosov-Nielsen-Olesen vortex[10]. This notation will help simplify the Euclidean e.o.m.

Since we have spend a long time deriving the BPST-instanton in the previous chapter, we keep this section short. We therefore sum up the relevant differences and similarities between this instanton and the BPST-instanton upfront:

1. The C_{S_E} of the theory is once again divided into disjoint sectors. In other words, there is a topological characteristic (i.e. topological charge Q) by which we can divide the instantons into distinct homotopy classes. We will find an instanton in the unit winding number sector, i.e. an instanton characterized by a topological charge $Q = 1$.

2. We will not have a simple equation such as $\boldsymbol{F}_{\mu\nu} = \pm\tilde{\boldsymbol{F}}_{\mu\nu}$ to our disposal to find the instanton. Instead, we will have to solve the Euclidean e.o.m. directly (and approximately). We will solve the e.o.m. using a rotationally symmetric ansatz containing just two free radial functions. The rotational symmetry is expected based on the

[4]The Landau-Ginzburg model is static, i.e. without reference to time. This is why the solution is interpreted to as a soliton.

principle of symmetric criticality, because the required asymptotics of the fields have rotational symmetry[33, p.159] (see the next section).

3. The ansatz will be a pure "curl", a configuration without a radial component. In other words, $a_\mu n_\nu = 0$ (n_μ being an outward pointing unit vector in the x_0x_1-plane). This is the reason why the solution is referred to as a "vortex".

4. We will solve the resulting e.o.m. in terms of the radial functions approximately in regions far away from the origin, where we can expand the instantons around the pure gauge background.

5. Although we will not demonstrated this here, it should be possible to present the instanton in the supplemented temporal gauge $a_0 = 0$, rather than it satisfying $a_\mu n_\nu = 0$ as it does when we derive it. We did change the gauge of the BPST-instanton after we found it. In this way, it becomes explicit that the instanton tunnels between the CS-vacua from equation 4.7.

The Finite S_E Field Configuration Space

In this section we demonstrate first point above, that the instantons can be divided amongst homotopy classes based on a topological charge. The discussion parallels section **??** where we did the same for the pure Yang-Mills theory.

For S_E to converge in the plane[5], a_μ and ϕ must tend to a pure gauge configurations as $x_\mu^2 = x_0^2 + x_1^2 \to \infty$, see equation 4.13. At $|x_\mu| = \infty$ both fields must be given by a gauge mapping u that only depends on the direction towards which the boundary $\partial\mathbb{R} \cong S^1$ is approached. The asymptotics of ϕ and a_μ are not independent, this is once again due to the vanishing of $D_\mu\phi$.

Let us use the polar coordinates ρ, θ in the x_0x_1-plane for convenience. It allows us to write partial and covariant derivatives in the angular direction as derivatives in θ. For instance, $n_\nu\epsilon_{\mu\nu}\partial_\nu = \frac{1}{\rho}\frac{d}{d\theta}$. This allows us to express u as some function $u(\theta) \equiv e^{i\alpha(\theta)}$. The pure gauge asymptotics of the instanton in this parameterization are then given by

$$\lim_{\rho\to\infty} \mathbf{\Phi}_{\text{inst.}}(\rho,\theta) = \left\{ \lim_{\rho\to\infty} \phi(\rho,\theta) = u(\theta), \quad \lim_{\rho\to\infty} a_\mu(\rho,\theta) = \frac{i}{g}\partial_\mu\alpha(\theta) \right\}, \tag{4.15}$$

where, just like u, the gauge and Higgs components only depend on θ.

This mapping u maps each point on the boundary $\partial\mathbb{R}^2 \cong S^1$ to a zero of an element of $U(1) \cong S^1$. Since $\Pi_1(S^1) \cong \mathbb{Z}$, this divides the u's into homotopy classes (and hence divides our configurations space into disconnected components). The associated winding number or topological charge for any finite S_E configuration, including the instantons, can be computed from u as well as $f_{\mu\nu}$ (Compare with equations 3.29, 3.30).

$$Q[u] = \frac{1}{2\pi i}\int_0^{2\pi} d\theta\; u(\theta)^{-1}\frac{d}{d\theta}u(\theta) = \frac{1}{2\pi}(\alpha(2\pi) - \alpha(0)) \tag{4.16}$$

$$Q[f_{\mu\nu}] = \frac{1}{4\pi i}\int d^2x\; \epsilon_{\mu\nu}f_{\mu\nu}. \tag{4.17}$$

[5]This is true for any finite S_E configuration, not just instantons.

To prove that these are equal one constructs a gauge dependent current $K_\mu = \frac{1}{2\pi i}\epsilon_{\mu\nu}a_\nu$ whose divergence is $\frac{1}{2\pi i}\epsilon_{\mu\nu}f_{\mu\nu}$ and whose asymptotics match those of a_μ.

$$Q[u] = \frac{1}{2\pi i}\int_0^{2\pi} \rho d\theta\; K_\mu n_\mu = \frac{1}{2\pi i}\int d^2x\; \partial_\mu K_\mu = \frac{1}{2\pi i}\int d^2x\; \epsilon_{\mu\nu}\partial_\mu a_\nu = Q[f_{\mu\nu}], \qquad (4.18)$$

where the second equality follows from Stokes's theorem.

Deriving the Instanton

We begin with minimizing the Euclidean action, equation 4.13. The resulting e.o.m. are[6]:

$$(D_\mu)^2\phi = \frac{\partial \mathcal{V}}{\partial(|\phi|^2)}\phi \quad \text{and} \quad \partial_\mu f_{\mu\nu} = j_\mu. \qquad (4.19)$$

These are, unsurprisingly, the Euclidean versions of the original ones, see equation 4.4.

We look for instantons in the unit winding number sector that we expect, based on the principle of symmetric criticality, to have additional rotation symmetry in the x_0x_1-plane. Let us therefore try

$$\mathbf{\Phi}_{\text{inst.}}(\rho,\theta) = \left\{\phi(\rho,\theta) = f(\rho)e^{i\theta}, \quad a_\mu(\rho,\theta) = \frac{a(\rho)}{\rho}\epsilon_{\mu\nu}n_\nu\right\}, \qquad (4.20)$$

where f and a are the radial functions that specify the instanton and that we are still required to find. The ansatz is a pure "curl": a_μ points in its entirety in the θ-direction, $a_\rho = 0$. This is not the maximally symmetric option, there could still have been a radial contribution to a_μ. However, such a radial contribution can always be written as the addition of a pure gauge, and hence, can always be gauged away. The mapping $u(\theta)$ that this ansatz uses is the identity mapping, $\alpha(\theta) = \theta$, which definitely produces an ansatz for which $Q = 1$. For smoothness we need to make sure that $f, a \to 1$ as $\rho \to \infty$ as well as that $f, a \to 0$ as $\rho \to 0$.

To find the instanton, we need to substitute the ansatz into the field equations and then solve them. This is made easier by using covariant vector notation, since we have access to vector identities. For instance, $\boldsymbol{D} = \boldsymbol{\nabla} - ig\,\boldsymbol{a}$ in this particular notation. This operator acting as a *covariant divergence* or *covariant gradient* in polar coordinates (with our ansatz for a_μ already substituted in) is given by

$$\boldsymbol{D}\phi = \frac{\partial\phi}{\partial\rho}\hat{\boldsymbol{\rho}} + \frac{1}{\rho}\left\{\frac{\partial\phi}{\partial\theta} - ig\,a(\rho)\phi\right\}\hat{\boldsymbol{\theta}}, \qquad (4.21)$$

$$\boldsymbol{D}\cdot\boldsymbol{a}' = \frac{1}{\rho}\frac{\partial(\rho\,\boldsymbol{a}'\cdot\hat{\boldsymbol{\rho}})}{\partial\rho} + \frac{1}{\rho}\frac{\partial(\boldsymbol{a}'\cdot\hat{\boldsymbol{\theta}})}{\partial\theta} - ig\,\boldsymbol{a}\cdot\boldsymbol{a}'. \qquad (4.22)$$

With both operators specified, the first equation of motion

$$\boldsymbol{D}\cdot(\boldsymbol{D}\phi) = \frac{\partial\mathcal{V}}{\partial\phi^*} \qquad (4.23)$$

[6]Notice the flipped potential. This is what we expect, since we are looking to find an instanton.

reduces, after substitution, to

$$\frac{1}{\rho}\frac{\partial}{\partial\rho}\left\{\rho\frac{\partial f}{\partial\rho}\right\} - \frac{f}{\rho^2}(1-g\,a)^2 = f(f^2-1). \tag{4.24}$$

Similarly, the second equation of motion[7]

$$\boldsymbol{\nabla}^2\boldsymbol{a} - \boldsymbol{\nabla}\cdot(\boldsymbol{\nabla}\cdot\boldsymbol{a}) = \boldsymbol{j} \tag{4.25}$$

reduces, after substitution, to

$$-\boldsymbol{\nabla}\times(\boldsymbol{\nabla}\times\boldsymbol{a}) = ig(\phi^*\boldsymbol{D}\phi - \phi\boldsymbol{D}\phi^*) \tag{4.26}$$

$$\frac{\partial}{\partial\rho}\left\{\frac{1}{\rho}\frac{\partial a}{\partial\rho}\right\}\hat{\boldsymbol{\theta}} = -\frac{2g}{\rho}(1-g\,a)f^2\,\hat{\boldsymbol{\theta}}, \tag{4.27}$$

where we used a vector calculus identity in the first step[8].

Even though the ansatz has made our equations of motion more palpable, we are still not able to solve them analytically. What we can do, however, is solve them far away from the origin by expanding around their asymptotic values $f, a = 1$. We expand

$$f(\rho) = 1 + \epsilon\,h(\rho) \quad \text{and} \quad a(\rho) = 1 + \epsilon g\rho\,b(\rho). \tag{4.28}$$

Linearizing in small ϵ gives us the following equations of motion for h and b.

$$\frac{1}{\rho}\frac{\partial}{\partial\rho}\left\{\rho\frac{\partial h}{\partial\rho}\right\} = 2h \quad \text{and} \quad \frac{\partial}{\partial\rho}\left\{\frac{1}{\rho}\frac{\partial(\rho b)}{\partial\rho}\right\} = 2b. \tag{4.29}$$

These are solved by the modified Bessel functions

$$h(\rho) = K_0(\sqrt{2}\rho) \quad \text{and} \quad b(\rho) = \sqrt{2}\,K_1(\sqrt{2}\rho). \tag{4.30}$$

This is the point at which the instanton can be computed over to supplemented temporal gauge, where it interpolates between the CS-vacua that differ by a single winding.

4.2.3 The Sphaleron in the Abelian Higgs model

In this section we derive the Abelian Higgs model sphaleron $\boldsymbol{\Phi}_{\text{sph.}}$ and its negative mode $\boldsymbol{\eta}$ in both the axial gauge ($a_1 = 0$) and supplemented temporal gauge ($a_0 = 0$ + boundary conditions). The Abelian Higgs model is an excellent toy model for the true EW theory, since the derivation of its sphaleron is much more transparant. The computation of $\boldsymbol{\eta}$ (from which one discerns the way in which the sphaleron decays) is also a useful exercise, since must be done numerically in the full EW theory. We begin in the axial gauge, as the derivation is more straightforward. Afterwards, we do the same in the supplemented temporal gauge. The latter is more interesting as the sphaleron resides on the barrier

[7] $\partial_\mu f_{\mu\nu} = \partial^2 a_\nu - \partial_\nu(\partial_\mu a_\mu) = j_\mu$

[8] Even though we use the curl identity, our space is two dimensional. Here $\boldsymbol{\nabla}\times$ produces a fictitious vector that points out of the x_0x_1-plane.

between neighboring CS-vacua, those which we discussed in section 4.1. We will illustrate this sphaleron with a figure in which its relation to these vacua becomes manifest. The latter computation of $\boldsymbol{\eta}$ uses the so-called *gradient flow equations*. These equations play a role in analyzing effective d.o.f. of certain field theories. The derivation here is based on the one found in book by Manton and Sutcliffe[30, ch.11 §3].

The Sphaleron in the Axial Gauge

Since saddle point configurations are also critical points of V ($\delta V = 0$), we look for sphalerons like we did for solitons: We simply stationarize V as given by equation 4.6. By choosing to work in the axial gauge, we replace D_1 with ∂_1 in V. With the D_1 gone, we can tell that the remaining gauge field a_0 plays a trivial role in the sphaleron: $\frac{1}{2}(\partial_1 a_0)^2$ is the only term in V that depends on a_0 while, most importantly, being positive definite. $a_0 = 0$ will therefore definitely minimize V. We need only calculate the Euler-Lagrange equation minimizing V for ϕ, which is given by

$$(\partial_1)^2\phi = -(1 - \phi^*\phi)\phi. \tag{4.31}$$

This is the same equation as the (anti-) kink soliton satisfied back in chapter 2. The ϕ portion of the sphaleron is therefore given by

$$\phi(x^1) = \phi_{\text{sph.}}(x^1) \equiv \tanh \frac{x^1}{\sqrt{2}}. \tag{4.32}$$

and the whole sphaleron is therefore

$$\boldsymbol{\Phi}_{\text{sph.}} = \{\phi = \phi_{\text{sph.}}, a_0 = 0\}. \tag{4.33}$$

Note that $a_0 = 0$ is coincidental in the axial gauge, we have not set set a temporal gauge constraint (this would not even be possible because it would overfix the gauge, making a_μ vanish entirely).

The Negative Mode

The (anti-) kink solution used to be a stable soliton, now it is an *unstable* sphaleron. This is because we are now considering a complex gauge theory. From that prior discussion we do know, however, that all possible real variations of ϕ will increase the energy. The negative mode will therefore be fully imaginary. For that reason, let us expand our variations $\delta\boldsymbol{\Phi}$ as

$$\boldsymbol{\Phi}_{\text{sph.}} + \delta\boldsymbol{\Phi} = \left\{\phi(x^1) = \phi_{\text{sph.}}(x^1) + i\eta(x^1), \qquad a_0(x^1) = 0 + a(x^1)\right\}, \tag{4.34}$$

as to make η real.

After substituting these into V and integrating by parts we obtain to quadratic order

$$V[\boldsymbol{\Phi}_{\text{sph.}} + \delta\boldsymbol{\Phi}] = V[\boldsymbol{\Phi}_{\text{sph.}}] + \int dx^1\, \eta\left(- \frac{\partial^2}{\partial {x^1}^2} - \operatorname{sech}^2 \frac{x^1}{\sqrt{2}}\right)\eta + \int dx^1 a\partial_1^2 a, \tag{4.35}$$

where there are no first order terms, since we expand around a critical point ($\delta V = 0$). The sphaleron energy is $V[\mathbf{\Phi}_{\text{sph.}}] = \frac{4\sqrt{2}}{3}$.

We can tell from the last term in equation 4.35 that the variation a cannot lower $V[\mathbf{\Phi}_{\text{sph.}}]$. On the other hand, the variation η can. We can see this by considering the eigenvalue equation

$$\Big(-\frac{\partial^2}{\partial {x^1}^2} - \operatorname{sech}^2 \frac{x^1}{\sqrt{2}} \Big) \eta = \lambda \eta, \tag{4.36}$$

which is an example of an integrable stationary Schrödinger equation. It has precisely what we are looking for, a *single* eigenfunction with a negative eigenvalue:

$$\eta(x^1) = \operatorname{sech} \frac{x^1}{\sqrt{2}}, \tag{4.37}$$

which has $\lambda = -\frac{1}{2}$. This solution is the Higgs component of the whole negative mode

$$\boldsymbol{\eta} = \Big\{ \eta(x^1) = i \operatorname{sech} \frac{x^1}{\sqrt{2}}, \quad a(x^1) = 0 \Big\}. \tag{4.38}$$

The Sphaleron in the Supplemented Temporal Gauge

Now we will switch to the supplemented temporal gauge where we get periodic CS-vacua. For $\mathbf{\Phi}_{\text{sph.}}$ this simply means a change of gauge.

In the supplemented temporal gauge the sphaleron solves the same Euler-Lagrange equation as before (equation 4.31) except with ∂_1's replaced with D_1's. The solution is now any time-independent gauge transformation $u(x^1)$ away from equation 4.33. For the sphaleron to properly interpolate between the CS-vacua, these u must satisfy the same boundary conditions as we imposed on them, equation 4.8. For instance, let

$$u(x^1) = u_{01}(x^1) = e^{i\alpha_{01}(x^1)} \equiv e^{i\frac{\pi}{2}(\tanh(x^1)-1)}, \tag{4.39}$$

then the associated sphaleron is

$$\mathbf{\Phi}_{\text{sph.}}(x^1) = \Big\{ \phi(x^1) = u_{01}(x^1)\, \phi_{\text{sph.}}(x^1), \quad a_1(x^1) = -\frac{1}{g} \partial_1 \alpha_{01}(x^1) \Big\}, \tag{4.40}$$

$$= \Big\{ \phi(x^1) = \tanh\Big(\frac{x^1}{\sqrt{2}}\Big) e^{i\frac{\pi}{2}(\tanh(x^1)-1)}, \quad a_1(x^1) = -\frac{\pi}{2g} \operatorname{sech}^2(x^1) \Big\} \tag{4.41}$$

as dictated by the way the fields must transform[9], see equation 4.3. This sphaleron resides on the barrier precisely beween the vacua with CS-numbers 0 and 1. As is therefore expected, its CS-number is $\frac{1}{2}$ (This can be verified explicitly using equation 4.9). Figure 4.4 shows this sphaleron.

[9]Since $a_0 = 0$ was part of the same sphaleron in the axial gauge, recall equation 4.33, a_0 remains zero under a time-independent gauge transformation. This is as it should be, otherwise the sphaleron in the supplemented temporal gauge would not be the gauge transformed version of the one in the axial gauge.

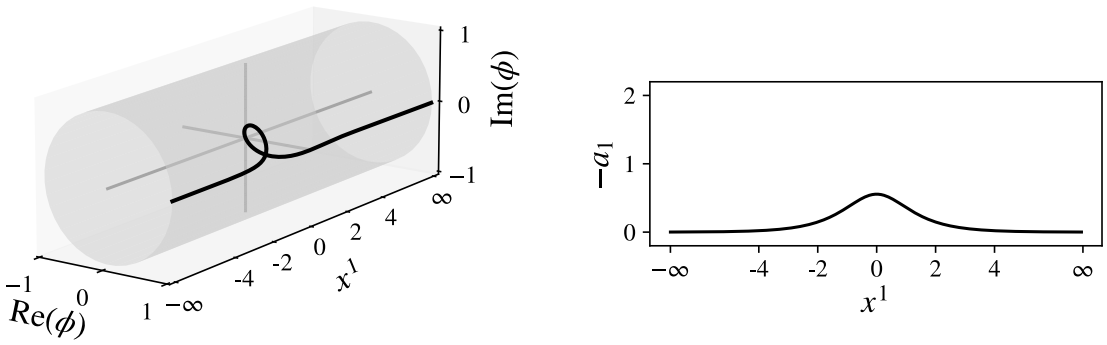

Figure 4.4: The Abelian Higgs model sphaleron, in the supplemented temporal gauge, that resides on the barrier between the vacua of figure 4.3. The Higgs and gauge fields are plotted on the left and right respectively.

The Negative Mode

To see how the sphaleron $\mathbf{\Phi}_{\text{sph.}}$ actually starts to decay (deform) into either vacuum, we need to rederive the negative mode $\boldsymbol{\eta}$ in the supplemented temporal gauge. In the axial gauge, it was convenient that the gauge field participated trivially in $\boldsymbol{\eta}$ (equation 4.38) this will no longer be the case. Here, $\boldsymbol{\eta}$ is recomputed using the gradient flow equations. These equations are used by Manton and Sutcliffe in their derivation[30, ch.11 §3].

The gradient flow equations are a set of first order dynamical equations different from the equations of motion. They instead describe motion through $\mathcal{C}$ on paths orthogonal to the contours of V. In other words, their motion makes configurations decay in the direction where V decreases most rapidly. This is why we can use them to find the negative mode of the sphaleron: their dynamics point in the direction of $\boldsymbol{\eta}$.

Consider, for instance, a classical dynamical system of an arbitrary but finite number of d.o.f. Its Lagrangian is given by

$$L(\boldsymbol{x}, \dot{\boldsymbol{x}}) = T(\boldsymbol{x}, \dot{\boldsymbol{x}}) - V(\boldsymbol{x}, \dot{\boldsymbol{x}}), \quad \text{where} \quad T(\boldsymbol{x}, \dot{\boldsymbol{x}}) = \frac{1}{2} g_{ij}(\boldsymbol{x}) \dot{x}^i \dot{x}^j \tag{4.42}$$

given some metric $g_{ij}(\boldsymbol{x})$ for the discrete coordinates x^i. For this system the equations of motion and gradient flow equations are[29]

$$\frac{d}{dt}(g_{ij}x^j) - \frac{1}{2}\frac{\partial g_{jk}}{\partial x^i}\dot{x}^j\dot{x}^k = -\frac{\partial V}{\partial x^i} \quad \text{and} \quad g_{ij}x^j = -\frac{\partial V}{\partial x^i}. \tag{4.43}$$

Most importantly, if $g_{ij}(\boldsymbol{x}) = \delta_{ij}$ (and hence there is no second term), then we see that the gradient flow equations are found by simply dropping a single time derivative. This is a heuristic rule that we will also use.

A interesting fact from a dynamical systems point of view is that these equations are used to describe the bulk dynamics of solitons[30, p.20]. In some sense, solitons behave like particles, they attract and repel each other. The gradient flow equations can be used to formulate an effective reduced dynamical system for these solitons (in terms of, for instance,

their centers of mass coordinates). Manton and Merabet used the gradient flow equations to study the dynamics of (anti-) kink solitons in the ϕ^4 theory[29] and others have examined the forces between the vortices (solitons) from the previous section[15] in this very model.

There is also a gradient flow equation for field theories (as well as gauge theories), where the coordinates have been replaced by fields[30, p.46]. In this case, the heuristic rule consists of dropping a covariant derivative D_0. When we work with gauge theories in which we have not fully fixed the gauge, we can check that the gradient flow equations do not dynamically generate (whichever still allowed) gauge transformations. Since gauge orbits are also contours of V, they should not. In the supplemented temporal gauge, this means that the gradient flow equations should not produce a time-independent gauge transformation.

Let us once again[10] expand the fields around the sphaleron as

$$\mathbf{\Phi}_{\text{sph.}} + \delta\mathbf{\Phi} = \left\{ \phi(x^1) = \phi_{\text{sph.}}(x^1) + i\eta(x^1), \qquad a_1(x^1) = 0 + a(x^1) \right\} \tag{4.44}$$

and use them to linearize the gradient flow equations (the gradient flow equations are themselves obtained by dropping a single covariant or partial time derivative from equation 4.4). Those equations ought to have no more than a single exponentially growing solution, in agreement with having a single negative mode.

These linearized gradient flow equations are[30, p.449]

$$\partial_0\eta = \partial_1(\partial_1\eta - ga\phi_{\text{sph.}}) - ga(\partial_1\phi_{\text{sph.}}) + (1 - \phi^2_{\text{sph.}})\eta \tag{4.45}$$

$$\partial_0 a = g\phi_{\text{sph.}}(\partial_1\eta - ga\phi_{\text{sph.}}) - g(\partial_1\phi_{\text{sph.}})\eta. \tag{4.46}$$

We mentioned that the gradient flow equations do not dynamically generate a gauge transformation, this can quickly be shown. From the gradient flow equations as well as equation 4.31 follows that

$$\partial_1\partial_0 a = g\phi_{\text{sph.}}\partial_0\eta. \tag{4.47}$$

Applying an infinitesimal time-independent gauge transformation $(i\phi_{\text{sph.}}\alpha, (\frac{i}{g}\,\partial_1\alpha))$ satisfying equation 4.8 this tells us that (multiplying either side by α and integrating by parts)

$$(i\phi_{\text{sph.}}\alpha)\, i\partial_0\eta - \left(\frac{i}{g}\,\partial_1\alpha\right)\partial_0 a. \tag{4.48}$$

The infinitesimal gauge transformation is thus orthogonal to time evolution $(i\partial_0\eta, \partial_0 a)$.

The exponentially growing solution from which we deduce $\boldsymbol{\eta}$ will be of the form

$$\eta'(x^\mu) = \eta(x^1)e^{\Gamma x_0} \quad \text{and} \quad a'(x_\mu) = a(x^1)e^{\Gamma x_0}. \tag{4.49}$$

which we try and substitute into the gradient flow equations. The spatial components $\eta(x^1)$ and $a(x^1)$ are part of the negative mode we are trying to find[11]. The procedure seems to

[10] Except that a_1 partakes instead of a_0. We also choose to postpone the application of a gauge transformation such as the one from equation 4.39 (required to have $\mathbf{\Phi}_{\text{sph.}}$ satisfy the correct boundary conditions) until after we have found $\boldsymbol{\eta}$.

[11] The dynamics of the gradient flow equations are not those of the e.o.m. The gradient flow equations and their evolution are used purely as tool to find the special configurations $\eta(x^1)$ and $a(x^1)$ that decrease $V[\mathbf{\Phi}_{\text{sph.}}]$ most rapidly.

work, the only negative mode appears to be[30, p.449]

$$\eta(x^1) = \tau\left(\operatorname{sech}\frac{x^1}{\sqrt{2}}\right)^\tau \quad \text{and} \quad a(x^1) = -\sqrt{2}g\left(\operatorname{sech}\frac{x^1}{\sqrt{2}}\right)^\tau, \tag{4.50}$$

where $\tau^2 - \tau - 2g^2 = 0$ and $\Gamma = \frac{\tau}{2}$. Choosing the positive root for τ makes sure it is a growing solution[12].

The expansion of the fields (equation 4.44) still needs to undergo a forced gauge transformation. Otherwise the fields do not satisfy the appropriate boundary conditions, equation 4.8. For instance, the negative mode of the sphaleron from equation 4.41 is

$$\boldsymbol{\eta}(x^1) = \left\{\eta(x^1) = \tau\left(\operatorname{sech}\frac{x^1}{\sqrt{2}}\right)^\tau e^{i\frac{\pi}{2}(\tanh(x^1)-1)}, \right. \\ \left. a(x^1) = -\sqrt{2}g\left(\operatorname{sech}\frac{x^1}{\sqrt{2}}\right)^\tau - \frac{1}{g}\operatorname{sech}^2(x^1)\right\}, \tag{4.51}$$

where we used the same time-independent gauge transformation $u_{01}(x^1)$ from equation 4.39. This is now the negative mode along which that sphaleron decays towards the vacua with CS-numbers 0 and 1. This fact is illustrated from multiple angles for the Higgs component of the sphaleron in figure 4.5 (The gauge component is far less interesting, the "lump" centered at the origin just grows or shrinks depending on the decay direction). To be precise, $\phi_{\text{sph.}} \pm 0.5\, i\eta$ are drawn in addition to the sphaleron. Both perturbed solutions already look remarkably similar to the vacua toward which they are decaying: In the dashed case the sphaleron loop is being blown up to almost encircle the cylinder, like the $N_{\text{CS}} = 1$ vacuum, while in the dotted case the loop has all but disappeared, like the $N_{\text{CS}} = 0$ vacuum. This is surprising, given that η is only tangent to the path of steepest descent of V to wards the vacua at the sphaleron point. This shows us that the field mode along which V decreases most rapidly does not change much when we move further down the barrier on either side. The shape of the barrier around the sphaleron is thus quadratic over a great range of N_{CS}.

4.3 The EW Sphaleron in the SM

The goal of this section will be to derive the famous $SU(2)$ sphaleron in the EW sector of the SM (what is also known as the Weinberg-Salam theory). It was originally found by Manton and Klinkhamer[28][23]. It exists at zero temperature, where it resides on a ~ 9 TeV barrier (the sphaleron mass). In complete analogy with the (1+1)-dimensional Abelian Higgs model, in the supplemented temporal gauge the barrier is located between (topologically distict) CS-vacua. Within the radial + temporal gauge (without the supplementary boundary condition) on the other hand, the barrier exists along an NCL from the vacuum to itself. Imposing both gauge conditions is not over-fixing the gauge, we are looking at a single configuration at one moment in time. We can therefore enforce the radial or temporal

[12]The appearance of various factors of $\sqrt{2}$ and g is a consequence of the metric used in our Lagrangian. Manton and Sutcliffe include a convenient prefactor of $\frac{1}{2}$ before the $(D_\mu\phi)^*(D^\mu\phi)$ term in their Lagrangian and they set $g = 1$, this makes sure that $g_{ij}(\boldsymbol{x}) = \delta_{ij}$ for them.

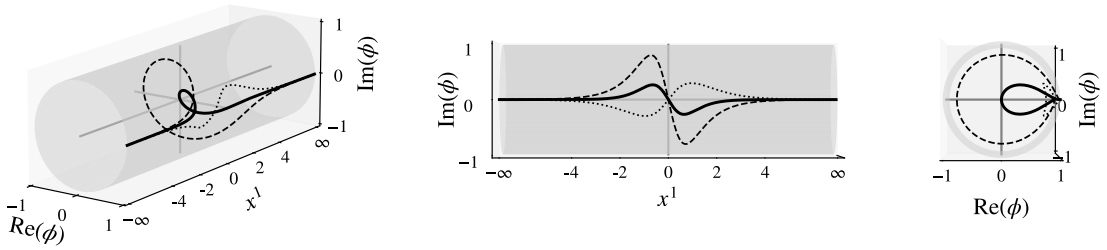

Figure 4.5: The deformation of the Higgs component of the sphaleron from figure 4.4 (solid black line) by the negative mode from equation 4.51. The dashed line is $\phi_{\text{sph.}} - 0.5\, i\eta$ and the dotted line is $\phi_{\text{sph.}} + 0.5\, i\eta$. We see how the sphaleron is quickly deformed towards a solution that resembles either of the vacua from figure 4.3. A front and side view is included for clarity.

gauge constraint globally and the other at the sphaleron's time slice. Manton chooses to enforce $A_r = 0$ globally when speaking about the EW sphaleron. It is in this gauge that we will go ahead and find the configuration.

The EW sector of the SM is an $SU(2)_L \times U(1)_Y$ gauge theory (Y being the weak hypercharge) that through SSB breaks down to $U(1)_{\text{EM}}$, the gauge group of electromagnetism: A mixed symmetry between a $U(1)$ subgroup of $SU(2)_L$ and $U(1)_Y$ determined by the Weinberg angle θ_W. After SSB, the massive gauge bosons that appear are the charged $W^{\pm}$ (or $W^{(\dagger)}$) and neutral Z^0. There are three, one for each broken gauge d.o.f. The Higgs attains a mass depending on its vacuum expectation value (VEV) and becomes a real, hence neutral, scalar field. The photon is the massless gauge boson of the remaining unbroken mixed $U(1)_{\text{EM}}$ gauge group.

We will derive the EW sphaleron in the limit $\theta_W \to 0$. In this limit, only $SU(2)_L$ breaks and produces three neutral equally massive gauge bosons for which we choose to retain the original notation A^a_μ. It is only these three fields that partake (in addition to the Higgs) in the EW sphaleron. The remaining $U(1)$ gauge boson ($U(1)_Y = U(1)_{\text{EM}}$ in this scenario) can safely be ignored in the derivation. For this reason, the sphaleron is known as the $SU(2)$ sphaleron. Turning θ_W back on is known to perturb the sphaleron's mass only minimally[23].

The derivation presented here is based on both the original papers on the EW sphaleron by Manton and Klinkhamer[28][23], as well as the more succinct computation found in the book by Manton and Sutcliffe[30, ch.11 §5].

4.3.1 The EW Theory

We begin the EW sphaleron derivation by summarizing the relevant details of the EW sector (at zero temperature and finite θ_W), as well as stating the conventions that we use throughout this computation. The most important part is, of course, the Lagrangian of the

bosonic fields. It is given by

$$\mathcal{L} = -\frac{1}{2}\,\mathrm{Tr}(\boldsymbol{F}_{\mu\nu}\boldsymbol{F}^{\mu\nu}) - \frac{1}{4}f_{\mu\nu}f^{\mu\nu} + (\boldsymbol{D}_\mu\phi)^\dagger(\boldsymbol{D}^\mu\phi) - \mathcal{V}(\phi^\dagger\phi). \tag{4.52}$$

The field strength tensors $F^a_{\mu\nu}$ and $f_{\mu\nu}$ of the $SU(2)_L$ and $U(1)_Y$ gauge fields, A^a_μ and a_μ respectively, are given by

$$F^a_{\mu\nu} = \partial_\mu A^a_\nu - \partial_\nu A^a_\mu + g\epsilon^{abc}A^b_\mu A^c_\nu, \tag{4.53}$$

$$f_{\mu\nu} = \partial_\mu a_\nu - \partial_\nu a_\mu. \tag{4.54}$$

Once again, the lower case letter refer to the abelian quantities.

In the EW Lagrangian we have stuck to the same conventions that we used during the BPST-instanton derivation. In particular, the $SU(2)_L$ gauge fields are presented in vector notation such that

$$\boldsymbol{A}_\mu = \frac{\tau^a}{2}A^a_\mu \quad \text{and} \quad \boldsymbol{F}_{\mu\nu}\frac{\tau^a}{2}F^a_{\mu\nu}, \tag{4.55}$$

where the τ^a's are once again the Pauli matrices.

The covariant derivative is given by

$$\boldsymbol{D}_\mu = \partial_\mu - ig\frac{\tau^a}{2}A_\mu - ig'\frac{1}{2}a_\mu, \tag{4.56}$$

which couples the complex Higgs doublet $\phi = (\phi_1, \phi_2)$ to the gauge fields of both symmetry groups at different strengths (g and g' for A^a_μ and a_μ respectively).

A general $SU(2)_L \times U(1)_Y$ gauge transformation $U = U_L U_Y$, acting on the Higgs and gauge fields, is made out of

$$U_L(x^\mu) = \exp\left(i\frac{\tau^a}{2}\theta^a(x^\mu)\right) \quad \text{and} \quad U_Y(x^\mu) = \exp\left(i\frac{1}{2}\alpha(x^\mu)\right), \tag{4.57}$$

where $\theta(x^\mu)$ and $\alpha(x^\mu)$ are the local gauge group parameter functions. Under such a transformation these fields transform as

$$\phi \to U\phi, \tag{4.58}$$

$$\boldsymbol{A}_\mu \to U_L^{-1}\boldsymbol{A}_\mu U_L + \frac{i}{g}U_L^{-1}\partial_\mu U_L, \tag{4.59}$$

$$a_\mu \to a_\mu + \frac{i}{g}U_Y\partial_\mu U_Y = a_\mu - \frac{1}{g}\partial_\mu\alpha. \tag{4.60}$$

In the full theory, the left-handed SM fermions interact as doublets with the $SU(2)_L$ gauge fields (in the fundamental representation, leptons paired with their neutrinos and quarks paired with their generation partners), while the right-handed particles do not participate and interact as singlets (i.e. in the trivial representation).

The effect of the $SU(2)_L$ and $U(1)_Y$ gauge transformations on each of the leptons is determined by their weak hypercharge T_3 and isospin Y. These are then conveniently included as operators (algebra elements) in the gauge transformations, picking up the right charges when the gauge transformation acts in each of the leptons. The factor of $\frac{1}{2}$, which begins appearing in equations 4.56 and 4.57, is the weak hypercharge of the Higgs field. Since we are only concerned with the Higgs field during this derivation, we have already substituted in this charge.

EW SSB and Gauge Boson Masses

The EW Lagrangian includes the famous "Mexican hat" potential $\mathcal{V}$, that results in SSB.

$$\mathcal{V}(\phi^\dagger\phi) = \lambda\left(\phi^\dagger\phi - \frac{v^2}{2}\right)^2. \tag{4.61}$$

In the process, the SM particles obtain their masses. For the gauge bosons we can tell that this happens in the following way.

A possible choice of VEV of the Higgs field (i.e. a possible value of ϕ that minimizes $\mathcal{V}$) is given by

$$\phi_0 = \frac{1}{\sqrt{2}}\begin{pmatrix}0\\ v\end{pmatrix}. \tag{4.62}$$

Only the mixed $U(1)$ gauge transformation

$$U_{\text{EM}}(x^\mu) = \exp\left(i\frac{\tau^3}{2}\alpha^a(x^\mu) + i\frac{1}{2}\alpha(x^\mu)\right) = \begin{pmatrix}e^{i\alpha(x^\mu)} & 0\\ 0 & 1\end{pmatrix} \tag{4.63}$$

leaves this VEV invariant. Hence it corresponds to the gauge symmetry of the electromagnetic interaction $U(1)_{\text{EM}}$ post SSB.

By substituting an expanded Higgs fields around ϕ_0 into the Lagrangian,

$$\phi(x^\mu) = \frac{1}{\sqrt{2}}e^{i\tau^a\xi^a(x)}\begin{pmatrix}0\\ v + H(x^\mu)\end{pmatrix}, \tag{4.64}$$

we can deduce what mass terms appear for the three broken and mixed $SU(2)_L \times U(1)_Y$ gauge bosons not included in $U(1)_{\text{EM}}$. Here, H and ξ^a correspond to a "radial" and "angular" excitation(s) in ϕ respectively. For that reason, H is a (electrically neutral) real valued scalar field. The angular fields ξ^a can be absorbed (or rotated away) by a local $SU(2)_L$ gauge transformation, these are the Goldstone bosons that get "eaten by the gauge fields". In this way, only a single Higgs d.o.f. remains: the post SSB Higgs field is simply H. The expanded covariant derivative term is responsible for the masses of the gauge bosons[13]. Substituting in the expanded version of ϕ with $\xi^a = 0$ gives

$$|\boldsymbol{D}\phi|^2 = \frac{1}{2}(\partial H)^2 + \frac{g^2}{8}\big[(A^1)^2 + (A^2)^2\big](H+v)^2 + \frac{1}{8}\big[g'a + gA^3\big]^2(H+v)^2, \tag{4.65}$$

from which we can tell that, using the conventions[14]

$$A^1_\mu A^{1\mu} + A^2_\mu A^{2\mu} = W^\dagger_\mu W^\mu \tag{4.66}$$

and

$$(g'a_\mu + gA^3_\mu)(g'a^\mu + gA^{3\mu}) = (g'^2 + g^2)Z_\mu Z^\mu + 0\cdot A_\mu A^\mu, \tag{4.67}$$

[13]The Lorentz indices have been suppressed, $(A^a)^2 = A^a_\mu A^{a\mu}$ and $|\boldsymbol{D}\phi|^2 = (\boldsymbol{D}_\mu\phi)(\boldsymbol{D}^\mu\phi)^\dagger$ etc.

[14]Complex fields halve, by convention, mass terms of the form $M_W^2 W^\dagger_\mu W^\mu$. On the other hand, scalar fields have an additional pre-factor of $\frac{1}{2}$, $\frac{1}{2}M_Z^2 Z_\mu Z^\mu$.

that $M_W = \frac{gv}{2\sqrt{2}}$ and $M_Z = \frac{v}{2}\sqrt{g'^2 + g^2}$. The Higgs mass itself can be found by considering the $\mathcal{V}$ term instead.

$$\mathcal{V}(\phi^\dagger\phi) = \lambda\left(\frac{1}{2}H^2 + vH\right), \tag{4.68}$$

from which we immediately deduce that $M_H = \sqrt{\lambda}$.

The mixing between $U(1)_Y$ and the $U(1)$ subgroup of $SU(2)_L$ (corresponding to τ^3) is quantified by the previously mentioned Weinberg angle θ_W. By convention,

$$\cos(\theta_W) = \frac{g'}{\sqrt{g'^2 + g^2}} \quad \text{and} \quad \sin(\theta_W) = \frac{g}{\sqrt{g'^2 + g^2}}. \tag{4.69}$$

4.3.2 The EW Sphaleron

We can now begin the actual (zero temperature) EW sphaleron derivation. We let the $\theta_W \to 0$. This leaves us with just the Higgs and $SU(2)_L$ gauge fields, whose gauge bosons now have equal masses, $M = \frac{gv}{2\sqrt{2}}$. The potential energy functional V, whose saddle point we are going to find, is given by

$$V[\Phi] = \int d^4x \left[\frac{1}{2}\operatorname{Tr}(\boldsymbol{F}_{ij}\boldsymbol{F}_{ij}) + (\boldsymbol{D}_i\phi)^\dagger(\boldsymbol{D}_i\phi) + \mathcal{V}(\phi, \phi^\dagger)\right]. \tag{4.70}$$

Take note that we have used $\boldsymbol{\Phi}$ as a surrogate for the complete collection of fields once again.

To make the derivation easier, we will normalize the Higgs field $\phi \to \frac{v}{\sqrt{2}}\phi$. This makes sure the VEV of ϕ is simply 1, $\phi_0 = (0, 1)$. This reproduces the conventions used in Manton's original paper[28] (Note the prefactor for the covariant derivative term).

$$V[\Phi] = \int d^4x \left[\frac{1}{2}\operatorname{Tr}(\boldsymbol{F}_{ij}\boldsymbol{F}_{ij}) + \frac{v^2}{2}(\boldsymbol{D}_i\phi)^\dagger(\boldsymbol{D}_i\phi) + \frac{\lambda v^4}{4}(\phi^\dagger\phi - 1)^2\right]. \tag{4.71}$$

At the end we can undo the scaling on ϕ and obtain the true Higgs field configuration of the sphaleron.

We will derive the sphaleron in radial + temporal gauge: $\boldsymbol{A}_0 = 0$ and $\boldsymbol{A}_i n_i = 0$ (n_i being an outward pointing normal vector in $\mathbb{R}^3$). This will fix the gauge of the fields almost completely, except for the global $U(1)_Y$ symmetry[15]. To get rid of this freedom as well (and therefore to fix the gauge completely), we force ϕ to take on a specific value along a predefined axis. Let us choose, for instance, the z-axis and make sure that $\phi \to (0, 1)$ as $x^3 \to \infty$. Manton calls this a "base point condition". With complete gauge fixing in place, this has become a true physical gauge, there is only a single vacuum:

$$\boldsymbol{\Phi}_{\text{vac.}} = \left\{\phi = \begin{pmatrix}0\\1\end{pmatrix}, \quad \boldsymbol{A}_\mu = 0\right\}. \tag{4.72}$$

[15] Global, since we ignored $U(1)_Y$'s gauge field.

Topology of the EW theory in the Temporal + Radial Gauge

The topology of the finite V field configurations space C_V is determined *completely* by the asymptotics of the Higgs and gauge fields as $|\vec{x}| \to \infty$. Each asymptotic being a unique[16] function $\mathbf{\Phi}^\infty$ that maps each point on the boundary of space $\partial\mathbb{R}^3$ to a zero of $\mathcal{V}$ (given that these functions satisfy the base point condition). The fields need to approach a zero of $\mathcal{V}$ for V to be finite (otherwise the configuration in question does not belong in C_V by definition). Let us call the space of asymptotic field configurations $\mathrm{Maps}(\partial\mathbb{R}^3 \to \ker\mathcal{V})$, then

$$C_V \cong \mathrm{Maps}(\partial\mathbb{R}^3 \to \ker\mathcal{V}) \cong \mathrm{Maps}(\partial\mathbb{R}^3 \to SU(2)) \cong \mathrm{Maps}(S^2 \to S^3). \tag{4.73}$$

The second equality follows from the theorem discussed in section 2.3.2 of chapter 2: $\ker V \cong G/H = (SU(2)_L \times U(1)_Y)/U(1)_{\mathrm{EM}} \cong SU(2)$. Note in particular that this topological argument is independent of the mixing of $SU(2)_L$ and $U(1)_Y$. The EW sphaleron stays an $SU(2)$ sphaleron at all mixing angles. The third equality follows from the fact that the boundary of space $\partial\mathbb{R}^3 \cong S^2$ and the gauge groups $SU(2) \cong S^3$. Note that, even though we deduce the topology of $\ker V$ from G/H, that the sphaleron will turn out to be a non-trivial configuration for the entire Higgs doublet (and not just H) at zero temperature.

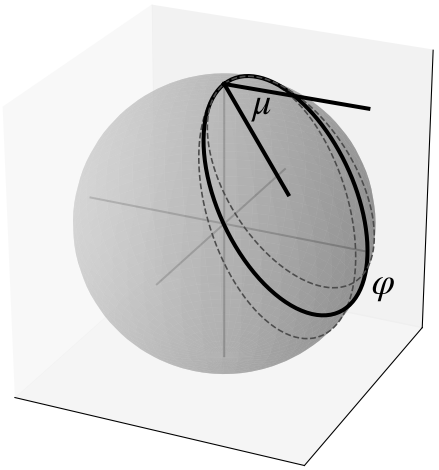

Figure 4.6: An alternative way to parameterize the points of S^2, taking S^1 cross sections of S^2 (parametrized by the azimuthal angle φ) at an polar angle μ.

We can already discuss the existence of solitons and sphalerons in the EW theory. Maps from S^2 to S^3 can always be deformed to the trivial map (mapping all of $\partial\mathbb{R}^3$ to ϕ_0). In other words, C_V has no disconnected components, $\Pi_0(C_V) = \Pi_0(\mathrm{Maps}(S^2 \to S^3)) = \mathbb{1}$. Hence, the EW theory does not have any solitons in addition to instantons. On the other hand, the topology of C_V is *not* trivial: $\Pi_1(C_V) \cong \Pi_1(\mathrm{Maps}(S^2 \to S^3)) = \Pi_3(S^3) = \mathbb{Z}$ (recall from section 2.3.1 that $\Pi_n(\mathrm{Maps}(S^m \to X) = \Pi_{n+m}(X))$. This is ultimately the reason why the EW sphaleron exists, there is an NCL in C_V inherited from a loop in the space of asymptotic field configurations $\mathrm{Maps}(\partial\mathbb{R}^3 \to \ker\mathcal{V})$.

The EW Sphaleron in the Temporal + Radial Gauge

To find the sphaleron, we begin with an NCL of asymptotic field configurations that crosses both the asymptotics of the vacuum and the asymptotics of the sphaleron. This becomes a loop in C_V itself by supplementing the field already known at the boundary $\partial\mathbb{R}^3$ using an ansatz over all of $\mathbb{R}^3$. The Higgs component of the loop of asymptotics $\mathbf{\Phi}^\infty(\theta, \varphi; \mu) =$

[16] Unique, since the covariant derivative term in V fixes the asymptotic behavior of $\boldsymbol{A}_\mu$ to that of ϕ.

$\{\phi^\infty(\theta,\phi;\mu), \boldsymbol{A}^\infty_\mu(\theta,\phi;\mu)\}$ is given by

$$\phi^\infty(\theta,\varphi;\mu) = \begin{pmatrix}\phi_1^\infty \\ \phi_2^\infty\end{pmatrix} = \begin{pmatrix}\sin\mu\sin\theta e^{i\varphi} \\ e^{-i\mu}(cos\mu + i\sin\mu\cos\theta).\end{pmatrix}, \tag{4.74}$$

where $\theta \in [0,\pi]$ is the polar angle (measured w.r.t. the z-axis) and $\varphi \in [0,2\pi]$ is the azimuthal angle (measured w.r.t. the x-axis) used to label the point of $\partial\mathbb{R}^3$. $\mu \in [0,\pi]$ is the loop paramater, it maps the point $\mu = 0,\pi$ to the vacuum.

This map covers all of $\ker\mathcal{V}$ once as μ goes from 0 to π. It therefore belongs to the homotopy class of unit winding number of $\Pi_1(\partial\mathbb{R}^3 \to \ker\mathcal{V}) \cong \Pi_3(S^3)$. The reason why this map covers all elements once, is because μ is essentially the second polar angle (recall μ's interval) in the triplet (μ,θ,ϕ) used as a conventional coordinate system for the points of S^3. Figure 4.6 illustrates as analogous coordinate system used to label the points of S^2. The figure also nice illustrates why the base point condition remains satisfied for each value of μ, it is the "pivot point" for the plane at which the S^1 cross section of S^2 are taken.

The asymptotic field configuration of the gauge fields $\boldsymbol{A}^\infty_\mu$ is not independent from ϕ^∞. The covariant derivative term in V need to vanish there also. This once again couples the asymptotic behaviors of the Higgs and gauge fields together. From ϕ^∞ we can construct the following gauge transformation, which maps each point on the boundary to an element of $SU(2)$:

$$U_\infty^{-1} = \begin{pmatrix}\phi_2^{\infty *} & \phi_1^\infty \\ -\phi_1^{\infty *} & \phi_2^\infty\end{pmatrix} = \Big|_{\mu=\frac{\pi}{2}} \quad \begin{pmatrix}\cos\theta & \sin\theta e^{i\varphi} \\ -\sin\theta e^{-i\varphi} & \cos\theta\end{pmatrix}. \tag{4.75}$$

By defining

$$\boldsymbol{A}^\infty_\alpha = \frac{i}{g} U_\infty^{-1}\partial_\alpha U_\infty, \quad \alpha = \{\theta,\varphi\}, \tag{4.76}$$

we make sure that $\boldsymbol{D}_\theta\phi^\infty = 0$ and $\boldsymbol{D}_\varphi\phi^\infty = 0$. We have thereby found the gauge component of $\boldsymbol{\Phi}^\infty(\theta,\varphi;\mu)$. It also allows us to write $\phi^\infty = U_\infty^{-1}\phi_0$, which shows us why the base point condition allows us to explicitly associate each zero of $\ker\mathcal{V}$ with an element of $G/H \cong SU(2)$.

The next step will be to put V, as given in equation 4.71, in spherical coordinates. Let $r^\alpha = (r,\theta,\varphi)$ be the vector $x^i = (x,y,z)$ in spherical coordinates, then the change of variables is specified by

$$R_\alpha{}^i = \frac{\partial x^i}{\partial r^\alpha}, \quad g^{\alpha\beta} = R^\alpha{}_i\, R^\beta{}_j\, g^{ij}, \quad g^{\alpha\beta} = \begin{pmatrix}1 & & \\ & \frac{1}{r^2} & \\ & & \frac{1}{r^2\sin^2\theta}\end{pmatrix}, \tag{4.77}$$

where $g^{\alpha\beta}$ is the inverse metric and $R_\alpha{}^i$ the inverse Jacobian. In any other coordinate

system, and specifically in spherical coordinates, V is given by

$$V[\mathbf{\Phi}] = \int \sqrt{\det g}\; d^3r \left[\frac{1}{2}g^{\alpha\rho}g^{\beta\sigma}\,\mathrm{Tr}(\boldsymbol{F}_{\alpha\beta}\boldsymbol{F}_{\rho\sigma}) + \frac{v^2}{2}g^{\alpha\beta}(\boldsymbol{D}_\alpha\phi)^\dagger(\boldsymbol{D}_\beta\phi) + \frac{\lambda v^4}{4}(\phi^\dagger\phi - 1)^2\right]$$

$$\begin{aligned} = \int r^2\sin^2\theta\; dr d\theta d\varphi \Bigg[&\frac{1}{r^2}\,\mathrm{Tr}(\boldsymbol{F}_{r\theta}\boldsymbol{F}_{r\theta}) + \frac{1}{r^4\sin^2\theta}\,\mathrm{Tr}(\boldsymbol{F}_{r\varphi}\boldsymbol{F}_{r\varphi}) \\ &+ \frac{1}{r^4\sin^2\theta}\,\mathrm{Tr}(\boldsymbol{F}_{\theta\varphi}\boldsymbol{F}_{\theta\varphi}) + \frac{v^2}{2}(\boldsymbol{D}_r\phi)^\dagger(\boldsymbol{D}_r\phi) + \frac{v^2}{2r^2}(\boldsymbol{D}_\theta\phi)^\dagger(\boldsymbol{D}_\theta\phi) \\ &+ \frac{v^2}{2r^2\sin^2\theta}(\boldsymbol{D}_\varphi\phi)^\dagger(\boldsymbol{D}_\varphi\phi) + \frac{\lambda v^4}{4}(\phi^\dagger\phi - 1)^2\Bigg]. \end{aligned} \tag{4.78}$$

We will now present the ansatz that completes $\mathbf{\Phi}^\infty(\theta,\varphi;\mu)$ over all of $\mathbb{R}^3$, here $r = |\vec{x}|$. It contains two, yet to be determined, radial functions f and h.

$$\phi(r,\theta,\varphi;\mu) = (1-h(r))\begin{pmatrix}0\\ e^{-i\mu}\cos\mu\end{pmatrix} + h(r)\phi^\infty(\theta,\varphi;\mu) \tag{4.79}$$

$$\boldsymbol{A}_\alpha(r,\theta,\varphi;\mu) = f(r)\boldsymbol{A}^\infty_\alpha(\theta,\varphi;\mu), \quad \alpha = \{\theta,\varphi\}, \tag{4.80}$$

for which the radial functions f and h have to satisfy

$$\lim_{r\to\infty} f,h = 1 \quad \text{and} \lim_{r\to 0} f,h = 0, \tag{4.81}$$

such that the asymptotic agree with our earlier results and such that (as $r \to 0$) the fields are smooth[17]. Note that the ansatz satisfies the radial gauge condition, $\boldsymbol{A}_r = 0$, because of equation 4.75.

We will now minimize V half way along the loop, at $\mu = \frac{\pi}{2}$, at what we suspect is the sphaleron point. At this point (see equation 4.75), the Higgs component of the field is simply given by

$$\phi(r,\theta,\phi) = h(r)\begin{pmatrix}\sin\theta e^{i\varphi}\\ \cos\theta\end{pmatrix}. \tag{4.82}$$

It has an additional symmetry $SO(3)$ and reflection symmetry[30, p.457]. This makes it, by the principle of symmetric criticality, the most likely candidate for the sphaleron configuration.

Plugging this ansatz into V gives us the following spherically symmetric functional

$$V[\mathbf{\Phi}] = \Big|_{\mu=\frac{\pi}{2}}\; 4\pi\int dr\left[\frac{4}{g^2}f'^2 + \frac{8}{g^2}\frac{f^2}{r^2}(f-1)^2 + r^2h'^2 + 2h^2(f-1)^2 + \frac{\lambda}{2}r^2(h-1)^2\right], \tag{4.83}$$

as the angular d.o.f. separate and can be integrated out. That the energy density is spherically symmetric at the sphaleron is precisely such an additional symmetry expected of a sphaleron.

[17] One might wonder whether the large r boundary condition for f is even required. As $\boldsymbol{A}^\infty_\mu$ is pure gauge, would that not make $\boldsymbol{F}_{\theta\varphi}$ vanish? This turns out not to be the case in polar coordinates, no terms in V turn out to vanish, specifically, $\mathrm{Tr}(\boldsymbol{F}_{\theta\varphi}\boldsymbol{F}_{\theta\varphi}) \neq\big|_{r=\infty}\; 0$.

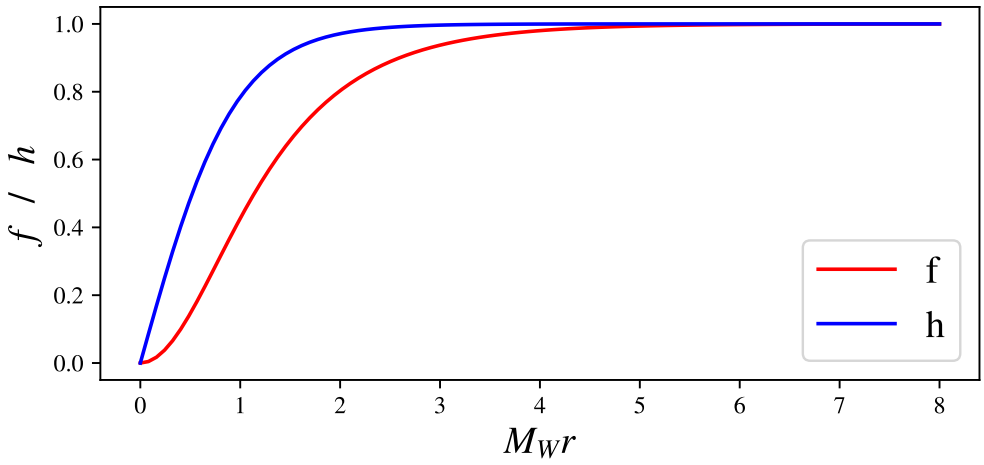

Figure 4.7: Plot of the approximate solutions of the radial functions that specify the sphaleron.

The variational equations for f and h obtained by minimizing V at $\mu = \frac{\pi}{2}$ are

$$r^2 f'' = 2f(f-1)(2f-1) + \frac{g^2 v^2}{4} r^2 h^2 (f-1), \tag{4.84}$$

$$(r^2 h')' = 2h(f-1)^2 + \lambda v^2 r^2 h(h^2-1). \tag{4.85}$$

These cannot be solved analytically, but it has been established that a smooth solution for f and h exists and a numerical solution as a function of λ has also been found[30, p.458]. The true EW sphaleron can now be found by substituting f and h into equation 4.80 at $\mu = \frac{\pi}{2}$, except that the Higgs field still needs to be shifted back, $\phi \to \frac{\sqrt{2}}{v}\phi$, to undo our normalization. Given the current day values of the Higgs mass (125 GeV) and Higgs VEV (246 GeV), the mass of this zero temperature EW sphaleron, in the $\theta_W \to 0$, limit comes out to be 9.11 TeV. In a paper by Tye and Wong[37], which we discuss in the next chapter, an approximate solution for f and h is given by

$$f(r) \approx 1 - \operatorname{sech}(aM_W r) \quad \text{and} \quad h(r) \approx \tanh(bM_W r), \tag{4.86}$$

where $a = 1.154$ and $b = 1.056$ are two numerically fitted parameters. Figure 4.7 shows a plot of these approximate solutions.

If this sphaleron would be put in the supplemented temporal gauge, then it would, like the sphaleron in the Abelian Higgs model, reside on a barrier between CS-vacua. In that case, the loop parameter μ is related to the CS-number of the fields[37]

$$N_{\text{CS}}(\mu) = \frac{1}{\pi}\left(\mu - \frac{\sin(2\mu)}{2}\right), \tag{4.87}$$

In other words, the N_{CS} of the sphaleron is $\frac{1}{2}$ when $\mu = \frac{\pi}{2}$ (which corresponds to the EW sphaleron residing on the barrier between CS-vacua with $N_{\text{CS}} = 0$ and $N_{\text{CS}} = 1$).

Chapter 5

Fermions in Sphaleron Backgrounds

We have discussed theories that have had solitons, instantons and sphalerons as special classical field configurations. Of these three, we have discussed the physical implications of instantons most fully: They bring about vacuum-to-vacuum tunneling that influences the quantum picture of the gauge field vacuum. For the pure Yang-Mills theory this meant the appearance of a vacuum angle θ, whose interpretation differs depending on the supplemented temporal or physical gauge used to quantize the theory. On the other hand, the previous chapter's discussion of sphalerons was purely classical: We saw the Abelian-Higgs model's classical vacuum structure have a similarly gauge dependent character (with CS-vacua in the supplemented temporal gauge), the same was true for the EW theory. The sphaleron's true physical significance comes about when fermions are finally introduced into the picture: fermionic quantum numbers can change in gauge field background with special topology such as instantons and sphalerons. This is going to be the topic of this chapter, in which we will pay special attention to the SM and its regular (non-thermal) EW sphaleron. In the case of the SM, these fermionic quantum numbers are the baryon B and lepton L_l numbers ($l = e, \mu, \tau$), for which violating processes related to the EW sphaleron exist. Moreover, fermions impact the vacuum angle θ of the EW and QCD gauge field vacuum, which we will also get to discuss.

One might wonder how B and L are supposed to be violated, since they are classically conserved. They are the charges corresponding to the four *global vector symmetries* $U(1)_{B/L_l}$ of the SM action. As it turns out, these symmetries disappear on a quantum level: they are said to be *anomalous*. In other words, these symmetries of the Lagrangian are only emergent in the classical limit, they are not true symmetries of nature. Hence, their currents J^μ_B and J^μ_l are not conserved, they are anomalous:

$$\partial_\mu J^\mu_B = \frac{g^2 N_f}{32\pi^2} F^a_{\mu\nu} \tilde{F}^{a\,\mu\nu} \quad \text{and} \quad \partial_\mu J^\mu_{L_l} = \frac{g^2 N_f}{32\pi^2} F^a_{\mu\nu} \tilde{F}^{a\,\mu\nu}, \tag{5.1}$$

where $N_f = 3$ is the number of generations in the SM. The right hands of these anomalies bear striking resemblance to the winding numbers we met in chapter 3 (such as equation 3.30), this is no coincidence, this is how instantons and sphalerons get involved. The

anomaly reflects the phenomenon that CS-number changes in the EW sector's gauge fields produce SM fermions. Specifically, when $\Delta N_{\text{CS}} = N$, such processes satisfy the selection rule[33, p.388][1]

$$\Delta L_e = \Delta L_\mu = \Delta L_\tau = \frac{1}{3}\Delta B = N, \tag{5.2}$$

hence $\Delta(B+L) = 6N$ and[2] $\Delta(B-L) = 0$: The transitions produce matter without anti-matter (or vice versa). Thus far such processes have not been observed, though they might be seen in (future) collider experiments[37][36][31]. Moreover, these processes might be a key-ingredient for generating the matter-antimatter asymmetry of te observable universe[33, ch.17 §4][26][32].

In section 5.1 we discuss the anomalies and their implications for the SM's quantum theoretic vacuum structure by first looking at a toy model with an anomaly. Its discussion brings together the topic of vacuum angles, which we discussed in regards to the pure Yang-Mills theory (section 3.3), with the EW sector we examined when deriving the EW sphaleron (section 4.3). As we alluded at the end of section 3.3.4, it turns out that having an anomalous physical symmetry can make the vacuum angles of specific gauge sectors unphysical. In the SM model, this happens to the θ angle of the EW sector. The θ angle of the QCD sector stays physical because the SM fermions are massive (obtain their mass through the Higgs mechanism). The difference in behavior is explained by the nature of these interactions: The $SU(2)_L \times U(1)_Y$ EW interaction is chiral, while the $SU(3)_c$ QCD interaction is vector instead. Furthermore, we will see how the existence of fermions shifts QCD's vacuum angle.

In section 5.2.1, we discuss a semiclassical technique to describe the non-conservation of fermionic quantum numbers such as B and L[33, ch.14, ch.15 §2][25]. Specifically, we describe electrons using Dirac spinors and make extensive use of the Dirac sea picture of energy levels of the Dirac Hamiltonian (to be interpreted semiclassically). The background gauge fields are instead treated as classical external parameters unchanged by the presence of the fermions, the technique therefore has its limitations[33, p.305]. Nonetheless, it predicts the production of particles as CS-number changes: The levels flow as the background fields changes, producing particles when a level crosses zero. The techniques reproduces the anomaly's effect and selection rules[3].

It has recently been proposed by Tye and Wong that sphaleron transitions might actually have a resonance feature[37][36][31], which makes sphaleron transitions much more likely to occur. If correct, sphaleron transition might be visible in future collider experiments at energies much lower than conventional beliefs suggest. It might even make them observable at the IceCube experiment[17]. At the moment, the implications of the resonance feature for the thermal EW sphaleron processes used in explanations of the origin the matter-antimatter asymmetry remain unexplored. To come up with their prediction, Tye and Wong used an alternative but novel technique, which they, however, did not spend

[1] These selection rules agree with the conservation of all other charges, such as electric charge. This must be so, otherwise there would have been anomalies in gauge symmetry in the SM. These turn a theory inconsistent, only anomalies in global symmetries are allowed.

[2] This second rule is an accidental symmetry within the SM caused by the right hand sides of the anomalies being the same.

[3] In this view, the anomaly is essentially a local version of the Atiyah-Singer index theorem[25].

much time on discussing in their original paper[37]. Follow-up papers have since then addressed these concerns[36][31]. Based on these works, we discuss conceptually, in section 5.3, the premises regarding vacuum structure that lay behind their technique. We also give a rudimentary overview of the phenomenology of sphaleron transitions in colliders, including the accepted wisdom regarding the degree of suppression the process experiences which Tye and Wong contradict.

5.1 SM Anomalies and Their Effect on the Vacuum Angles

In this section, we discuss SM anomalies further: We examine why they exist and we argue what consequences they have for the vacuum angle of the EW and QCD sector. As we will see, the angle of the EW sector disappears while the QCD angle sticks around.

We notice that a symmetry is anomalous exists when it fails to survive quantization. We can tell by looking at the path integral measure: The path integral measure itself (hence the partition function) is not invariant under the corresponding classical symmetry, even though the Lagrangian is. This was first shown by Fujikawa[18], who considered the effect of axial rotations on the path integral measure.

5.1.1 The Fujikawa Anomaly Derivation and the Vacuum Angle

Before talking about the SM, let us consider what Fujikawa's results can tell us about the vacuum angle of a simpler theory that has an anomaly. For the actual derivation we refer to the original paper[18], we instead highlight the important consequences of the non-invariance of the measure.

Let us, for instance, consider a QCD-like theory with a single massless quark, as discussed by Schwichtenberg[34]

$$\mathcal{L} = -\frac{1}{4} G^a_{\mu\nu} G^{a\,\mu\nu} + \bar{\psi}\gamma^\mu (i\partial_\mu - g A_\mu)\psi, \tag{5.3}$$

where $G^a_{\mu\nu}$ is the $SU(3)_c$ gauge field tensor, A_μ are its gauge fields, γ^μ are the Dirac matrices and where ψ the quark's Dirac spinor. Naively it appears, since this model is a Yang-Mills theory with fermions, that its gauge sector must have a vacuum angle θ. As it turns out, is does not.

Let us begin by noticing that this model has two global symmetries (one is vector and one is axial),

$$U(1)_V : \psi \to e^{i\phi_v}\psi \quad \text{and} \quad U(1)_A : \psi \to e^{i\gamma^5\phi_a}\psi, \tag{5.4}$$

given the "fifth" Dirac matrix $\gamma^5 = -i\gamma^0\gamma^1\gamma^2\gamma^3$. Note that the $U(1)_A$ symmetry appears because the quark is massless, mass terms (or a Yukawa interaction terms) would break the axial symmetry explicitly. Of these two symmetries, $U(1)_A$ becomes anomalous. According to Fujikawa, under such a $U(1)_A$ rotation the path integral measure transforms non-trivially, producing a term that can be absorbed into the Lagrangian[18][34]:

$$\mathcal{L} \to \mathcal{L} + \frac{g^2\phi_a}{16\pi^2} G^a_{\mu\nu}\tilde{G}^{a\,\mu\nu}. \quad \mathcal{L}_{\text{eff}} = \mathcal{L} - \frac{g^2\theta}{32\pi^2} F^a_{\mu\nu}\tilde{F}^{a\,\mu\nu} \tag{5.5}$$

From this term the anomaly is derived by functional variation of the partition function[21]. Specifically, $U(1)_A$'s anomalous current, $J_5^\mu = \psi\gamma^\mu\gamma^5\psi$, satisfies

$$\partial_\mu J_5^\mu = \frac{g^2}{8\pi^2} G^a_{\mu\nu}\tilde{G}^{a\,\mu\nu}. \tag{5.6}$$

At the time, the existence of this anomaly was not a new result[2][6]. It had historically first been computed using a triangle diagram. Even today, computing such a diagram is a quick way of determining whether a current is anomalous. Conventionally, anomalies have been labeled by the symmetries of the particles and currents appearing at the vertices. This makes this model's anomaly an $SU(3)_c^2 U(1)_A$ anomaly. As it turns out, these anomalies are actually 1-loop exact[4].

Not the anomaly itself, but the newly produced Fujikawa-term lets us say something about the vacuum angle θ of this model's gauge sector. The term looks remarkably similar to the θ-term that appears in the Yang-Mills Lagrangian given a particular θ-sector, recall equation 3.62. *If $U(1)_A$ would have been a true symmetry of the system* (which we know it is not, since it is anomalous), then we could have concluded that the vacuum angle θ has been turned unphysical by the fermions: Under, what would have been, a symmetry transformation, $\theta \to \theta + 2\phi_a$ according to equation 5.5. This means θ cannot have any physical consequences, since we are free to perform symmetry transformations in any way we like. In particular, we could choose $\phi_a = -\frac{\theta}{2}$ to set $\theta = 0$, it is then said that θ "can be rotated away by an axial transformation". θ cannot not show up in a physical quantity.

Nontheless, θ is still unphysical in this theory for almost this exact reason. This is because we can very easily use J_5^μ to construct a proper conserved current $\tilde{J}_5^\mu$, which must correspond to some true $U(1)_A$ symmetry of the system, let us call it $\tilde{U}(1)_A$. In particular, let it transform $\psi \to \exp(i\tilde{Q}_5\phi)\psi$ using its charge $\tilde{Q}_5$. Constructing such a new current dates back to the original paper on the Yang-Mills vacuum structure by Jackiw and Rebbi[22] as well as the paper by Callan, Dashen and Gross[9], both of which we have discussed before. More in depth discussions about this construction can also be found in the book by Cheng and Li[11, ch.16 §3] as well as other sources[36][34].

We construct $\tilde{J}_5^\mu$ as the difference

$$\tilde{J}_5^\mu = J_5^\mu - \frac{g^2}{8\pi^2} K^\mu, \tag{5.7}$$

where we use the fact that $G^a_{\mu\nu}\tilde{G}^{a\,\mu\nu}$ can be written as the divergence of some current depending on the gauge fields. We have done this before, recall equation 3.31. Let

$$\frac{1}{4} G^a_{\mu\nu}\tilde{G}^{a\,\mu\nu} = \partial_\mu K^\mu, \tag{5.8}$$

then $\tilde{J}_5^\mu$ is actually the conserved current we were looking for, it is conserved on account on equations 5.6 and 5.8. Therefore, we have implicitly found the true $\tilde{U}(1)_A$ symmetry that can rotate θ away. ($\tilde{U}(1)_A$ transformations still produce Fujikawa terms in the partition function.)

[4] They receive no further corrections from higher order diagrams.

Note that this whole story was only possible because the Lagrangian had an axial symmetry (that turned out to be anomalous) which we could "fix" and use to rotate θ away. If the quark would have been massive, then this axial symmetry would have been explicitly broken en de argument could not have proceeded: θ would have remained physical.

5.1.2 An Original Argument for the Vanishing of the Vacuum Angle

Rotating away θ in the partition function using $\tilde{U}(1)_A$ is the more modern view on the vanishing of vacuum angles. The original argument in the papers by Jackiw and Rebbi[22] and Callan, Dashen and Gross[9] had a different form and used state vector notation. This argument also occurs from time to time in literature[11, ch.16 §3][34], including the papers by Tye et. al. on resonant sphaleron transitions[36][31]. We present it here, employing the notation from section 3.3.4 to refer to quantities such as the Hamiltonian H, large gauge transformations T and the θ-vacuum state $|\theta\rangle$.

Let us begin by recalling that K^μ is not gauge invariant, which includes large gauge transformations. This means that the current $\tilde{J}_5^\mu$ and the charge $\tilde{Q}_5$ are not gauge invariant either, this a feature of these quantities. In particular, under a large gauge transformation T (that has $N_{\mathrm{CS}} = 1$ and hence maps between CS-vacua for which $\Delta N_{\mathrm{CS}} = 1$), $\tilde{Q}_5$ transforms as[11, p.491][9][22][36]

$$\tilde{Q}_5 \to T^{-1}\tilde{Q}_5 T = \tilde{Q}_5 + 2n \quad \Rightarrow \quad [\tilde{Q}_5, T^n] = 2n\, T^n. \tag{5.9}$$

Additionally, note that the conservation of $\tilde{Q}_5$ can be written as

$$[\tilde{Q}_5, H] = 0. \tag{5.10}$$

Equation 5.9 implies that under the symmetry transformation $\exp(i\tilde{Q}_5\phi) \in \tilde{U}(1)_A$, that the θ-vacuum of this model's gauge sector satisfies

$$T e^{i\tilde{Q}_5\phi}\,|\theta\rangle = e^{i(\tilde{Q}_5+2)\phi}\,T\,|\theta\rangle = e^{i(\theta+2\phi)} e^{i\tilde{Q}_5\phi}\,|\theta\rangle\,. \tag{5.11}$$

The equation shows that $\exp(i\tilde{Q}_5\phi)\,|\theta\rangle$ is an eigenstate of T with eigenvalue $e^{i(\theta+2\phi)}$, see section 3.3.4. In addition, we know it is an eigenstate H on account of equation 5.10. The transformed state is therefore another θ-vacuum, $\exp(i\tilde{Q}_5\phi)\,|\theta\rangle = |\theta + 2\phi\rangle$. In other words, $\tilde{U}(1)_A$ transformations map between θ-sectors. Since $\exp(i\tilde{Q}_5\phi)$ is a global symmetry of the theory, we must identify the initial and final state: $|\theta\rangle = |\theta + 2\phi\rangle$ for arbitrary ϕ. In other words, all θ-vacua are physically equivalent and identified. In particular, they have the same energy because of equation 5.10,

$$H\,|\theta + 2\phi\rangle\,|\theta\rangle = e^{i\tilde{Q}_5\phi}\,H\,|\theta\rangle = E_\theta\,|\theta + 2\phi\rangle\,. \tag{5.12}$$

We have "collapsed" the band structure (recall figure 3.4) of this theory's gauge sector, θ has turned unphysical. This agrees with the result from simply rotating θ away in the Lagrangian.

Cheng and Li give a further argument to explain why θ has all of a sudden disappeared[11, p.491]: The instanton corrections to matrix elements of operators O, such as we discussed in section 3.3.4 (O can itself have some chirality, say k), now satisfy

$$e^{i\theta}\,\langle n+1|\,O\,|n\rangle \sim \delta_{(n+1)-n,k}. \tag{5.13}$$

In particular,

$$\langle n|\, e^{-iHt}\, |m\rangle \sim \delta_{n,m}. \tag{5.14}$$

Tunneling between n-vacua has therefore ceased: There is no longer a θ-vacuum. Once again this argument requires the fermions to be massless.

5.1.3 Anomalies, Vacuum Angles and the Strong CP Problem in the SM

The QCD-like theory with massless quark is an example of a scenario where an axial current obtained an axial anomaly in the presence of a vector interaction. We can now turn our attention to the SM, which, on the other hand, has no axial (or chiral) symmetries. The SM only has the four aforementioned global vector symmetries $U(1)_{B/L_l}$ that classically correspond to the conservation of baryon number B and three lepton numbers L_l ($l = e, \mu, \tau$). Their currents, as we have seen, are anomalous, equation 5.1.

Notice that only the gauge fields of the SM's chiral interaction, the EW sector, appears in the anomaly. There is no contribution from the vector QCD-sector. As we alluded to in the introduction, the chiral and vector nature of these interaction are responsible: The measure pays attention to each interaction's character when producing Fujikawa terms. Let us discuss the vector rotation $U(1)_{B/L/B+L}$ as made out of a left and right handed component, $U(1)_V \sim U(1)_{L+R}$. Then the Fujikawa term for the EW sector comes from the $U(1)_L$ component alone. For the QCD sector, the measure produces both an $U(1)_L$ and $U(1)_R$ term that cancel out with each other[25]. In any case, we can construct some conserved $\tilde{J}^\mu_B$ (or instead $\tilde{J}^\mu_L$ or some combination $\tilde{J}^\mu_{B+L}$) that we can use to rotate the EW vacuum angle away.

The Strong CP Problem

In the SM, the quarks have the Cabibbo-Kobayashi-Maskawa (CKM) mass matrix M that introduces some CP violation into the SM through the QCD sector. This matrix is one that we would like to real and diagonal when we work with it. In general, this requires us to perform an axial rotation on our system (the partition function) nonetheless[34]. As a consequence, the vacuum angle is shifted w.r.t. its innate value by the generated Fujikawa-term.

$$\theta \to \bar{\theta} \equiv \theta + \mathrm{Argdet}(M), \tag{5.15}$$

where $\mathrm{Argdet}(M)$ is the argument of the complex phase which is the determinant of the unitary CKM matrix. (This is also visible in the simple one quark model discussed above: introducing a mass term $m\bar{\psi}\psi$ and performing a chiral transformation, which is no longer a symmetry, transforms this term into $e^{i\phi}\, m\bar{\psi}\psi$.)

According to experiment[21] $\bar{\theta} \ll 10^{-10}$, which is exceptionally small for a variable that is, at least in the SM, completely unconstrained: There is almost (or possibly exact) cancellation of the vacuum angle and the mass matrix phase angle. Since CP violation is generated by the $\bar{\theta}$-term, the experimental size of $\bar{\theta}$ presents a puzzle, the so-called *strong CP problem*: Why is CP violated so weakly in QCD[5]? In principle, we have already seen a solution, if a single quark in the SM is massless, for instance the u-quark, then the SM

[5]Having massive fermions and thus a vacuum angle θ, including its term in the Lagrangian, does not

obtains a new axial symmetry. The current will then be anomalous and the QCD vacuum angle can then be rotated out. This solution, however, appears to be ruled out on theoretical grounds[21]. Other explanations are considered, such as the *Peccei-Quinn mechanism* where θ is taken so be field whose particles are termed *axions*[16].

5.2 Spectral Flow and Non-conservation of Fermion Number

In this section we discuss a specific semiclassical technique that can predict phenomena of fermions in external (topological) bosonic fields (such as gauge fields). One such phenomenon is charge fractionalization: Field states occur with a fractional electric charge when fermions are placed in a (anti-) kink soliton background, this has been observed in condensed matter systems[33, ch.15 §1].

Specifically, we present and summarize, based on chapter 14 and 15 from the book by Rubakov[33], the way in which this technique is used to discuss the non-conservation of fermionic quantum numbers and its connection with CS-number changes. We keep this discussion largely conceptual, highlighting the key points and leaving the computational details to the book itself. The most important prediction of the technique is that it reproduces the anomaly's consequences such as the selection rules from a different point of view. An analogous technique in Euclidean spacetime was used by 't Hooft in his famous work on the production of fermions in instanton backgrounds[1], which was later shown to be equivalent to the technique as we apply it here[33, p.336].

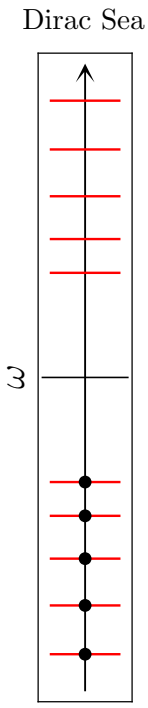

Figure 5.1

As it turns out, the interaction of fermions with bosonic fields (not necessarily gauge fields) can in many cases be probed by treating the fermions as a classical Dirac spinors in a classical bosonic field configuration chosen independently as an external parameter. As we will see, the flow of eigenvalues of the classical Dirac Hamiltonian can tell us about the fermions states. In reality, the presence of fermions changes the background field ever so slightly. For this technique to work, it is therefore required that this effect is negligible. According to Rubakov this happens in quite a few circumstances. In his example of charge fractionalization, the fermion mass (or Higgs VEV) needs to be much smaller than the energy of the background field configuration[33, p.331].

5.2.1 The Dirac Equation, its Energy Levels and the Dirac Sea

Before looking at the spectral flow of the Hamiltonian, let us briefly summarize what the classical spectrum of the Dirac Hamiltonian looks like in absence of bosonic background fields. Then we can discuss the adequacy of this picture and motivate its use in the semiclassical technique when applied to particle physics.

immediately imply that QCD violates CP. For that we need instantons to exist as well, which do exist in this model since fermions do not change anything about the classical Euclidean action of Yang-Mills component.

The Dirac equation is the e.o.m. of Dirac spinors $\psi(x)$ and can be written in an explicitly Lorentz invariant way as well as one that resembles the Schödinger equation ($\hbar = 1$):

$$(i\gamma^\mu \partial_\mu - m)\psi = 0 \quad \text{or} \quad i\partial_0\psi = \left(-i\alpha^i\partial_i + m\beta\right)\psi \equiv H\psi, \tag{5.16}$$

where H is called the Dirac Hamiltonian and $\alpha^i \equiv \gamma^0\gamma^i$ and $\beta = \gamma^0$. The Dirac "gamma" matrices γ^μ form a Clifford algebra $\{\gamma^\mu, \gamma^\nu\} = 2\eta^{\mu\nu}$. The representation depends on the dimensionality of spacetime.

The equation was once used by Dirac in an attempt to formulate a relativistic version of quantum mechanics for a single particle predating quantum field theory, the spinor was then interpreted as a wave function.

In (3+1)-dimensional spacetime, the solution of the Dirac equation are plane waves of the form[33, ch.14 §2]

$$\psi_{\vec{p}}(x) = e^{i\omega x^0 + i\vec{p}\cdot\vec{x}}\, u_{\vec{p}}, \quad \text{given that} \quad \omega^2 - |\vec{p}|^2 = m^2, \tag{5.17}$$

where τ^i are the Pauli matrices and the constant spinor $u_{\vec{p}} = (u_{\vec{p},L}, u_{\vec{p},R})$ has interdependent components. If we choose $u_{\vec{p},L}$ free, $u_{\vec{p},L} \equiv u_L$, then

$$u_{\vec{p},R} = \frac{\tau^i p^i + \omega}{m}\, u_L, \tag{5.18}$$

For the plane wave, the eigenvalues of the H are simply the frequencies ω. $\vec{p}$ is the conversed momentum of the wave, extracted from the solution using the operator $P_i = -i\partial_i$: $P_i\psi_{\vec{p}} = p_i\psi_{\vec{p}}$.

We can ascribe to these waves a conserved angular momentum $\vec{L}$ that contains a classical equivalent of spin $\vec{s}$. Their operators are

$$L_i = -\epsilon_{ijk}x_j\partial_k + s_i, \quad \text{where} \quad s^i = \begin{pmatrix} \frac{1}{2}\tau^i & \\ & \frac{1}{2}\tau^i \end{pmatrix}. \tag{5.19}$$

The spin portion of the operator can be used to characterize the wave, since for each ω and $\vec{p}$ there are two independent solutions. They either have their spin aligned in or against the direction of motion, i.e. the helicity of the solution. $u_{\vec{p}} = u_\pm$, where

$$\frac{s^i p^i}{|\vec{p}|}u_\pm = \pm\frac{1}{2}u_\pm. \tag{5.20}$$

The spectrum of H will be continuous unless we put the system in a box, let us therefore impose boundary condition $\psi\left(x^i = -\frac{L}{2}\right) = \psi\left(x^i = \frac{L}{2}\right)$ for all spatial coordinates of the theory. Only a discrete number momenta and energies remain,

$$\vec{p} = \vec{p}_{\vec{n}} = \frac{2\pi}{L}\vec{n} \quad \text{with} \quad \omega = \omega_{\vec{n}} = \sqrt{|\vec{p}_{\vec{n}}|^2 + m^2}, \tag{5.21}$$

given some lattice vector $\vec{n}$ whose components are integers. The spectrum is given as the red lines in figure 5.1.

The Dirac Sea Picture and its Relevance to QFT

If the Dirac equation would have been the relativistic Schödinger equation and ψ the single particle wave function, then its spectrum would have been unbounded from below: There is no (lowest energy) ground state. Dirac found a solution in the many particle version of the problem (with spinors $\psi(x_1, x_2, \cdots)$): The state with all countably infinite number of negative energy states filled up by a fermion can be treated as the vacuum instead, see figure 5.1 (the black dots denote the occupied levels). Such a vacuum works for fermions because of Pauli's exclusion principle: There is no way for the fermions to start jumping down as there can only be one fermion per level. This is referred to as the *Dirac sea* picture of relativistic quantum mechanics. In this picture, the absence of a particle in a negative energy state (a "hole" in the Dirac sea) is interpreted as a positron.

Since the true relativistic theory of fermions is QFT, in which one quantizes the field (not wave function[6]) ψ, one might wonder whether the classical spectrum of H is in any way interesting[7] and whether a Dirac sea picture is even possible. Moreover, one might wonder whether the Dirac sea interpretation with its holes is adequate for particle physics as opposed to solid state physics[8]. As it turns out, a Dirac sea like picture is available for QFT.

In regular QFT (in a box), the field operator ψ and its Hermitian conjugate $\psi^\dagger$ are schematically

$$\psi(\vec{x}) = \sum_{\vec{p}} b_{\omega,\vec{p}}\, e^{i\vec{p}\cdot\vec{x}} + c^\dagger_{\omega,\vec{p}} e^{-i\vec{p}\cdot\vec{x}} \quad \text{and} \quad \psi^\dagger(\vec{x}) = \sum_{\vec{p}} b^\dagger_{\omega,\vec{p}}\, e^{-i\vec{p}\cdot\vec{x}} + c_{\omega,\vec{p}} e^{i\vec{p}\cdot\vec{x}}. \tag{5.22}$$

Here, $b^\dagger_{\omega,\vec{p}}$ and $c^\dagger_{\omega,\vec{p}}$ create particles and antiparticles of momentum $\vec{p}$ respectively, while $b_{\omega,\vec{p}}$ and $c_{\omega,\vec{p}}$ annihilation them.

To turn this algebra into one that mimics the Dirac sea story, we perform a so-called Bogoliubov transformation on $c^\dagger_{\omega,\vec{p}}$ and $c_{\omega,\vec{p}}$ of the antiparticles. Specifically, we replace $c^\dagger_{\omega,\vec{p}} \to b_{-\omega,\vec{p}},\ c_{\omega,\vec{p}} \to d^\dagger_{-\omega,\vec{p}}$. In other words, we re-interpret the annihilation of an antiparticle with the creation of a negative energy particle. This mapping preserves the expected algebra when we transform the vacuum with it: For instance, annihilation of the vacuum $c_{\omega,\vec{p}}|0\rangle = b^\dagger_{-\omega,\vec{p}}|0\rangle' = 0$ when $|0\rangle' = \Pi_{\omega<0,\vec{p}}\, d^\dagger_{\omega,\vec{p}}|0\rangle$, which reflects the idea that the Dirac vacuum is already filled with negative energy fermions. Rubakov claims that studying these classical eigenvalues works and is in agreement with the QFT[33, p.305].

5.2.2 The Concept of Spectral Flow

If we introduce a bosonic field background as external parameter to these fermions and we start to change these new fields, then the levels can start to shift. Because the change of these levels is continuous, as long as we move them along some contractible closed path, the levels match back up with themselves. If there are instead NCLs of bosonic field configurations,

[6] This is where the historical term "second quantization" came form.

[7] At the very least, the relativistic corrections to the momentum of the particle can be used to compute radiative corrections to the Hydrogen atom.

[8] The valence band of a solid can be regarded as a Dirac sea, holes in that band occur readily.

such as the path on which a sphaleron resides[9], then there is the possibility that the levels mismatch. Such a loop (in whatever quantum picture of the gauge field vacuum one prefers) is associated with a change in CS-number. Such a mismatch of the initial and final levels means there must have been some *spectral flow* (the crossing of levels through $\omega = 0$) at some point along the loop of fields. (This point is the sphaleron in theories where they exist.) The corresponding eigenspinors of zero energy at those points are called *zero modes*.

The mismatch of levels translates to mismatches of fermionic quantum number between this initial and final states. The quantum numbers can be fermion numbers (such as baryon and lepton number) or, for instance, the difference between the number of left and right handed particles. For example, in the case a fermion number is violated, this would mean that the level corresponding to the classical solution with zero particles (associated in QFT with $|0\rangle$) connects to a state that has one particle more (associated with a state $b^\dagger |0\rangle$). Most importantly, *the mismatching of the fermionic quantum numbers is equivalent to the existence of an anomaly in the corresponding current of the charge*. The technique therefore reproduces the anomaly's effect such as the explicit form of the selection rules.

Spectral Flow in a Simple Model

To illustrate his point, Rubakov considers a (1+1)-dimensional theory of a free massless fermion that obtains a vector interaction with a $U(1)$ gauge field. In particular[33, p.298], $\gamma^0 = \tau^1$, $\gamma^1 = i\tau^2$ and $\gamma^5 = -\gamma_0\gamma^1 = \tau^3$. Let us summarize his results[33, ch.15 §2]. There will not be any particle creation in this model, instead we will see an axial symmetry become anomalous.

In the absence of the gauge fields, the theory is exactly the one we discussed above[10]. Because the theory is massless, the Dirac equation separates for the top χ and bottom η spinors of $\psi = (\chi, \eta)$[33, p.336].

$$(i\partial_0 - i\partial_1)\chi = 0 \tag{5.23}$$

$$(i\partial_0 + i\partial_1)\eta = 0, \tag{5.24}$$

which are both solved by any traveling wave $\chi = \chi(x_1 + x_0)$ and $\eta = \eta(x_0 - x_1)$. The model has both a vector $U(1)_V : \psi \to e^{i\phi_v}\psi$ and axial symmetry $U(1)_A : \psi \to e^{i\gamma^5\phi_a}\psi$ symmetry, or equivalently two chiral symmetries $U(1)_L : (\chi, \eta) \to (e^{i\phi_L}\chi, \eta)$ and $U(1)_R : (\chi, \eta) \to (\chi, e^{i\phi_R}\eta)$. This means a conservation of both the left handed and right handed current J^μ_L, J^μ_R and charges N_L, N_R individually.

$$J^\mu_L = \bar{\psi}\frac{1+\gamma^5}{2}\psi \quad \text{and} \quad J^\mu_R = \bar{\psi}\frac{1-\gamma^5}{2}\psi \tag{5.25}$$

Let us introduce the gauge fields $A_\mu(x^0, x^1)$ such that x^0 is treated simply as an external parameter (and not a variable under which A_μ is dynamic). Then the spectral flow itself is

[9] Alternatively, take an instanton in Euclidean spacetime with its imaginary time taking the role of the loop parameter. This requires a modified technique, the one we referred to famously used by t'Hooft[1]. It can also be found in the book by Rubakov[33, ch.17].

[10] Except for the absence of the mass gap.

found by solving the eigenvalue equation[33, p.341]

$$H_D(x^0)\psi_{\omega(x^0)}(x^1) = \omega(x^0)\psi_{\omega(x^0)}(x^1), \tag{5.26}$$

where we must use the instantaneous Dirac Hamiltonian

$$H_D(x^0) = -i\alpha(\partial_1 - igA_1(x^0, x^1)). \tag{5.27}$$

The eigenvalue equation can be solved in terms of pure left handed $\psi_{\omega(x^0),L} = (\chi_{\omega(x^0)}, 0)$ and righthanded $\psi_{\omega(x^0),R} = (0, \eta_{\omega(x^0)})$ eigenspinors, the resulting spectrum turns out to be[33, p.343]

$$\omega_n(x^0) = \frac{2\pi n}{L} + \frac{g}{L}\int_{-\frac{L}{2}}^{\frac{L}{2}} A_1(x^0, x^1)dx^1, \tag{5.28}$$

$$\omega_n(x^0) = \frac{2\pi n}{L} - \frac{g}{L}\int_{-\frac{L}{2}}^{\frac{L}{2}} A_1(x^0, x^1)dx^1, \tag{5.29}$$

for both types of spinors respectively. The gauge fields of this model match those of the (1+1)-dimensional Abelian Higgs model, except that they are constrained to live between $\pm\frac{L}{2}$. In particular, they still have the same CS-vacua, recall figure 4.3 (and imagine $\pm\infty \to \pm\frac{L}{2}$ and ignoring the Higgs part). The gauge terms in the above expressions count the change in the CS-number of the gauge fields, see equation 4.9. If we make the gauge fields transition between the vacua with $N_{\text{CS}} = 0, 1$ as x^0 goes from $-\infty$ to ∞, then the spectral flow occurs as in figure 5.2. One level crosses $\omega = 0$ for either handedness.

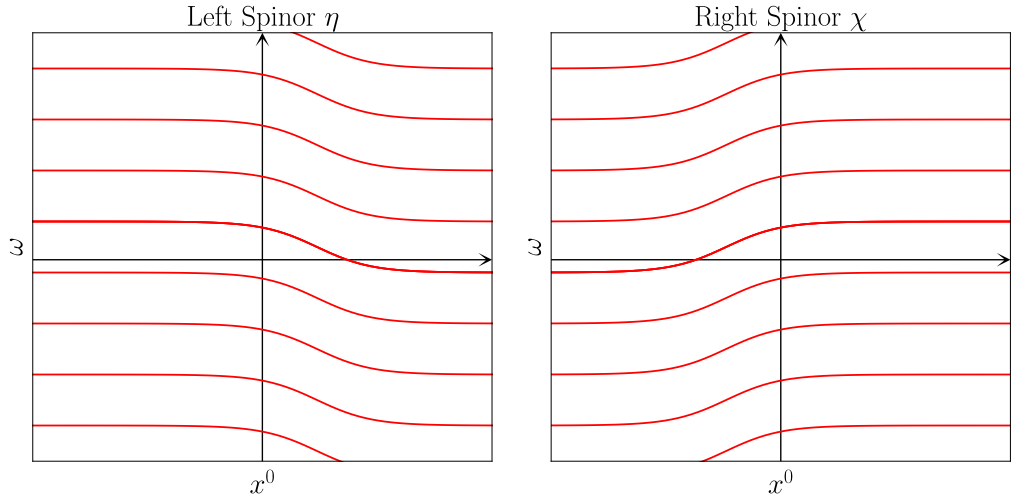

Figure 5.2: Spectral flow of the instantaneous Dirac Hamiltonian H_D for the left and right handed eigenspinors $\psi_{\omega_n,L/R}(x^1)$ as a function of x^0.

This is not the whole story yet, the movement of the levels in independent from the actual field evolution. The eigenspinors simply form a x^0-dependent basis for the configuration

$$\psi(x^0, x^1) = \sum_n A_n(x^0)\,\psi_{\omega_n(x^1),L} \;+\; B_n(x^0)\,\psi_{\omega_n(x^1),R}. \tag{5.30}$$

The evolution of the field $\psi(x^0, x^1)$ itself (in other words the coefficients) is given by the new Dirac equations

$$(i(\partial_0 - igA_0) - i(\partial_1 - igA_1))\chi = 0 \quad \text{and} \tag{5.31}$$

$$(i(\partial_0 - igA_0) + i(\partial_1 - igA_1))\eta = 0. \tag{5.32}$$

The levels themselves might move, but a configuration starting out in some level might not follow along (the coefficients might not stay constant) as the gauge fields change. Rubakov demonstrated that the field does follow along[33, p.341] when A_μ changes adiabatically. If the field starts out (at $x^0 = -\infty$) as some particular eigenspinor $\psi_{\omega_M(x^0)}$ the configuration stays proportional to $\psi_{\omega_M(x^0)}$ as x^0 changes:

$$\psi(x^0, x^1) \sim \exp\left(-i\int_\infty^{x^0} dt\, \omega_n(t)\right)\psi_{\omega_M(x^0)}. \tag{5.33}$$

Thus for any physical change in the gauge fields that causes in the CS-number to change slowly, the selection rule for the physical change in the quantum numbers (classical charges of the field $\psi(x^0, x^1)$) is

$$\Delta N_L = -\Delta N_R = \Delta N_{CS}. \tag{5.34}$$

Further Remarks

- In this problem, the right handed levels all crossed zero from below. In more complicated scenarios, some levels might also cross down from above. ΔN_R would then have been their difference. Such a difference of crossing eigenvalues of a differential operator like H_D is called the analytic index of the operator. The change in x^0 is indirectly a change in the CS-number of the fields, known as a topological index of the gauge fields. That these two quantities are equal (the selection rule) is a consequence of the so-called Atiyah-Singer index theorem. That this can be proved by direct substitution is a property of two dimensional models[33, p.345].

- The anomalies for this model in its regular form are[33, p.345]

  $$\partial_\mu J^\mu_L = \frac{e}{4\pi}\epsilon_{\mu\nu}F^{\mu\nu} \quad \text{and} \quad \partial_\mu J^\mu_R = -\frac{e}{4\pi}\epsilon_{\mu\nu}F^{\mu\nu}, \tag{5.35}$$

  which upon integration of a particular background $A_\mu(x^0, x^1)$ reproduce this selection rule. Thus the non-conservation of fermionic quantum number presented here is equivalent to the one the anomaly predicts.

- In the non-adiabatic scenario, the movement of the levels is still the same, but jumping from ω_M to a limited number of other levels has become allowed[33, p.343]. Jumping from left handed to right handed states is still prevented as well as evolution from negative energy to positive energy states and vice versa. After the transition, there can only be an additional number of positive energy levels filled together with an equal amount of holes in the states with energies below zero. In other words, the left handed and right handed spinors are still related: The "electric" charge of the particles is conserved, $\Delta(N_L + N_R) = 0$, otherwise the theory would be inconsistent.

- The model we have discussed has been very similar to the (1+1)-dimensional Abelian Higgs model we considered in chapter 4, except for the absence of the Higgs field (and a Yukawa term that should be added if there were fermions). This model has precisely the same spectral flow, which occurs on the sphaleron. Moreover, by making the interaction chiral instead of vector, the lepton current itself becomes anomalous[11]. This model mimics the EW sector of the SM accurately. There, a single level crosses from below for each quark and lepton as we traverse over the sphaleron. Thus a particle from each kind is produced in a sphaleron process. This reproduces the anomalies and selection rules from the start of the chapter[25].

- Anomalies in global $U(1)$ are an example of an abelian anomaly. These are generally related to the Atiyah-Singer index theorem and sphalerons as discussed above. On the other hand, non-abelian anomalies are not, though they are analyzed in terms of spectral flow (See the article on the $SU(3)$ sphaleron[24], Klinkhamer's and Rupp's Review *Sphalerons, Spectral Flow and anomalies*). According to these sources, not being able to globally impose Gauss's law (recall section 3.3.3) plays an important role.

5.3 Resonant Instanton/Sphaleron Transitions in the SM

In this section, we will discuss the possibility of a "resonance" feature that $\Delta(B+L)$ violating processes in the EW sector of the SM might have in collider experiments (mediated by instantons or sphalerons depending on the center of mass energy). The "resonance" refers to the concept of *resonant tunneling*, which is a phenomenon in QM, but whose QFT analogue is thought to similarly exist. Having such a feature supposedly enlarges the cross section of such transitions considerably. Knowing more about these cross sections in the laboratory might also give us more insight into sphalerons transitions that might have occurred in the early universe. The idea was put forth by originally Tye and Wong[37], since then their view has been clarified and their calculations improved[36][31]. In addition, their views have also been scrutinized[3]. In the context of this thesis we highlight the conceptual details of the procedure and their relation with the quantum theoretic vacuum structure of the SM. For the particulars of the computations themselves we refer to these papers as well as other sources[21].

5.3.1 Tye and Wong's Disagreement with the Conventional View

Consider the $|\Delta N_{\mathrm{CS}}| = 1$ reaction[12] that can occur during a proton-proton collision

$$q + q \to 3\bar{l} + 7\bar{q} + X, \quad \text{such as} \quad u + u \to e^+\mu^+\tau^+\,\bar{b}\bar{b}\bar{b}\,\bar{c}\bar{c}\bar{c}\,\bar{u} + X \tag{5.36}$$

with a quark-quark center of mass energy E_{qq}. From the discussions in the previous section, one might think that a sphaleron process produces one of each electrically charged SM

[11] Since the particles carry a charge because of the interaction, a second fermion with the opposite charge should be added to make the theory consistent.

[12] X are any other (in)directly produced particles that conserve electric charge.

fermion as a single energy level crosses zero for each species. This is only true for the SM leptons (recall equation 5.2) and not the quarks (because of the CKM matrix mixing, we only know $\Delta B = 1$).

In literature[36], it is accepted that no matter the size of E_{qq} w.r.t. the laboratory (zero temperature) value of the sphaleron energy $E_{\text{sph.}} \sim 9$ TeV, that such processes are exponentially suppressed. Specifically, the $(B+L)$-violating fraction of all EW reactions (a ratio of cross sections)

$$\kappa(E_{qq}) = \frac{\sigma(E_{qq}, |\Delta N_{\text{CS}}| \neq 0)}{\sigma(E_{qq}, |\Delta N_{\text{CS}}| \neq 0) + \sigma(E_{qq}, |\Delta N_{\text{CS}}| = 0)} \tag{5.37}$$

is thought to be dominated by the $|\Delta N_{\text{CS}}| = 1$ transitions,

$$\kappa(E_{qq}) \approx \frac{\sigma(E_{qq}, |\Delta N_{\text{CS}}| = 1)}{\sigma(E_{qq}, |\Delta N_{\text{CS}}| = 0)}. \tag{5.38}$$

The value turns out to be

$$\kappa(E_{qq} > E_{\text{sph.}}) < 10^{-70}. \tag{5.39}$$

Furthermore

$$\kappa \sim e^{-\frac{4\pi}{\alpha_w}} \rightarrow \kappa \sim e^{-\frac{2\pi}{\alpha_w}} \tag{5.40}$$

as $E_{qq} \approx 0 \ll E_{\text{sph.}}$ grows to $E_{qq} \gg E_{\text{sph.}}$. Note that $\alpha_w = \frac{g^2}{4\pi} \approx \frac{1}{30}$, where g is the EW coupling constant.

There are two exponential suppressions at play that limit the reaction[36]. Firstly, tunneling through instantons dominates the transition at $E_{qq} \approx 0 \ll E_{\text{sph.}}$, however the smallness of the EW coupling constant g prevents the reaction (see the left hand side of equation 5.40) from taking place: $g \approx 0.0645$, such that tunneling $\Gamma \sim \exp\left(-(16\pi^2)/(g^2)\right) \sim 10^{-160}$. Thus instanton-mediated $B+L$ violation turns out to be exponentially suppressed. Rather than tunnel, the fields must thus actually traverse the barriers between the CS-vacua. The ~ 9 TeV EW sphaleron therefore sets a lower limit on the energy threshold at which these predicted processes could start to become observable in experiments. Secondly however, a suppression exists at $E_{qq} > E_{\text{sph.}}$ as the process must first create a sphaleron background for the reaction to take place in[13], leading to a suppression that remains at high energies (the right hand side of equation 5.40). This renders observations of such processes supposedly impossible with current generation colliders[36].

Tye and Wong contradict these established views. In their first paper[37], they applied a novel technique to probe the suppression of these processes when the transitions are resonant. Firstly, they show that their technique produces the correct tunneling suppression as $E_{qq} \rightarrow 0$ (equation 5.40). Secondly, they conclude that sphaleron transitions at $E_{qq} > E_{\text{sph.}}$ are, in contrast to the conventional belief, unsuppressed. In their original paper they deduced

$$\kappa(E_{qq} > E_{\text{sph.}}) \sim \frac{1}{3} 10^{-2}, \tag{5.41}$$

[13]This is different for thermal EW sphaleron transitions in the early universe, those reactions are not expected to be suppressed above $E_{\text{sph.}}$ in the first place[32].

which is a discrepancy of more or less 67 orders of magnitude with equation 5.39 at those energies.

In their second paper[36], they discuss the significance of what they call multisphalerons: transitions for which $|\Delta N_{\mathrm{CS}}| > 1$. They claim these are crucial to their observed estimate of κ. In the conventional literature these are neglected (recall equation 5.37), because they are supposedly multiply suppressed. However, according to Tye and Wong, the resonance feature prevents this. For instance, they show that a double sphaleron is only single suppressed[14]. Furthermore, the paper discusses the premises of their technique. A further analysis on that topic was done by Tye and Qiu[31].

Let us explain their results by discussing their novel technique. Since it relies on the existence of resonant tunneling in QFT, we therefore begin by discussing the conceptual details of resonant tunneling in QM first.

5.3.2 Resonant Tunneling in Quantum Mechanics

To explain resonant tunneling in quantum mechanics, let us use the simple one dimensional example by Tye and Wong[36]: Consider the scenario portrayed in figure 5.3, where an electron wave packet initially in region A is send to impinge on a double barrier.

Chances are that the predominant picture of the tunneling is as follows: Part of the wave function transmits the first barrier and part of it reflects back, then the same thing happens for the second barrier for the part that went through the first. In section 3.1.1, we saw how to calculate the transmission amplitude $T(A \to B, E)$ and $T(B \to C, E)$ for each of these barriers individually, which are the same function of E given that the barriers are the same $T(A \to B, E) = T(B \to C, E) \equiv T$. We computed these amplitudes by calculating an approximate wave function in the classically forbidden regions, by approximation, those decay exponentially inside the barriers. The square of the ratio of the wave function amplitudes on either end of the barrier then give the transmission probability $|T|^2$. If the tunneling rate $\Gamma(A \to B) = \Gamma(B \to C) \equiv \Gamma = |T|^{-2} \sim e^{-S}$ for one barrier (where we compare the rate with one computed from an instanton calculation with Euclidean action S), then $\Gamma_{\mathrm{tot.}} = \Gamma^2 = e^{-2S}$ is a good estimate for the total tunneling rate for the double barrier, at least according to our story. However, not all tunneling events proceed this way.

A double barrier such as this gives rise to resonant tunneling. This means that there are certain plane wave wave functions of specific energies E' for which $\Gamma_{\mathrm{tot.}} = \Gamma^2$ is a poor estimate for the total tunneling rate. These special plane waves go through the double barrier almost as if it was not there. If a plane wave component with energy E' is the dominant part of our initial wave packet, than it would large tunnel through as such. The reason for the resonance effect is that the wave function crosses the barrier and transitions into an approximate bound state for the intermittent region B[36]. To see that $\Gamma_{\mathrm{tot.}} = e^{-2S}$ is a poor estimate, realize that unperturbed movement through the barriers means that

[14] They phenomenologically support their idea by counting powers of g in a double 't Hooft vertex diagram describing a $|\Delta N_{\mathrm{CS}}| = 2$ transition[36]. It shows inner cancellation of powers of g, which they argue to be a consequence of the resonance feature and leads to the single overall suppression of the whole diagram.

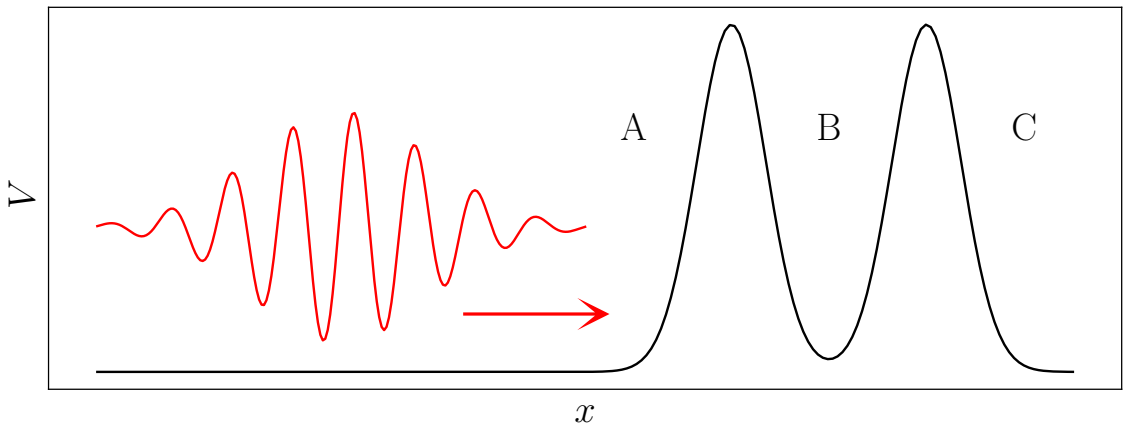

Figure 5.3: Wave packet electron impinging on a double barrier from region A. Resonant tunneling into region C occurs when the particle can transition onto an approximate bound state of region B.

transition times add up: $t(A \to C) = t(A \to B) + t(B \to C)$. Hence[36],

$$\Gamma(A \to C) = \frac{1}{t(A \to C)} = \frac{\Gamma(A \to B)\Gamma(B \to C)}{\Gamma(A \to B) + \Gamma(B \to C)} \sim e^{-S}, \tag{5.42}$$

which is only approximately singly suppressed.

In the case that the number of barriers increases arbitrarily, the approximate bound states become Bloch waves, such as the periodic potentials we discussed in section 3.3.4. This means that a plane wave that matches in frequency will tunnel through resonantly. This will be important for the field theory problem we will discuss right now.

5.3.3 The Conceptual Premises behind the Reduction to a QM Problem

The technique that Tye and Wong apply has its roots in the works by Banks, Bender and Wu[4]. They attempted to formulate a version of the WKB procedure that would work for systems with more than one quantized degree of freedom $\psi(x_n)$.

The WKB procedure then obtains an additional step: One must first compute the most probable escape path (MPEP), which is the specific curve $x_n(\mu)$ (given some parameter $\mu \in [0, 1]$) that begins and ends at the points between which the tunneling should take place. Specifically, the curve is found by minizing an expression such as equation 3.3. One then substitutes this path into the classical Lagrangian $L(x_n, \dot{x}_n)$ and chain-rules all of the dynamics onto μ alone[37], $\dot{x}_n(\mu) = \frac{\partial x_n}{\partial \mu}\dot{\mu}$. One then obtains some dynamical system for μ

$$L(\mu, \dot{\mu}) = \frac{m(\mu)}{2}\dot{\mu}^2 - V(\mu), \tag{5.43}$$

where both the "mass" as well as the potential can be μ dependent. After quantizing this reduced theory,

$$\left(-\frac{1}{2m}\frac{\partial^2}{\partial \mu^2} + V(\mu)\right)\psi(\mu) = E\psi(\mu), \tag{5.44}$$

(which required computing the Hamiltonian and promoting μ and its momentum to non-commuting operators), one can apply the regular WKB procedure, that is writing down the approximate solutions for the wave function $\psi(\mu)$.

This technique extends well into field theory, which under certain circumstances can be seen or approximated as infinite-dimensional quantum mechanics[15]. For example, the technique by Banks, Bender and Wu was used by Coleman in his famous paper *Fate of the false vacuum: Semiclassical theory*[13]. It has been shown that this WKB result agrees with the tunneling amplitudes computed using instantons[8][38]. The reduced dynamical system in the case of field theory is found by integrating out the spatial coordinates of the fields, rather then simply plugging the coordinates into the Lagrangian:

$$L(\mu, \dot{\mu}) = \int d^3x \, \mathcal{L}(\phi(x;\mu), \partial_\mu \phi(x;\mu)), \tag{5.45}$$

one then still obtains a reduced Lagrangian of the same form.

In the Schödinger functional formalism, one could think of $\psi(\mu)$ as a cross section of the whole wave functional $\Psi[\phi]$ (all field modes integrated out except the mode along μ), that supposedly captures the relevant physics (such as the resonance feature) of the tunneling process. This approximation is only valid when the wave functional is approximately separable for this mode. Interactions with the other neglected modes can effect the time scale τ over which the approximate bound states in region B are metastable. Their effect can effectively be taken into account as a form of decay[36]. Such as by introducing a non-unitary decay term into the Hamiltonian, effecting τ. The resonant tunneling becomes unnoticeable when $t(A \to C) > \tau$, so making sure that the neglected modes are irrelevant is crucial.

Tye and Wong's Approach

Ultimately, Tye and Wong want to use this WKB procedure to compute κ. They want to describe the scattering of the colliding particles as scattering of the wave functional of the SM fields in the EW sector in the potential along the $(B + L)$-violating modes[36]. According to them, a modified version of Manton's path[37] through the sphaleron (as well as another path for comparison) is an approximate ansatz for the MPEPs of this process. Since μ is directly related to the CS-number, recall equation 4.87, it has effectively become the relevant dynamical variable. They successfully integrate out the fields along the Manton loop in the Lagrangian and obtain[36]

$$L(\mu, \dot{\mu}) = \frac{m(\mu)}{2}\dot{\mu}^2 - V(\mu) \tag{5.46}$$

$$m(\mu) = 44\,\mathrm{TeV}/g^3v^2 \tag{5.47}$$

$$V(\mu) = 4\,\mathrm{TeV}(\sin^2\mu + 0.46\sin^4\mu)/g. \tag{5.48}$$

[15]The easiest example is a free massive scalar field ϕ described by the Klein-Gordon equation. Its field modes are all independent, one can therefore write down a wave functional for $\Psi(\phi)$ in terms of the amplitudes of each of the field modes α_n: $\Psi(\phi) = \psi(\alpha_n)$.

They also compute a similar system for another supposed MPEP, to compare and contrast with the Manton path. If the results differ by a lot, chances are the one (but probably both) of the paths are in no way close to MPEPs, invalidating their computation. They were in agreement however (see below).

The important property is the translational EW CS-symmetry of the potential not being gauge, but global[36]: In a CS-number change in the EW sector quarks and leptons are produced, thus the fermion numbers can be used to label each minimum (making them physically distinct). The potential is thus periodic. This is essentially how, according to Tye and Wong, the EW and QCD vacuum structures differ and why QCD retains its vacuum angle θ. The closest mode in QCD conceptually to a $B + L$ violating direction is simply the vacuum-to-vacuum path along which instantons tunnel and no particles are produced. However Manton's view of Yang-Mills and QCD reveals (the pendulum view, which Tye and Wong use) that the apparent periodic symmetry of CS-vacua is gauge: There is no resonant tunneling between $|n\rangle$ vacua in Yang-Mills or QCD in the same way as there is no resonant tunneling in the quantum mechanical pendulum. Disagreement on the nature of this symmetry has been a point of contention with the view[3]. Later works have even taken the slight a periodicity due to the fermion masses into account[31] making the periodic EW CS-symmetry only approximate.

Assuming that their view of the EW sector is correct, the periodicity of the resulting quantum system has Bloch waves as solutions with an energy band spectrum such as we discussed in section 3.3.4. Such a Bloch wave analysis is thus impossible for QCD. In their paper, Tye and Wong compute this spectrum numerically[37]. If an initial wave packet of $\psi(\mu)$ describing field state before the scattering of particles, then it is located at one of the minima of the potential. Resonant tunneling of an instanton / sphaleron process occurs when the plane waves component in in $\psi(\mu)$ fall within a energy band of the periodic potential.

To demonstrate some prediction of the theory, consider quark-quark scattering at small energies $E_{qq} \ll E_{\text{sph.}}$. An important property of the spectrum is that the lowest lying bands are really thin and are spaced far apart. According to Tye and Wong, the initial wave function $\psi(\mu)$ obtains its energy spread from the parton distributions of the quarks of the colliding protons[37][36]. At these small energies, they argue that the spread of E_{qq} contained within $\psi(\mu)$ is much larger than any particular resonant tunneling band. The rate κ can therefore be estimated as the relative overlap[37][36]

$$\kappa \sim \frac{\text{total band width overlap}}{\text{total band gap overlap} + \text{total band width overlap}} \equiv e^{\frac{4\pi}{\alpha_W}C}, \tag{5.49}$$

which they compute numerically. For ease of comparing, they define these estimates equal to a typical tunneling term with free parameter C (which in theory should be 1 for tunneling at $E_{qq} = 0$ in a pure Yang-Mills theory, recall the left hand side of equation 5.37). As it turns out, $C \approx 1.1$ for the Manton path[37][36] and about 1.35 for the alternative path. Hence, the Bloch wave analysis reproduces the expected tunneling rates (the discrepancy exists because the EW sector is not a pure Yang-Mills theory.).

Furthermore, the bands grow in size exponentially as $E_{qq} \to E_{\text{sph.}}$. From this they predict that the $(B+L)$-violating transitions are completely unsupressed above $E_{\text{sph.}}$, which is the main result of their paper.

Chapter 6

Discussion and Conclusion

Let us start this chapter by discussing and summarizing the results of each of the core chapters 2-5.

Chapter 2

In chapter 2 we began our investigations of classical field configurations of interest for QFT by studying the soliton. They are non-trivial field configurations that are static and stable (i.e. not the vacua), which means they are the minima of a theory's potential energy functional V. A soliton can be considered regular or topological, which refers to the origin of its stability.

Regular solitons exist because dissipative and amplifying effects balance out in a region of C_V, the space of finite V field configurations. In that region there is a local minimum of V, a regular soliton. If perturbed hard enough, such that the fields leave this region, the soliton can still be made to decay. The stability of a topological soliton, on the other hand, is absolute.

Topological solitons exist because there is no path through C_V that connects them to a vacuum: Any attempt at deforming a topological soliton into a vacuum is met with V blowing up. Thus the topological soliton configurations are separated from the vacua by infinite potential energy barriers, so under time evolution they cannot decay. In the chapter we discussed two topological solitons: the (anti-) kink soliton in ϕ^4-theory and the monopole solitons in the $SO(3)$ Georgi-Glashow model.

In general, C_V consisting of disconnected components (i.e. the fundamental homotopy group $\Pi_0(C_V)$ is non-trivial) hints at the existence of topological solitons. This happens because C_V inherits its topology from the requirements put on the fields needed for V to converge. If V contains a potential term $\int d^d x\, \mathcal{V}(\phi(x))$, then this term forces the fields to approach one of $\mathcal{V}$'s zeros at the d-dimensional boundary of space[1] $\partial\mathbb{R}^d$. Thus $C_V \cong \text{Maps}(\partial\mathbb{R}^d \to \ker \mathcal{V})$. If the number of such mappings is discrete (such as in the ϕ^4-theory) or when these mappings fall into homotopy classes (such as in the $SO(3)$ Georgi-

[1] $\partial\mathbb{R}^d$ is the space of the coordinates that remains once the limit $|\vec{x}| \to \infty$ is taken. For instance in $\mathbb{R}^2$, $\partial\mathbb{R}^2$ is the circle S^1 of points at "infinity", which characterizes the ways one can walk away from the origin.

Glashow model), then C_V gets similarly split up. The sectors of C_V can be labeled by topological charges associated with the discrete mappings or homotopy classes (generally winding numbers). In the case of SSB from the gauge group G to some subgroup H, such as in the $SO(3)$ Georgi-Glashow model, the relation $\ker \mathcal{V} \cong G/H$ can be used to deduce $\Pi_0(C_V)$. In that model $\Pi_0(C_V) \cong \mathbb{Z}$, which hints at the possibility of there being a countably infinite number of topological solitons.

$\Pi_0(C_V) \neq \mathbb{1}$ is a necessary but insufficient condition to prove the existence of solitons. V only obtains a true minimum (i.e. soliton) on each disconnected sector of C_V when the functional is positive definite (which is generally the case) and when these minima cannot be shown to disappear under scaling arguments such as those used to prove Derrick's theorem.

Chapter 3

In chapter 3 we discussed instantons and examined the classical and quantum picture of the gauge field vacuum. Instantons are essentially the topological solitons of the Euclidean action S_E, which live in the space of finite S_E configurations C_{S_E} of various field theories. Like solitons, they exist because $\Pi_0(C_{S_E})$ is non-trivial. Classically, they appear as trajectories / events in Euclidean time that connects classical vacua together. They are relevant in QM and QFT because their S_E determines the corresponding tunneling amplitudes between the associated vacuum / ground states.

In particular, we discussed instantons and vacuum structure of the pure $SU(2)$ Yang-Mills theory in (3+1)-dimensions. The model has a countably infinite number of instantons, as $\Pi_0(C_{S_E}) = \Pi_0(\text{Maps}(\partial\mathbb{R}^4 \to SU(2))) = \Pi_0(\text{Maps}(S^3 \to S^3)) = \mathbb{Z}$, labeled by the corresponding topological charge Q of which the $Q = 1$ solution is the famous BPST-instanton. The supplemented temporal gauge, $\boldsymbol{A}_0 = 0$ with an additional boundary constraint, gives the instantons their desired vacuum-to-vacuum event structure, the theory has a countably infinite number of topologically distinct homotopy classes of CS-vacua labled by the CS-number N_{CS}. They are separated by large gauge transformations and the instantons tunnel between them. Specifically, the instanton with charge Q interpolates between vacua such that $\Delta N_{\text{CS}} = Q$.

We subsequently discussed what quantum picture this tunneling corresponds to. We saw that there are two different views. In the original works by Jackiw and Rebbi[22] and Callan, Dashen and Gross[9], large gauge transformations are treated as global symmetries, since they are not gauge symmetries according to $\boldsymbol{A}_0 = 0$ Hamiltonian field theory, only small ones are. Upon canonical quantization, each homotopy class of classical CS-vacua, whose vacua are mutually connected by small gauge transformations, then gets their own n-vacuum state $|n\rangle$. The Hilbert space separates into a set of ladders / superselection sectors and the true vacuum state in each is the θ-vacuum $|\theta\rangle$. This is the "periodic potential picture" of the Yang-Mills vacuum. The θ can appear in physical quantities, it is a defining constant of the theory.

On the other hand, if one insists that large gauge transformations are gauge symmetries nonetheless, then one obtains Manton's view. There is then only a single vacuum state $|\Omega\rangle$. This view occurs naturally in physical gauges where every $\boldsymbol{F}_{\mu\nu}$ configuration uniquely specifies some $\boldsymbol{A}_\mu$ and the CS-vacua never appear. In this view, the instantons tunnel along

an NCL in the Euclidean field configuration space from the vacuum to itself, giving rise to a "pendulum picture" of the gauge field vacuum. θ can be introduced by inserting a topological term into the original Lagrangian, reproducing the θ-dependent physics from the other picture. Therefore, both views ultimately agree on the physics.

Chapter 4

In chapter 4 we discussed sphaleron configurations, saddle points of the potential energy V living in C_V, for the first time. They reside on the top of the smallest possible potential energy barriers separating the vacua of a theory. In the case such a theory has a single unique vacuum (in a physical gauge) or a countably infinite number of CS-vacua (in a supplemented temporal gauge), then the sphaleron changes its appearance accordingly (just as the Yang-Mills instantons did). In a physical gauge, $\Pi_1(C_V) \cong \mathbb{Z}$ proves the existence of sphalerons as long as V is positive definite and scaling arguments do not preclude their existence.

We began by examining the sphaleron (and instanton) in the (1+1)-dimensional Abelian Higgs model, a toy model for the EW theory. We observed the aforementioned gauge-dependent vacuum structure. The specific physical gauge we chose was an axial gauge. We derived the sphaleron in both aforementioned gauges including its negative mode. The mode shows how the configuration deforms towards either a single vacuum or towards distinct CS-vacua depending on the gauge.

Then we derived the $SU(2)$ sphaleron in the EW sector of the SM in a physical gauge (in the $\theta_W \to 0$ limit) after briefly reviewing the bosonic part of the EW theory. In this gauge, we explicitly show that $\Pi_1(C_V) = \mathbb{Z}$ by studying the topology of the theory. We derived the Euler-Lagrange equations for this sphaleron explicitly by first constructing a family of NCLs in C_V (in terms of two free functions) and by subsequently minimization of V over the remaining degrees of freedom. In terms of Higgs VEV and the EW coupling constant, the sphaleron mass, or height of the barrier, turns out to be ~ 9 TeV if these equations are solved numerically.

Chapter 5

In chapter 5 we finally introduced (interactions with) fermions into our theories. In the discussion that followed, the concept of the anomaly, a classical symmetry that does not exist at the quantum level (whose current J^μ is thus actually not conserved), was paramount. If the right symmetries are anomalous, then these theories are effected in fundamental ways: Vacuum angles can turn unphysical and sphalerons (and instantons) can start to play a role in processes that violate specific fermionic quantum numbers. For instance, the EW sector of the SM has anomalous baryon and lepton currents J^μ_B and $J^\mu_{L_l}$, hinting at the possibility of baryon B and lepton number L violating processes. Such reactions might be produced in collision experiments and they could have occurred in the early universe. In the latter case, the thermal EW sphaleron might help explain how the matter-antimatter asymmetry of the observable universe was generated. These processes satisfy the selection rule $\Delta L_e = \Delta L_\mu = \Delta L_\tau = \frac{1}{3}\Delta B$.

Firstly, we examined the effect of fermions on the vacuum angles of the QCD and EW gauge sectors of the SM. If the right symmetries of the classical Lagrangian are anomalous, then the path integral measure produces a θ-term under an corrected version of the symmetry. This term is shown to cancel out against the preexisting θ-term that picks out a θ-sector, turning θ nonphysical. The four global SM vector anomalies turns the EW vacuum angle unphysical. The QCD vacuum angle, however, remains because there is to global axial symmetry to become anomalous (SM fermions have mass because of the Higgs mechanism). Nonetheless, the QCD vacuum angle (and thus de degree of C and CP violation) is exceptionally small, this is the so-called strong CP problem.

Secondly, we studied a semiclassical technique that explains the connection between sphalerons and the violation of fermionic quantum numbers (such as the SM's B and L, i.e. particle production), reproducing the effect of the anomaly. In the technique, fermions are represented as classical Dirac spinors that reside in an external gauge field background. In the case of the sphaleron, one studies the spectral flow of their Dirac Hamiltonian (the movement of the eigenvalues), viewed in a Dirac sea-like picture, when traversing the sphaleron loop. Depending on the kind of anomaly and nature of the interaction (vector, chiral, etc.) levels get raised out of, or fall into, the sea, corresponding to the creation and / or annihilation of fermions. Ultimately, a change in the CS-number of the gauge fields results in the shifting of the levels, quantified by the Atiyah-Singer index theorem. In the SM, this produces the selection rule $\Delta L_l = \Delta B/3 = \Delta N_{\mathrm{CS}}$ for a $(B+L)$-violating reaction.

Thirdly, we examined the recently proposed by Tye, Wong (and later Qiu) possibility that sphaleron process occurring in collider experiment could have a resonance feature[37][36][31], analogous to resonant tunneling in QM. The cross section of such processes is then predicted to be 67 orders of magnitude larger at energies above the sphaleron mass, which is where it is conventionally expected that sphaleron transitions remain suppressed. The feature makes sphaleron processes more likely to be observed in future colliders. The technique that was used to make these predictions is based on applying the WKB procedure to QFT (in the Schrödinger functional formalism), reducing the complicated scattering calculation into a one dimensional quantum mechanics problem with the CS-number as (indirectly) quantized variable. This QM problem has resonant tunneling, because it contains the periodic potential $V(N_{\mathrm{CS}})$ along the sphaleron loop, which is now a supposedly global symmetry in the EW theory (as opposed to QCD), since fermions are produced when the N_{CS} changes in the EW sector. Periodic potentials have Bloch wave solutions, which take the resonant tunneling feature implicitly into account. If the technique works, that this resonance feature must exist in QFT too. The technique was not invented by Tye and Wong, it has its roots in the works by Banks, Bender and Wu[4], which has seen applications[13][8][38].

Conclusion

In this thesis we set out to understand solitons, instantons and especially sphalerons. We have discussed what defined them, why they exist and what predictions can be made with them. For the various theories discussed, the table in figure 6.1 lists whether any of these configurations is present.

We notice especially the relevance of topology in all aspects of these problems. Firstly, we saw that the topology of configuration spaces C (in terms of homotopy groups) is responsible for their existence. The connectedness of such a space Π_0 revealing solitons (when $C = C_V$) and instantons (when $C = C_{S_E}$), while having an NCL in C_V, characterized by $\Pi_1(C_V)$, reveals the existence of a sphaleron.

Secondly, we noticed how important topology is for the violations of fermionic quantum numbers. The spectral flow technique revealed that the gauge and fermion fields can only be wound simultaneously: The levels of the Dirac Hamiltonian get shifted under a change of CS-number. In the QFT, this corresponded to the creation of particles.

We also got to understand that for the application of these semiclassical techniques it is important that one has a proper understanding of the connection between the classical and quantum theoretic vacuum structure of the field theory in question. Firstly, we saw that the quantum theoretic picture of the gauge field vacuum depends on the residual gauge freedom the moment one start quantizing. This gave rise to a crystal or alternatively a pendulum picture of the Yang-Mills vacuum structure. The reason was that one needs to carefully analyze the way in which such a residual gauge freedom shows up in the Hamiltonian formalism.

Secondly, understanding how the quantum theoretic vacuum structure of the SM changes when fermions are introduced is crucial for the resonance feature of the sphaleron transition to exist. The symmetry of the periodicity of $V(N_{\mathrm{CS}})$ (the potential along the $(B+L)$-violating mode in which the Bloch wave states of reduced QM problem live) must be global (not gauge). Tye and Wong argue that these are global, because changes in N_{CS} produce particles[36]. The importance of this point was made clear in Tye and Wong's second article, in which they responsed to criticisms by Bachas and Tomaras [3] concerning the existence of Bloch waves.

Table of Theories			
Model	Topological Soliton	Instanton	Sphaleron
(3+1)-dim. $SO(3)$ Georgi-Glashow	X	X	
(1+1)-dim. Abelian Higgs		X	X
(3+1)-dim. $SU(2)$ Yang-Mills		X	
(3+1)-dim. $SU(2)$ Yang-Mills + Higgs (EW)			X
(3+1)-dim. $SU(3)$ Yang-Mills + Higgs (QCD)			XXX

Figure 6.1: Table of theories with the existence of solitons, instantons or sphalerons marked. Three X's denotes the existence of three different classes of the particular configuration type.

Bibliography

[1] (a) G. 't Hooft. "Symmetry Breaking through Bell-Jackiw Anomalies". In: *Physical Review Letters* 37.1 (July 1976), pp. 8–11. ISSN: 0031-9007. DOI: 10.1103/PhysRevLett.37.8. URL: https://link.aps.org/doi/10.1103/PhysRevLett.37.8; (b) G. 't Hooft. "Computation of the quantum effects due to a four-dimensional pseudoparticle". In: *Physical Review D* 14.12 (Dec. 1976), pp. 3432–3450. ISSN: 0556-2821. DOI: 10.1103/PhysRevD.14.3432. URL: https://link.aps.org/doi/10.1103/PhysRevD.14.3432.

[2] Stephen L. Adler. "Axial-Vector Vertex in Spinor Electrodynamics". In: *Physical Review* 177.5 (Jan. 1969), pp. 2426–2438. ISSN: 0031-899X. DOI: 10.1103/PhysRev.177.2426. URL: https://link.aps.org/doi/10.1103/PhysRev.177.2426.

[3] Constantin Bachas and Theodore Tomaras. "Band structure in Yang-Mills theories". In: *Journal of High Energy Physics* 2016.5 (May 2016), p. 143. ISSN: 1029-8479. DOI: 10.1007/JHEP05(2016)143. URL: http://link.springer.com/10.1007/JHEP05(2016)143.

[4] (a) Thomas Banks, Carl M. Bender, and Tai Tsun Wu. "Coupled Anharmonic Oscillators. I. Equal-Mass Case". In: *Physical Review D* 8.10 (Nov. 1973), pp. 3346–3366. ISSN: 0556-2821. DOI: 10.1103/PhysRevD.8.3346. URL: https://link.aps.org/doi/10.1103/PhysRevD.8.3346; (b) Thomas Banks and Carl M. Bender. "Coupled Anharmonic Oscillators. II. Unequal-Mass Case". In: *Physical Review D* 8.10 (Nov. 1973), pp. 3366–3378. ISSN: 0556-2821. DOI: 10.1103/PhysRevD.8.3366. URL: https://link.aps.org/doi/10.1103/PhysRevD.8.3366.

[5] A.A. Belavin et al. "Pseudoparticle solutions of the Yang-Mills equations". In: *Physics Letters B* 59.1 (Oct. 1975), pp. 85–87. ISSN: 03702693. DOI: 10.1016/0370-2693(75)90163-X. URL: https://linkinghub.elsevier.com/retrieve/pii/037026937590163X.

[6] J. S. Bell and R. Jackiw. "A PCAC puzzle: $\pi 0 \to \gamma\gamma$ in the σ-model". In: *Il Nuovo Cimento A* 60.1 (Mar. 1969), pp. 47–61. ISSN: 0369-3546. DOI: 10.1007/BF02823296. URL: http://link.springer.com/10.1007/BF02823296.

[7] Claude W. Bernard and Erick J. Weinberg. "Interpretation of pseudoparticles in physical gauges". In: *Physical Review D* 15.12 (June 1977), pp. 3656–3659. ISSN: 0556-2821. DOI: 10.1103/PhysRevD.15.3656. URL: https://link.aps.org/doi/10.1103/PhysRevD.15.3656.

[8] (a) Khalil M. Bitar and Shau-Jin Chang. "Vacuum tunneling and fluctuations around a most probable escape path". In: *Physical Review D* 18.2 (July 1978), pp. 435–452. ISSN: 0556-2821. DOI: 10.1103/PhysRevD.18.435. URL: https://link.aps.org/doi/10.1103/PhysRevD.18.435; (b) Khalil M. Bitar and Shau-Jin Chang. "Vacuum tunneling of gauge theory in Minkowski space". In: *Physical Review D* 17.2 (Jan. 1978), pp. 486–497. ISSN: 0556-2821. DOI: 10.1103/PhysRevD.17.486. URL: https://link.aps.org/doi/10.1103/PhysRevD.17.486.

[9] C.G. Callan, R.F. Dashen, and D.J. Gross. "The structure of the gauge theory vacuum". In: *Physics Letters B* 63.3 (Aug. 1976), pp. 334–340. ISSN: 03702693. DOI: 10.1016/0370-2693(76)90277-X. URL: https://linkinghub.elsevier.com/retrieve/pii/037026937690277X.

[10] James Charbonneau. *Introduction to the Ginzburg-Landau Equations*. Tech. rep. 2005.

[11] Ta-Pei Cheng and Ling-Fong Li. *Gauge Theory of Elementary Particle Physics: Problems and Solutions*. illustrate. Clarendon Press, 1984, p. 536. ISBN: 9780198519614.

[12] Sidney Coleman. *Aspects of Symmetry*. Cambridge University Press, Aug. 1985. ISBN: 9780521318273. DOI: 10.1017/CBO9780511565045. URL: https://www.cambridge.org/core/product/identifier/9780511565045/type/book.

[13] Sidney Coleman. "Fate of the false vacuum: Semiclassical theory". In: *Physical Review D* 15.10 (May 1977), pp. 2929–2936. ISSN: 0556-2821. DOI: 10.1103/PhysRevD.15.2929. URL: https://link.aps.org/doi/10.1103/PhysRevD.15.2929.

[14] Roger F. Dashen, Brosl Hasslacher, and André Neveu. "Nonperturbative methods and extended-hadron models in field theory. III. Four-dimensional non-Abelian models". In: *Physical Review D* (1974). ISSN: 05562821. DOI: 10.1103/PhysRevD.10.4138.

[15] Sophia Demoulini and David Stuart. "Gradient flow of the superconducting Ginzburg–Landau functional on the plane". In: *Communications in Analysis and Geometry* 5.1 (1997), pp. 121–198. ISSN: 10198385. DOI: 10.4310/CAG.1997.v5.n1.a3. URL: http://www.intlpress.com/site/pub/pages/journals/items/cag/content/vols/0005/0001/a003/.

[16] Wilco J. den Dunnen. "Vacuum structure of the strong interaction with a Peccei-Quinn symmetry". PhD thesis. 2008.

[17] John Ellis, Kazuki Sakurai, and Michael Spannowsky. "Search for sphalerons: IceCube vs. LHC". In: *Journal of High Energy Physics* (2016). ISSN: 10298479. DOI: 10.1007/JHEP05(2016)085. arXiv: 1603.06573.

[18] Kazuo Fujikawa. "Path-Integral Measure for Gauge-Invariant Fermion Theories". In: *Physical Review Letters* 42.18 (Apr. 1979), pp. 1195–1198. ISSN: 0031-9007. DOI: 10.1103/PhysRevLett.42.1195. URL: https://link.aps.org/doi/10.1103/PhysRevLett.42.1195.

[19] David J. Griffiths and Darrell F. Schroeter. *Introduction to Quantum Mechanics*. Cambridge University Press, Aug. 2018. ISBN: 9781316995433. DOI: 10.1017/9781316995433. URL: https://www.cambridge.org/core/product/identifier/9781316995433/type/book.

[20] Richard Healey. "Gauge Symmetry and the Theta-Vacuum". In: *EPSA Philosophical Issues in the Sciences*. Dordrecht: Springer Netherlands, 2010, pp. 105–116. ISBN: 9789048132515. DOI: 10.1007/978-90-481-3252-2_11. URL: http://link.springer.com/10.1007/978-90-481-3252-2%7B%5C_%7D11.

[21] Tomas Heldeweg. "Sphaleron solutions and their phenomenology in the electroweak theory". PhD thesis. 2018.

[22] R. Jackiw and C. Rebbi. "Vacuum Periodicity in a Yang-Mills Quantum Theory". In: *Physical Review Letters* 37.3 (July 1976), pp. 172–175. ISSN: 0031-9007. DOI: 10.1103/PhysRevLett.37.172. URL: https://link.aps.org/doi/10.1103/PhysRevLett.37.172.

[23] F. R. Klinkhamer and N. S. Manton. "A saddle-point solution in the Weinberg-Salam theory". In: *Physical Review D* 30.10 (Nov. 1984), pp. 2212–2220. ISSN: 0556-2821. DOI: 10.1103/PhysRevD.30.2212. URL: https://link.aps.org/doi/10.1103/PhysRevD.30.2212.

[24] F.R. Klinkhamer and C. Rupp. "A sphaleron for the non-Abelian anomaly". In: *Nuclear Physics B* 709.1-2 (Mar. 2005), pp. 171–191. ISSN: 05503213. DOI: 10.1016/j.nuclphysb.2004.12.027. arXiv: 0410195 [hep-th]. URL: https://linkinghub.elsevier.com/retrieve/pii/S055032130401034X.

[25] Frans R. Klinkhamer and Christian Rupp. "Sphalerons, spectral flow, and anomalies". In: *Journal of Mathematical Physics* 44.8 (Aug. 2003), pp. 3619–3639. ISSN: 0022-2488. DOI: 10.1063/1.1590420. arXiv: 0304167 [hep-th]. URL: http://aip.scitation.org/doi/10.1063/1.1590420.

[26] V.A. Kuzmin, V.A. Rubakov, and M.E. Shaposhnikov. "On anomalous electroweak baryon-number non-conservation in the early universe". In: *Physics Letters B* 155.1-2 (May 1985), pp. 36–42. ISSN: 03702693. DOI: 10.1016/0370-2693(85)91028-7. URL: https://linkinghub.elsevier.com/retrieve/pii/0370269385910287.

[27] N. S. Manton. "The inevitability of sphalerons in field theory". In: *Philosophical Transactions of the Royal Society A: Mathematical, Physical and Engineering Sciences* 377.2161 (Dec. 2019), p. 20180327. ISSN: 1364-503X. DOI: 10.1098/rsta.2018.0327. arXiv: 1903.11573. URL: https://royalsocietypublishing.org/doi/10.1098/rsta.2018.0327.

[28] N. S. Manton. "Topology in the Weinberg-Salam theory". In: *Physical Review D* 28.8 (Oct. 1983), pp. 2019–2026. ISSN: 0556-2821. DOI: 10.1103/PhysRevD.28.2019. URL: https://link.aps.org/doi/10.1103/PhysRevD.28.2019.

[29] N. S. Manton and H. Merabet. "$\phi 4$ kinks - Gradient flow and dynamics". In: *Nonlinearity* 10.1 (Jan. 1997), pp. 3–18. ISSN: 0951-7715. DOI: 10.1088/0951-7715/10/1/002. URL: https://iopscience.iop.org/article/10.1088/0951-7715/10/1/002.

[30] Nicholas Manton and Paul Sutcliffe. *Topological Solitons*. Cambridge University Press, June 2004. ISBN: 9780521838368. DOI: 10.1017/CBO9780511617034. URL: https://www.cambridge.org/core/product/identifier/9780511617034/type/book.

[31] Yu-Cheng Qiu and S.-H. Henry Tye. "Role of Bloch waves in baryon-number violating processes". In: *Physical Review D* 100.3 (Aug. 2019), p. 033006. ISSN: 2470-0010. DOI: 10.1103/PhysRevD.100.033006. arXiv: 1812.07181. URL: https://link.aps.org/doi/10.1103/PhysRevD.100.033006.

[32] Valerii A. Rubakov and Mikhail E. Shaposhnikov. "Electroweak baryon number non-conservation in the early Universe and in high-energy collisions". In: *Uspekhi Fizicheskih Nauk* 166.5 (1996), pp. 493–537. ISSN: 0042-1294. DOI: 10.3367/UFNr.0166.199605d.0493. arXiv: 9603208 [hep-ph]. URL: http://ufn.ru/ru/articles/1996/5/d/.

[33] Valery Rubakov. *Classical Theory of Gauge Fields*. Princeton: Princeton University Press, Dec. 2009. ISBN: 9781400825097. DOI: 10.1515/9781400825097. URL: http://www.degruyter.com/view/books/9781400825097/9781400825097/9781400825097.xml.

[34] (a) Jakob Schwichtenberg. *Demystifying the QCD Vacuum: Part 1 - The Standard Story*. URL: http://jakobschwichtenberg.com/demystifying-the-qcd-vacuum-part-1/ (visited on 06/13/2020); (b) Jakob Schwichtenberg. *Demystifying the QCD Vacuum: Part 2 - The Subtleties No One Talks About*. URL: http://jakobschwichtenberg.com/demystifying-the-qcd-vacuum-part-2/ (visited on 06/13/2020); (c) Jakob Schwichtenberg. *Demystifying the QCD Vacuum: Part 3 - The Untold Story*. URL: http://jakobschwichtenberg.com/demystifying-the-qcd-vacuum-part-3-the-untold-story/ (visited on 06/13/2020); (d) Jakob Schwichtenberg. *Demystifying the QCD Vacuum: Part 4 - Physical Implications of θ*. URL: http://jakobschwichtenberg.com/demystifying-the-qcd-vacuum-part-4-physical-implications-of-theta/ (visited on 06/13/2020); (e) Jakob Schwichtenberg. *Demystifying the QCD Vacuum: Part 5 - Anomalies and the Strong CP Problem*. URL: http://jakobschwichtenberg.com/demystifying-the-qcd-vacuum-part-5-anomalies-and-the-strong-cp-problem/ (visited on 06/13/2020).

[35] (a) Clifford Henry Taubes. "The existence of a non-minimal solution to the SU(2) Yang-Mills-Higgs equations on $\mathbb{R}^3$: Part I". In: *Communications in Mathematical Physics* 86.2 (June 1982), pp. 257–298. ISSN: 0010-3616. DOI: 10.1007/BF01206014. URL: http://link.springer.com/10.1007/BF01206014.

[36] S.-H. Henry Tye and Sam S.C. Wong. "Baryon number violating scatterings in laboratories". In: *Physical Review D* 96.9 (Nov. 2017), p. 093004. ISSN: 2470-0010. DOI: 10.1103/PhysRevD.96.093004. URL: https://link.aps.org/doi/10.1103/PhysRevD.96.093004.

[37] S.-H. Henry Tye and Sam S.C. Wong. "Bloch wave function for the periodic sphaleron potential and unsuppressed baryon and lepton number violating processes". In: *Physical Review D* 92.4 (Aug. 2015), p. 045005. ISSN: 1550-7998. DOI: 10.1103/PhysRevD.92.045005. arXiv: 1505.03690. URL: https://link.aps.org/doi/10.1103/PhysRevD.92.045005.

[38] Stefan Vandoren and Peter van Nieuwenhuizen. "Lectures on instantons". In: (Feb. 2008). arXiv: 0802.1862. URL: http://arxiv.org/abs/0802.1862.

Acknowledgements

I want begin this section by thanking my supervisor and first examiner prof. dr. Daniël Boer. Firstly, for being given the opportunity to work on this subject that I personally really enjoy. Secondly, for the many fruitful and insightful conversations we have had during the year. Thirdly, for the constructive and in-depth feedback on this thesis and associated presentation as they were being written and outlined. Lastly, for continuing to supervise in the coming years for a related PhD project.

I want to thank prof. dr. Rob G.E. Timmermans for reading and commenting on my thesis as well as my final presentation.

I want to thank my friends, especially Fabian IJpelaar and Björn Boer. Fabian, for helping me out when I got stuck as well as being there to bounce ideas back and forth with at the university. Our thorough, long, exciting (and possible slightly distracting) discussions on QFT will not be forgotten. Björn, for the many fun evenings we have enjoyed and encouraging discussions we have had about our studies and life. Both, for helping me de-stress and for supporting me when I needed it.

I want to thank both my parents for the support throughout the year. My mother for taking care of much of the household activities, allowing me to focus on my project. My father for the time of leisure / recreation he has provided, the breaks have helped me a lot. Both, for the support and motivation they have given me.